First Quarter
1993

AFRRI Reports

REPORT DOCUMENTATION PAGE

Form Approved
OMB No. 0704-0188

1 AGENCY USE ONLY *(Leave blank)*	2 REPORT DATE	3 REPORT TYPE AND DATES COVERED
	May 1993	Reprints/Technical

4 TITLE AND SUBTITLE

AFRRI Reports, First Quarter 1993

5 FUNDING NUMBERS

PE: NWED QAXM

6 AUTHOR(S)

7 PERFORMING ORGANIZATION NAME(S) AND ADDRESS(ES)

Armed Forces Radiobiology Research Institute
8901 Wisconsin Avenue
Bethesda, MD 20889-5603

8 PERFORMING ORGANIZATION REPORT NUMBER

SR93-1 - SR93-12

9 SPONSORING/MONITORING AGENCY NAME(S) AND ADDRESS(ES)

Defense Nuclear Agency
6801 Telegraph Road
Alexandria, VA 22310-3398

10 SPONSORING/MONITORING AGENCY REPORT NUMBER

11 SUPPLEMENTARY NOTES

12a DISTRIBUTION/AVAILABILITY STATEMENT

Approved for public release; distribution unlimited.

12b DISTRIBUTION CODE

13 ABSTRACT *(Maximum 200 words)*

This volume contains AFRRI Scientific Reports SR93-1 through SR93-12 for January-March 1993.

14 SUBJECT TERMS

15 NUMBER OF PAGES
80

16 PRICE CODE

17 SECURITY CLASSIFICATION OF REPORT	18 SECURITY CLASSIFICATION OF THIS PAGE	19 SECURITY CLASSIFICATION OF ABSTRACT	20 LIMITATION OF ABSTRACT
UNCLASSIFIED	UNCLASSIFIED	UNCLASSIFIED	SAR

CONTENTS

Scientific Reports

INT. J. RADIAT. BIOL., 1993, VOL. 63, NO. 1, 37–46

Effects of WR-1065 and WR-151326 on survival and neoplastic transformation in C3H/10T$\frac{1}{2}$ cells exposed to TRIGA or JANUS fission neutrons

E. K. BALCER-KUBICZEK*†, G. H. HARRISON†, C. K. HILL‡ and W. F. BLAKELY§

(Received 10 March 1992; revision received 15 June 1992, accepted 19 August 1992)

Abstract. We demonstrated the ability of aminothiols WR-1065 and WR-151326, each at concentration 1 mM, to protect C3H 10T$\frac{1}{2}$ cells against the transforming effects of fission neutrons under two distinct sets of experimental conditions. Experiments with WR-1065 were performed with stationary cultures of C3H 10T$\frac{1}{2}$ cells, and a TRIGA reactor-generated fission neutron field at the Armed Forces Radiobiology Research Institute (USA). Experiments with WR-151326 were performed with proliferating cultures of C3H 10T$\frac{1}{2}$ cells and a JANUS reactor-generated fission neutron field at the Argonne National Laboratory (USA). Radioprotectors were present before, during, and after irradiation for total periods of 35 min (WR-151326; 10 min pre-incubation) or 1 h (WR-1065; 30 min pre-incubation). Bioavailability of WR-1065 and WR-151326 in extracellular medium under experimental conditions simulating those of the transformation experiments was studied by measuring oxidation rates in the presence of attached C3H 10T$\frac{1}{2}$ cells in plateau and exponential phase of growth for periods of up to 5 h. Estimated half-lives for autoxidation of WR-1065 or WR-151326 were approximately 8 min or 1 h regardless of the proliferative status of cells. In the absence of WR-compounds, dose response data for transformation induction by neutrons from TRIGA and JANUS reactors were fitted to a common curve with a linear coefficient of about 7×10^{-4}/Gy. WR-151326 and WR-1065 were found to provide significant radioprotection by factors of $1{\cdot}79 \pm 0{\cdot}08$ and $3{\cdot}23 \pm 0{\cdot}19$, respectively, against fission neutron-induced neoplastic transformation. No significant protection against neutron-induced cell lethality was observed.

1. Introduction

The use of chemical agents for protection against the acute effects of irradiation was first investigated by Patt *et al.* (1949), but it was only within the past several years that antimutagenic and antineoplastic properties were discovered (Marquardt *et al.* 1974, Maisin *et al.* 1978, Mori *et al.* 1983, Milas *et al.* 1984, Grdina *et al.* 1985a,b, 1989a,b, 1991, Nagy and Grdina 1986, Hill *et al.* 1986, Nagy *et al.* 1986, Corn *et al.* 1987, Grdina and Sigdestad 1989, Nassi-Calo *et al.* 1989, Schwartz *et al.* 1988, Carnes and Grdina 1992). Earlier protection studies found that the most effective compounds were phosphorothioates that must be dephosphorylated to produce an active free thiol (Mori *et al.* 1983, Smoluk *et al.* 1988). The benchmark radioprotector remains WR-2721 and its associated free thiol WR-1065. However, WR-151327, a structural analogue of WR-2721, showed promise as being equally effective against high-LET radiations (Sigdestad *et al.* 1986, Steel *et al.* 1987); WR-151326, one of the compounds investigated in the present study, is an associated thiol of WR-151327.

Progress in protector research has led to a number of postulated mechanisms of action, including free radical scavenging, chelation of metal ions, oxygen depletion, restoration of damaged target molecules by hydrogen atom or electron donation, and the enhancement of DNA repair or cell recovery processes, or a combination of these mechanisms (Livesy and Reed 1987, Aguilera *et al.* 1992). These mechanisms are generally consistent with the ability of thiols to reduce several types of DNA lesions linked to cell lethality, and with better protection against low-LET radiations than high-LET radiations (Nagy and Grdina 1986, Sigdestad *et al.* 1986, Afzal and Ainsworth 1987, Schwartz *et al.* 1988, van Ankeren *et al.* 1989, Murray *et al.* 1990). On the other hand, cell mutation and transformation are caused by non-lethal types of DNA damage. Although the supporting data are sparse, some aspects of thiol protection for the endpoint of radiation-induced cell killing appear to differ significantly from those for mutation, transformation or tumour induction. Some of these differences are: that, for these late effects, protection factors are usually higher (Patt *et al.* 1949, Maisin *et al.* 1978, Milas *et al.* 1984, Grdina *et al.* 1985a,b, 1989a,b, 1991, Grdina and Sigdestad

*Author for correspondence.
†Department of Radiation Oncology, University of Maryland School of Medicine, Baltimore MD 21201, USA.
‡Department of Radiation Oncology, Southern California Cancer Research Laboratory, University of Southern California School of Medicine, Los Angeles CA 90015, USA.
§Radiation Biophysics Department, Armed Forces Radiobiology Research Institute, Bethesda MD, 20889-5145, USA.

0020-7616/93 $10.00 (c) 1993 Taylor & Francis Ltd

1989); protection can occur for drug administration postirradiation (Grdina *et al.* 1989b); protection can occur at drug concentrations lower than those required for protection from killing by chemicals or radiation (Marquardt *et al.* 1974, Hill *et al.* 1986, Nagy *et al.* 1986). One of us (Hill *et al.* 1986) previously reported the anti-neoplastic effect of WR-1065 following low-LET irradiation of actively growing C3H/10T½ cells. While this study clearly demonstrated protection against γ-ray-induced neoplastic transformation in the C3H/10T½ assay, there has been no corresponding published study on WR protection against high-LET irradiation.

In this report we present the results of two independent investigations of the potential of WR protectors to mitigate at the cellular level the carcinogenic action of neutrons. Important applications may be established for these agents in neutron therapy, military or occupational exposures, and space exploration, depending on the neutron dose range within which protection may be demonstrated. Protective effects of WR-1065 on fission neutron-induced lethality and neoplastic transformation were studied at the Armed Forces Radiobiology Research Institute (AFRRI) TRIGA reactor facility, using plateau cultures of C3H/10T½ cells. Independently, the protective effects of WR-151326 on fission neutron-induced lethality and neoplastic transformation were studied at the Argonne National Laboratory (ANL) JANUS reactor, using exponential cultures of C3H/10T½ cells. In addition, some supporting pharmacokinetic data for WR-1065 and WR-151326 were obtained at AFRRI by one of us (W.F.B.). Although the same transformation assay and protector concentration of 1 mM were used for both protectors, the studies were not coordinated, leading to differences in treatment protocols detailed below.

2. Materials and methods

2.1. *Cells, culture conditions, and bioassays*

Subconfluent parent cultures of C3H/10T½ cells were used to initiate exponential or plateau cultures using previously reported materials and methods (Han and Elkind 1979, Hill *et al.* 1982, Balcer-Kubiczek *et al.* 1987, 1988, 1991, Balcer-Kubiczek and Harrison 1991). In JANUS neutron experiments with or without WR-151326, 3–4-day-old actively growing cultures at 10^6 cells per flask were used. Confluent monolayers for TRIGA neutron experiments with or without WR-1065 were obtained by growing cells for 18 days with medium changes every 5 days. Under these conditions the number of cells per flask reached a saturation density of $6{\cdot}8 \times 10^6$ cells per flask. Experiments were performed 3 days after the last medium change. Flow cytometry measurements indicated that more than 97% of the cells were in G_1 phase. Experiments were performed at 37 °C.

Cell survival was determined by colony-forming ability while neoplastically transformed foci were identified according to published criteria (Reznikoff *et al.* 1973a,b, IARC/NCI/EPA Working Group 1985). The endpoint of transformants per surviving cell was calculated by the null method of Han and Elkind (1979) with uncertainties determined according to our modified analysis (Balcer-Kubiczek *et al.* 1987). In addition, we determined the average number of transformants per dish as recommended by IARC/NCI/EPA (1985) with uncertainties calculated according to the published methods (Hieber *et al.* 1987).

2.2. *Radioprotectors*

S-2-(3-aminopropylamino)ethyl phosphorothioic acid (WR-1065, lot BK71365) was obtained from the Division of Cancer Treatment, National Institutes of Health, Bethesda, MD. 3-[3-Methylaminopropylamino]propanethiol dihydrochloride (WR-151326, lot BL00101) was obtained from the Division of Experimental Therapeutics, Walter Reed Army Medical Center, Washington, DC. Glutathione and cysteine for pharmacokinetic studies were obtained from Sigma Chemical Company, St Louis, MO. Structures and selected properties of these radioprotectors, including half-lives for autoxidation measured in the present study, are listed in Table 1.

2.2.1. *Treatment with WR-151326.* WR-151326 treatment in the present experiments was similar to that previously described for WR-1065 combined with ^{60}Co γ-irradiation (Hill *et al.* 1986). Briefly, WR-151326 stock was freshly prepared on the day of each experiment as a 1-M stock solution in 3 ml of phosphate-buffered saline (PBS) and sterilized by filtration through a 0·2 μm filter. It was added to prewarmed complete medium at a final concentration of 1 mM and used to fill flasks 10 min before irradiation. Medium containing drug was not removed until the cells were harvested after the end of the irradiation. The total exposure time to WR-151326 was kept constant at 35 min. After completion of irradiation and/or WR-151326 treatment, cells were rinsed twice with PBS, then trypsinized, counted, and plated for survival and transformation

Table 1. The structural formula and some properties of the thiols used in the present studies

Compound[a]	Structure	Net charge at pH 7.2[b]	Autoxidation $t_{\frac{1}{2}}$, min[c]
WR-1065	$NH_2(CH_2)_3NH(CH_2)_2SH$	+2	8 ± 1 (7)
WR-151326	$CH_3NH(CH_2)_4NH(CH_2)_4SH$	+2	55 ± 3 (5)
Cysteine	NH_2CHCH_2SH COOH	+1	19 ± 2 (5)
Glutathione	$NH_2CH(CH_2)_2CONHCHCONHCOOH$ COOH CH_2SH	−1	70 ± 28 (5)

[a] All rates determined by the use of 1 mM thiol. See §2 for experimental details.

[b] Murray *et al.* 1990).

[c] Half-life in the culture medium at 37°C is based on pooled data from experiments with exponential or stationary cultures. Values are the variance-weighted means and standard errors. The number of experiments, each consisting of three to six measurements per time point in Figure 1, is indicated in parentheses.

as described previously (Han and Elkind 1979, Hill *et al.* 1982).

2.2.2. *Treatment with WR-1065.* The day before each experiment, WR-1065 was weighed out, sealed under nitrogen in 50 ml tubes, and stored at −20°C. Immediately prior to use, WR-1065 was dissolved in warm medium withdrawn from a medium-filled flask. This thiol stock solution was sterilized by filtration as above, and then added back to flasks to obtain 1 mM final concentration in flasks designated as drug-treatment groups. The WR-1065 concentration in individual flasks based upon weight was routinely checked by titration with Ellman's reagent; the methods are described below in §2.2.3. Thiol level in medium determined spectrophotometrically agreed well to within uncertainties with the thiol concentration based upon weight.

Neutron irradiations were initiated 30 min after the beginning of exposure to WR-1065; the total exposure time to WR-1065 was 1 h for all samples. After completion of neutron irradiation and/or drug treatment, medium was removed, cellular monolayers were rinsed twice with growth medium and flasks refilled with fresh warm medium before being returned to Baltimore, where cells were dissociated and plated for survival and transformation determination as described previously (Balcer-Kubiczek *et al.* 1987, 1988, 1991, Balcer-Kubiczek and Harrison 1991).

2.2.3. *Thiol oxidation assay.* Bioavailability of thiols in the media was measured using Ellman's assay, which is based on the reaction of sulphydryl-containing radiation protectors with 5,5′-dithiobis-(2-nitrobenzoic acid) (DTNB or Ellman's reagent, Sigma, St Louis, MO). Our protocol involved a modification of methods described by Held and Melder (1987).

Briefly, to simulate the conditions of studies with JANUS or AFRRI neutrons, exponential or plateau cultures of C3H/10T½ cells were used as described above for transformation experiments. Designated thiols were added at the final concentration of 1 mM to serum-containing custom-made medium (10% fetal bovine serum, 90% Eagle's basal medium, standard composition, but without phenol red indicator). Cultures were incubated in the presence of drugs at 37°C. At varying intervals of up to 5 h, 0·1 or 1 ml medium samples were withdrawn from flasks. The sulphydryl content remaining in medium was determined by the addition of 10 µl of 10 mM DTNB in phosphate buffer to the reaction sample. The total volume of the reaction solution was 1 ml with a pH of 7·0–7·4. After 6 min, during which the colour develops after reaction with DTNB due to the liberated *p*-nitrothiophenol anion, the increase in absorbance at 412 nm was measured with a spectrophotometer (Ellman 1959, Suzuki *et al.* 1990). Standard curves were generated with glutathione. The thiol content in medium from non-drug control flask was measured and found to be negligible compared to medium that did not come in contact with cells.

2.3. *Neutron irradiations*

Characteristics of the ANL and AFRRI fission neutron sources were previously described (Marshall and Williamson 1985, Zeman *et al.* 1988). Both JANUS and TRIGA reactors generate neutrons with average energy of <1 MeV, and γ-contamination of <5%. In our studies of the radioprotective effects of WR-1065 with TRIGA neu-

trons, irradiations were performed using a dose-rate of 0·1 Gy min^{-1} at doses of $<0{\cdot}9$ Gy, and a dose-rate of 0·3 Gy min^{-1} at doses $\geq 0{\cdot}9$ Gy, so that all exposure times were <10 min. In experiments on the radioprotective effects of WR-151326 with JANUS neutrons, all irradiations were performed using a dose-rate of 0·25 Gy min^{-1} (Grdina *et al.* 1989a).

2.4. *Data analysis*

The thiol oxidation data pooled from individual experiments were analysed by log-linear regression, and half-life times ($T_{\frac{1}{2}}$) for autoxidation of each compound in medium were expressed as a reciprocal of the slope times ln 2. The standard errors for the $T_{\frac{1}{2}}$ values were calculated from the slope variance.

Pooled sets of dose-response data on cell survival with or without the WR thiol were analysed using a single linear-quadratic equation with a least-squares fit.

Quantitative analysis of dose-response curves for cell transformation was performed by the simultaneous fitting of transformation data obtained with neutrons alone and in combination with a WR compound. The protection against neutrons, expressed as a dose-modifying factor (DMF), was calculated for WR-1065 and WR-151326 from data obtained with and without a radioprotector present. We used a modification of the three-parameter method, originally described for determining oxygen enhancement ratios from survival data (Pike and Alper 1965, Harrison and Balcer-Kubiczek 1980). Briefly, sets of observations with or without a radiation protector were treated as if there were a common intercept for both sets of data. Two linear dose-response curves were then described by three parameters (a common intercept and two slopes), instead of the four (two intercepts and two slopes), needed for fitting a straight line to each set of observations separately by the standard method. The simultaneous three-parameter fit is a statistically rigorous and efficient means for determining protection factors as the ratio of slope for the radiation-only curve to the slope of each radioprotector curve. The standard error for DMF was determined by a slope variance ratio. Details of required procedures, including a test for the sufficiency of the common intercept, were similar to those described in Pike and Alper (1964). Accordingly, for each pooled set of the data with and without a protector, the three-parameter fit was compared with the four-parameter fit by the F-ratio. For the data presented here, no gain in the precision of the slope estimates resulted by adding a fourth parameter.

3. Results

3.1. *Thiol oxidation studies*

The spontaneous oxidation of a variety of sulphydryl compounds in media has been studied by other investigators (Held and Melder 1987, Suzuki *et al.* 1990), but none of these data were previously obtained for C3H/10T½ cells and/or WR-1065 or WR-151326. The rate of thiol oxidation *in vitro*, which affects protector efficacy, may depend on several factors, including type of media, buffer, cell density, proliferative state and type of cells, as well as the nature and concentration of the thiol (Biaglow *et al.* 1984, Held and Melder 1987). Our purpose was to estimate thiol levels in medium above the cells at the time of neutron irradiation, replicating as closely as possible the conditions described above for transformation experiments. Two other well-studied thiols, glutathione and cysteine, were included for comparison with the literature data (Biaglow *et al.* 1984, Held and Melder 1987).

Although the between-experiments values varied considerably, the hierarchy of autoxidation rates of each thiol, shown in Figure 1, was retained in all experiments. There was no clear difference between the rates measured for a given thiol in the presence of exponential or plateau cultures, indicating a secondary importance of the proliferative state of cells.

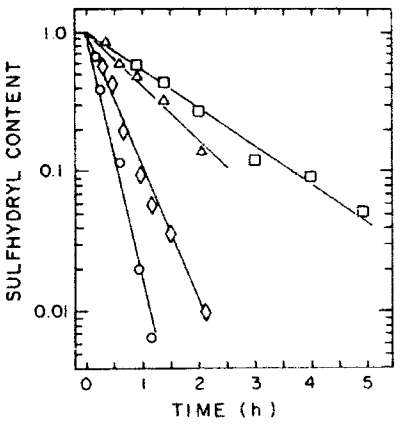

Figure 1. Spontaneous oxidation of glutathione (□), WR-151326 (△), cysteine (◇) and WR-1065 (○) at 37°C measured in the presence of C3H/10T½ cells. Drugs were prepared at 1 mM in complete medium without phenol red indicator. Sulphydryl concentrations were measured at times indicated on the abscissa. Shown are values relative to the maximum. Solid lines are the best fit to the data pooled from five to seven experiments with exponentially growing or density-inhibited cultures. Half-lives calculated from these data are shown in Table 1.

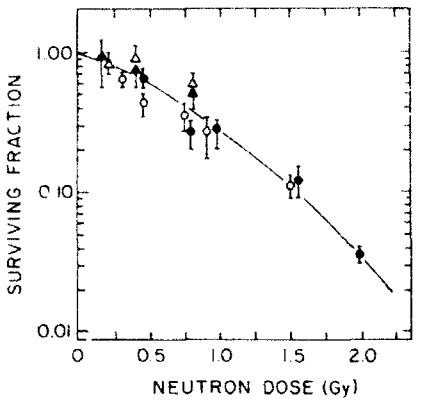

Figure 2. Survival of exponentially growing C3H/10T½ cells exposed to JANUS neutrons with (▲) or without (△) WR-151326, and density-inhibited C3H/10T½ cells exposed to AFRRI neutrons with (●) or without (○) WR-1065 at 37°C. Drugs were prepared at 1 mM in complete, serum-containing medium and were present before, during and after irradiation according to protocols shown in Figures 3 and 4 (inserts). The solid line is the best fit to the pooled data in Table 2.

Consistent with the pattern reported by Held and Melder (1987), glutathione oxidized slowly, while cysteine was oxidized rapidly. The rates of oxidation of WR-1065 were similar to the values for cysteine, while the rates for WR-151326 fell always between those for cysteine and for glutathione. The half-life for each thiol shown in Table 1 is the weighted mean of the $T_{\frac{1}{2}}$-values obtained from the time-course of oxidation measured in sequential samples from the same flask. Of special interest was a 7-fold difference in the $T_{\frac{1}{2}}$-values for WR-1065 and WR-151326, whose chemical structures are very similar (Table 1). Comparison of our present data with the literature results for glutathione and cysteine confirms that the thiol autoxidation rates vary considerably with the chemical composition of tissue culture medium, demonstrating the need for these measurements in individual model systems (e.g. Held and Melder 1987).

3.2. *Effect of WR thiols on cell survival*

Neutron survival data, obtained in experiments that involved protection protocols, are shown in Figure 2; for additional information see Table 2. A paired comparison of data points, with or without WR compound, indicated no apparent protective effect of WR-151326 or WR-1065 at 1 mM. These results agree with observations from related experiments with C3H/10T½ cells reported earlier (Hill *et al.* 1986). Neutron-only survival curves were consistent with previous results reported separately for JANUS and TRIGA neutron-irradiated C3H 10T½ cells (Hill *et al.* 1982, Balcer-Kubiczek and Harrison 1983, Balcer-Kubiczek *et al.* 1988, 1991). The lack of appreciable repair of potentially lethal or sublethal damage with neutrons and α-particles in doses <3 Gy was previously reported for several systems, including C3H/10T½ cells (Masuda 1971, Han and Elkind 1979, Suzuki *et al.* 1988, Balcer-Kubiczek *et al.* 1988, Hagasawa *et al.* 1990, reviewed by Hendry 1991). In contrast, significant changes in survival responses were observed during confluent holding of C3H/10T½ cells exposed to X-rays (Terasima *et al.* 1985, Nagasawa *et al.* 1990).

3.3. *Effect of WR thiols on cell transformation*

Neutron-transformation data for C3H/10T½ cells, obtained in experiments that involved protection protocols at the JANUS or TRIGA reactor facilities, are summarized in Table 2. High dose-rate data for exponential cultures agree well with corresponding data for plateau cultures. The present result supports our previous findings reported for the AFRRI neutrons (Balcer-Kubiczek *et al.* 1988, 1991). No independent JANUS data for plateau cultures are available for comparison.

The neutron-only data were pooled for calculation of dose modifying factors (Figures 3 and 4). Consistent with our previous transformation results, the dose–response curve fitted to the combined data obtained in this study was compatible with linearity in the low-to moderate range of neutron doses examined. The curve provided an initial slope estimate of about 7×10^{-4} transformants per surviving cell, in agreement with those reported previously for JANUS or TRIGA neutrons (Han and Elkind 1978, Hill *et al.* 1982, Balcer-Kubiczek *et al.* 1991).

An examination of the effect of WR-151326 or WR-1065 present during irradiation (Figures 3 and 4), demonstrates that both radioprotectors, at 1 mM, significantly reduced the incidence of transformation in C3H/10T½ cells. The WR-1065 protocol in experiments with AFRRI neutrons produced more protection (DMF $= 3{\cdot}23 \pm 0{\cdot}19$) than did a WR-151326 protocol with JANUS neutrons (DMF $= 1{\cdot}79 \pm 0{\cdot}08$).

4. Discussion

These present findings support the central result of Hill *et al.* (1986) that moderate thiol therapy can mitigate radiation-induced cell transformation *in*

vitro, and can do so at drug doses lower than that required for protection against cell killing. Further, our results are consistent with available data on protection against carcinogenic effects *in vivo* (Maisin *et al.* 1978, Grdina *et al.* 1991, Carnes and Grdina 1992).

In the present experiments, protection by WR-1065 and WR-151326 against neoplastic cell transformation was characterized by slope changes of transformation induction curves suggesting that, in combination with fission neutrons, WR-1065 and WR-151326 are dose-modifying; thus, no loss of protection should be anticipated at low neutron doses. Although this result is a consequence of the constraint that the data were fit to a linear model, nevertheless in the present case this model can be accepted as a good approximation. For our previous neutron data the quadratic component was negligible (Hill *et al.* 1982, Balcer-Kubiczek *et al.* 1991). For the limited neutron-plus-protector data, only a linear fit was justified in the statistical sense.

The slope values found for JANUS and TRIGA neutrons based on the individual data sets (Table 2) obtained in the present experiments with, respectively, exponential and plateau cultures of C3H 10T½ cells, were virtually the same as the initial slope found for exponential cultures of these cells in transformation experiments carried out at ANL or AFRRI before (Hill *et al.* 1982, Balcer-Kubiczek and Harrison 1983, concurrently (Balcer-Kubiczek *et al.* 1991, and after (Balcer-Kubiczek in preparation), the experiments with radioprotectors. When these different data subsets were analysed by the linear-quadratic model, differences among dose-linear terms were less than one standard error, and dose-quadratic terms were always negligible. This indicates that, without radioprotectors, the dose-response functions for transformation by ANL or AFRRI neutrons obtained with proliferating or stationary cultures are similar.

With regard to the relative efficacy of WR-1065 and WR-151326, some limited insights can be gained by comparing the corresponding thiophosphate derivatives, WR-2721 and WR-151327,

Table 2. Pooled data from experiments on neoplastic transformation and survival of C3H 10T½ cells exposed to 1 mM WR thiols and/or fission neutrons

Condition	Dose (Gy)	SF (PE)[c] ± SE	N[d]	X[d]	Y[d]	P[d]	$X/N \pm$ SE [e] $\times 10^2$	$T \pm$ SE [f] $\times 10^4$
AFFRI TRIGA fission neutrons								
No protector	Concurrent control	(0·63)	280	0	280	239	0	<0·15
	0·3	0·67 ± 0·12	174	11	163	225	6·3 ± 2·0	2·90 ± 0·87
	0·45	0·43 ± 0·08	191	14	179	307	7·3 ± 2·0	2·14 ± 0·66
	0·75	0·35 ± 0·08	229	31	199	282	13·5 ± 2·2	5·00 ± 0·93
	0·9	0·27 ± 0·10	337	53	288	299	15·7 ± 2·3	5·26 ± 0·78
	1·5	0·11 ± 0·02	138	34	108	228	24·6 + 4·8	10·78 ± 2·10
+ WR1065[a]	0	(0·58)	142	0	142	248	0	<0·28
	0·45	0·64 ± 0·11	203	2	201	247	0·98 ± 0·70	0·40 ± 0·20
	0·75	0·28 ± 0·08	103	8	96	397	7·8 ± 2·7	1·77 ± 0·72
	0·9	0·26 ± 0·06	310	12	299	317	3·9 ± 1·1	1·14 ± 0·36
	1·5	0·12 ± 0·03	335	41	296	353	12·2 ± 1·9	3·51 ± 0·58
	2·0	0·035 ± 0·01	230	38	202	311	12·2 ± 2·3	4·17 ± 0·79
Argonne Laboratory JANUS fission neutrons								
No protector	Historic control	(0·70)	2425	6	2419	244	0·3 ± 0·1	0·10 ± 0·04
	0·21	0·82 ± 0·12	207	7	200	228	3·4 ± 1·3	1·51 ± 0·57
	0·41	0·89 ± 0·12	158	11	149	227	7·0 ± 2·1	2·58 ± 0·87
	0·78	0·63 ± 0·08	146	24	124	275	16·4 ± 3·4	5·94 ± 1·27
+ WR151326[b]	0·21	0·88 ± 0·37	81	2	79	294	2·5 + 1·8	0·85 ± 0·52
	0·41	0·77 ± 0·25	54	2	52	216	3·7 ± 2·6	1·75 ± 1·33
	0·78	0·63 ± 0·21	49	6	43	378	12·2 ± 5·0	3·47 ± 1·37

[a] 1 mM WR-1065 added 30 min prior to neutron irradiation. Cells kept at 37°C, total exposure time 1 h.

[b] 1 mM WR-151326 added 10 min prior to neutron irradiation. Cells kept at 37°C, total exposure time 35 min.

[c] SF (PE), surviving fraction (plating efficiency).

[d] N, X, Y, P, total number of dishes, number of transformants of type 2 or 3 (Reznikoff *et al.* 1973b, IARC/NCI/EPA Working Group 1985), number of dishes without transformants, number of cells per dish corrected for plating efficiency of unirradiated cells, or surviving fraction and plating efficiency of irradiated cells.

[e] Transformation rate per dish (IARC/NCI/EPA Working Group 1985) and its standard error (Hieber *et al.* 1987).

[f] Transformation rate per survivor (Han and Elkind 1979) and its standard error (Balcer-Kubiczek *et al.* 1987).

for protection against high-LET radiations. For the endpoint of animal lethality, Steel *et al.* (1987) observed no marked difference in protection between WR-2721 and WR-151327 after AFRRI neutron irradiation. However, WR-151327 was more effective than WR-2721 in the study of Sigdestad *et al.* (1986) with two reactor-produced neutron fields (DOSAR, Health Physics Research Reactor at Oak Ridge National Laboratory, Oak Ridge TN, and JANUS) and with higher-energy cyclotron-produced neutrons (FERMILAB).

We do not have direct evidence that, at the equimolar concentrations, WR-1065 is more effective than WR-151326. Attempts to explain the observed differences in DMF for WR-1065 and WR-151326 in our experiments are hindered by uncertainty over the possible contributions of the pre-incubation period, the nature of the thiol and other aspects of experimental designs at ANL and AFRRI. Of these factors, the proliferative status of cells seems the less important, since no correlation between the effect of thiols and the cell cycle distribution was observed in the study of Murray *et al.* (1990). The latter also studied the development of radioprotection *in vitro* as a function of drug pretreatment time for various thiols, including WR-1065 and WR-151326, at 37°C. They found that the time-course of

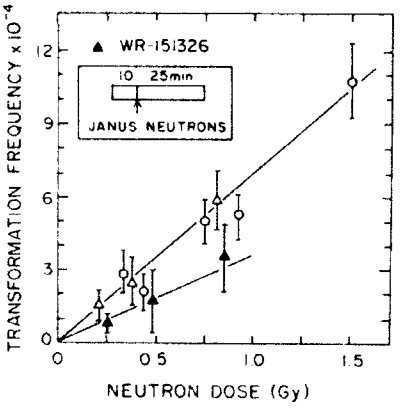

Figure 3. The effect of WR-151326 on cell transformation by fission neutrons. The neutron-only dose–response curve represents a fit to data for exponentially growing C3H/10T½ cells exposed to JANUS neutrons (△) and to density-inhibited C3H/10T½ cells exposed to AFRRI neutrons (○); ▲ = transformation frequencies measured with JANUS neutrons when WR-151326 at 1 mM was added 10 min before the irradiation. Solution for the three-parameter model: common intercept = $(-0{\cdot}013 \pm 0{\cdot}092) \times 10^{-4}$ transformants/surviving cell, slopes for neutron-only or in combination with WR-151326 are $(6{\cdot}89 \pm 0{\cdot}06) \times 10^{-4}$/Gy or $(3{\cdot}85 \pm 0{\cdot}31) \times 10^{-4}$ Gy, respectively. Goodness of fit: chi-square = 12·1, degrees of freedom = 9 ($p = 0{\cdot}79$).

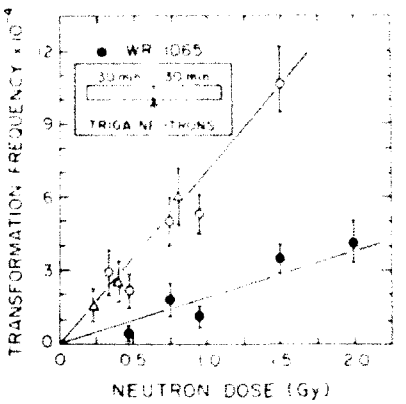

Figure 4. Effect of WR-1065 on cell transformation by fission neutrons. Transformation frequencies measured with AFRRI neutrons when WR-1065 at 1 mM was added 30 min before irradiation. Other details are the same as for Figure 3. Solution for the three-parameter model: common intercept = $(-0{\cdot}17 \pm 0{\cdot}08) \times 10^{-4}$ transformants surviving cell, slopes for neutron-only or in combination with WR-1065 are $7{\cdot}07 \pm 0{\cdot}11) \times 10^{-4}$ Gy or $(2{\cdot}19 \pm 0{\cdot}22) \times 10^{-4}$ Gy, respectively. Goodness of fit: chi-square = 16·2, degrees of freedom = 11 ($p = 0{\cdot}87$).

protection development for these WR thiols was similar; a minimum 30-min pretreatment was required for each of the drugs before reaching a full protection level. Compared with WR-1065, a 1·5-fold higher extracellular concentration of WR-151326 was needed to achieve the same level of protection. These differences, which are consistent overall with our results, could be attributed, at least in part, to differences in the kinetics of the redistribution of the thiols (Table 1 and Figure 1). Those drugs that oxidize rapidly (cysteine, WR-1065) also reach an equilibrium of intracellular and extracellular compartments rapidly. In some cases equilibrium is complete within 1 min (Calabro-Jones *et al.* 1988, Dennis *et al.* 1989). While the supporting data are limited, the corresponding trend for thiols that oxidize slowly (glutathione, WR-151326) can be expected. These considerations make it tempting to speculate that the lower DMF we observed for WR-151326 could be due to a lower intracellular drug concentration, due in turn to the pharmacology of the compound coupled with the shorter preirradiation drug exposure time.

For cell killing and animal lethality, thiol protective capability was reported to decrease with an increase in LET in some studies (Sigdestad *et al.* 1986, Steel *et al.* 1987), but a more complex picture emerged from the study of the protection by WR-2721 against the effects of high-energy heavy-charged particle beams (Afzal and Ainsworth 1987). A similar conclusion regarding protection in regard

to LET can tentatively be reached by comparing our present neutron data in Figure 4 with previously determined transformation data for WR-1065 and low-LET radiation (Hill *et al.* 1986). Although WR-1065 afforded significant radioprotection against fission neutron radiation (DMF ≈ 3), a protection factor of about 6 was reported for this thiol, based on Hill's transformation results with a lower LET source (Grdina and Sigdestad 1989). We note, however, that several cellular studies showed WR-1065 to give an equally effective protection against mutation after exposure to low- and high-LET irradiations (Grdina *et al.* 1985a,b, 1989a,b, Nagy and Grdina 1986, Hill *et al.* 1986, Nagy *et al.* 1986, Grdina and Sigdestad 1989). Clearly, the efficacy of WR compounds to protect against neoplastic effects should be further investigated over a broad range of LET.

In summary, the emerging evidence for protection against mutation and carcinogenesis provides a more optimistic picture for aminothiol applications than did the earlier data for protection against acute cytotoxicity. Further investigation is warranted of whether radioprotectors can be administered at low doses so that side-effects can be avoided, and whether they can also be administered *after* unexpected exposures.

Acknowledgements

This work was supported by Grants CA 50629 and CA 42808 from the National Cancer Institute, and by the Armed Forces Radiobiology Research Institute, Defense Nuclear Agency, under work unit 4620. The authors thank Dr Eric Kearsley for his helpful discussions and comments, and Dr Nincita Lomax for supplying WR-1065 for this study. We wish to acknowledge Ms D. M. Mosbrook (AFRRI), Mr W. A. McCready and Mr J. Klaff (UMAB School of Medicine) for expert technical assistance, Mr G. Holmblab for the efficient running of the JANUS reactor, and Ms B. A. Williams for the dosimetric support at AFRRI.

References

Afzal, S. M. J. and Ainsworth, E. J., 1987. Radioprotection of mouse colony forming units-spleen against heavy-charged particle damage by WR2721. *Radiation Research*, **109,** 118–126.

Aguilera, J. A., Newton, G. L., Fahey, R. C. and Ward, J. F., 1992. Thiol uptake by Chinese hamster cells and aerobic radioprotection as a function of the net charge on the thiol. *Radiation Research*, **130,** 194–204.

Balcer-Kubiczek, E. K. and Harrison, G. H., 1983. Oncogenic transformation of C3H 10T½ cells by X-rays, fast-fission neutrons, and cyclotron-produced neutrons. *International Journal of Radiation Biology*, **44,** 377–386.

Balcer-Kubiczek, E. K. and Harrison, G. H., 1991. 'Inter silvas Academi quaerere verum': reply to Letter to the Editor by M. M. Elkind. *International Journal of Radiation Biology*, **59,** 1477–1482.

Balcer-Kubiczek, E. K., Harrison, G. H. and Thompson, B. W., 1987. Repair time for oncogenic transformation in C3H 10T½ cells subjected to protracted X-irradiation. *International Journal of Radiation Biology*, **51,** 219–226.

Balcer-Kubiczek, E. K., Harrison, G. H., Zeman, G. H., Mattson, P. J. and Kunska, A., 1988. Lack of inverse dose-rate effect on fission neutron induced transformation of C3H 10T½ cells. *International Journal of Radiation Biology*, **54,** 531–536.

Balcer-Kubiczek, E. K., Harrison, G. H. and Hei, T. K., 1991. Neutron dose-rate experiments at the AFRRI nuclear reactor. *Radiation Research*, **128,** S65–S70.

Biaglow, J. E., Issels, R. W., Gerweck, L. E., Varnes, M. E., Jacobson, B., Mitchell, J. B. and Russo, A., 1984. Factors influencing the oxidation of cysteamine and other thiols: implication for hyperthermic sensitization and radiation protection. *Radiation Research*, **100,** 298–312.

Calabro-Jones, P. M., Aguilera, J. A., Ward, J. F., Smoluk, G. D. and Fahey, R. C., 1988. Uptake of WR-2721 derivatives by cells in culture: identification of the transported form of the drug. *Cancer Research*, **48,** 3634–3640.

Carnes, B. A. and Grdina, D. J., 1992. *In vivo* protection by the aminothiol WR-2721 against neutron-induced carcinogenesis. *International Journal of Radiation Biology*, **61,** 567–576.

Corn, B. W., Liber, H. L. and Little, J. B., 1987. Differential effects of radical scavengers on X-ray-induced mutation and cytotoxicity in human cells. *Radiation Research*, **109,** 100–108.

Dennis, M. F., Stratford, M. R. L., Wardman, P. and Watts, R. R., 1989. Increase in intracellular cysteine after exposure to dithiothreitol: implications in radiobiology. *International Journal of Radiation Biology*, **56,** 877–883.

Ellman, G. L., 1959. Tissue sulfhydryl groups. *Archives of Biochemistry and Biophysics*, **82,** 70–77.

Grdina, D. J. and Sigdestad, C. P., 1989. Radiation protectors: the unexpected benefits. *Drug Metabolism Reviews*, **20,** 13–42.

Grdina, D. J., Peraino, C., Carnes, B. A. and Hill, C. K., 1985a. Protective effect of S-2-(3-aminopropylamino) ethyl phosphorothioic acid against induction of altered hepatocyte foci in rats treated once with gamma radiation within one day after birth. *Cancer Research*, **45,** 5379–5381.

Grdina, D. J., Nagy, B., Hill, C. K., Wells, R. L. and Peraino, C., 1985b. The radioprotector WR1065 reduces radiation-induced mutations at the hypoxanthine phosphoribosyl transferase locus in V79 cells. *Carcinogenesis*, **6,** 929–931.

Grdina, D. J., Sigdestad, C. P. and Carnes, B. A., 1989a. Protection by WR1065 and WR151326 against fission-neutron induced mutation at the hgprt locus in V79 cells. *Radiation Research*, **117,** 500–510.

Grdina, D. J., Nagy, B., Hill, C. K. and Sigdestad, C. P., 1989b. Protection against radiation-induced mutagenesis in V79 cells by 2-[(aminopropyl)-

amino]ethanethiol under conditions of acute hypoxia. *Radiation Research*, **117,** 251–258.

GRDINA, D. J., WRIGHT, E. J. and CARNES, B. A., 1991. Protection by WR-151327 against late effects damage from fission-spectrum neutrons. *Radiation Research*, **128,** S124–S127.

HAN, A. and ELKIND, M. M., 1979. Transformation of mouse C3H 10T½ cells and single and fractionated doses of X-rays and fission-spectrum neutrons. *Cancer Research*, **39,** 123–130.

HARRISON, G. H. and BAECER-KUBICZEK, E. K., 1980. The oxygen enhancement ratio for d(80 + Be) + La and d(80 + La + Be) neutrons. *Radiation Research*, **83,** 90–98.

HEED, K. D. and MELDER, D., 1987. Toxicity of the sulfhydryl-containing radioprotector dithiothreitol. *Radiation Research*, **112,** 544–554.

HENDRY, J. H., 1991. The slower cellular recovery after higher-LET irradiations, including focuses on the quality of DNA breaks. *Radiation Research*, **128,** S114–S116.

HIEBER, L., PONSEL, G., ROOS, H., FENN, S., FROMKE, E. and KELLERER, A. M., 1987. Absence of a dose rate effect in the transformation of C3H 10T½ cells by α-particles. *International Journal of Radiation Biology*, **52,** 859–869.

HILL, C. K., BUONOGURO, F. M., MYERS, C. P., HAN, A. and ELKIND, M. M., 1982. Fission-spectrum neutrons at reduced dose rate enhance neoplastic transformation. *Nature*, **298,** 67–68.

HILL, C. K., NAGY, B., PERAINO, C. and GRDINA, D. J., 1986. 2-[Aminopropyl ethanethiol (WR-1065) is anti-neoplastic and anti-mutagenic when given during ^{60}Co gamma-ray irradiation. *Carcinogenesis*, **7,** 665–668.

IARC/NCI/EPA WORKING GROUP, 1985. Cellular and molecular mechanisms of cell transformation and standardization of transformation assays of established cell lines for prediction of carcinogenic chemicals: overview and recommended protocols. *Cancer Research*, **45,** 2395–2399.

LIVESY, J. C. and REED, D. J., 1987. Chemical protection against ionizing radiation. *Advances in Radiation Biology*, **13,** 285–341.

MAISIN, J. R., MATTELIN, G. and LAMBIET-COLLIER, M., 1978. Chemical protection against the long-term effects of a single whole-body exposure of mice to ionizing radiation. II. Cause of death. *Radiation Research*, **74,** 415–435.

MARSHALL, I. R. and WILLIAMSON, F. S., 1985. Microdosimetric spectra measurements of JANUS neutrons. *Radiation Protection Dosimetry*, **13,** 111–113.

MARQUARDT, H., SAPOZINK, M. D. and ZEDECK, M. S., 1974. Inhibition by cysteamine-HCl on oncogenesis induced by DMBA without affecting toxicity. *Cancer Research*, **34,** 3387–3390.

MASUDA, K., 1971. Survival of synchronized L cells irradiated with 14 MeV neutrons. *International Journal of Radiation Biology*, **20,** 85–86.

MILAS, L., HUNTER, N., STEPHENS, C. L. and PETERS, L. J., 1984. Inhibition of radiation carcinogenesis by S-2-(3-aminopropyl-amino) ethyl phosphorothioic acid. *Cancer Research*, **44,** 5567–5569.

MORI, T., WATANABE, M., HORIKAWA, M., NIKAIDO, P., KIMURA, H., AOYAMA, T. and SUGAHARA, T., 1983. WR-2721, its derivative and their radioprotective effects on mammalian cells in culture. *International Journal Radiation Biology*, **44,** 41–53.

MURRAY, D., PRAGER, A., VANANKEREN, S. C., ALTSCHULER, E. M., KERR, M. S., TERPY, N. H. A. and MILAS, L., 1990. Comparative effect of the thiols dithiothreitol, cysteamine and WR-151326 on survival and on the induction of DNA damage in cultured Chinese hamster ovary cells exposed to gamma radiation. *International Journal of Radiation Biology*, **58,** 71–91.

NAGASAWA, H., ROBERTSON, J. and LITTLE, J. B., 1980. Induction of chromosomal aberrations and sister chromatid exchanges by alpha particles in density-inhibited cultures of 10T½ and 3T3 cells. *International Journal of Radiation Biology*, **57,** 735–744.

NAGY, B. and GRDINA, D. J., 1986. Protective effects of 2-[aminopropyl amino]ethanethiol against bleomycin and nitrogen mustard-induced mutagenicity in V79 cells. *International Journal of Radiation Oncology, Biology and Physics*, **12,** 1475–1478.

NAGY, B., DALE, P. J. and GRDINA, D. J., 1986. Protection against cis-diamine-di-chloroplatinum II cytotoxicity and mutagenicity in V79 cells by free radical scavenger 2-[aminopropyl amino]-ethane-thiol. *Cancer Research*, **46,** 1132–1135.

NASSI-CALO, L., MELLO-FILHO, A. C. and MENEGHINI, R., 1989. o-Phenanthroline protects mammalian cells from hydrogen peroxide-induced gene mutation and morphological transformation. *Carcinogenesis*, **10,** 1055–1057.

PATT, H. M., TYREE, E. B., STRAUBE, R. L. and SMITH, D. E., 1949. Cysteine protection against X-irradiation. *Science*, **110,** 213–214.

PIKE, M. C. and ALPER, T., 1964. A method for determining dose-modification factors. *British Journal of Radiology*, **37,** 458–462.

REZNIKOFF, C. A., BRANKOW, D. W. and HEIDELBERGER, C., 1973a. Establishment and characterization of a cloned line of C3H mouse embryo cells sensitive to post-confluence inhibition of cell division. *Cancer Research*, **33,** 3231–3238.

REZNIKOFF, C. A., BERTRAM, J. S., BRANKOW, D. W. and HEIDELBERGER, C., 1973b. Quantitative and qualitative studies of chemical transformation of cloned line of C3H mouse embryo cells sensitive to postconfluence inhibition of cell division. *Cancer Research*, **33,** 3239–3249.

SCHWARTZ, J. L., GIOVANAZZI, S. M., KARRISON, T., JONES, C. and GRDINA, D. J., 1988. 2-[Aminopropyl amino]-ethanethiol-mediated reductions in ^{60}Co gamma-ray and fission-spectrum neutron-induced chromosome damage in V79 cells. *Radiation Research*, **113,** 145–157.

SIGDESTAD, C. P., GRDINA, D. J., CONNOR, A. M. and HANSON, W. R., 1986. A comparison of radioprotection from three neutron sources and ^{60}Co by WR-2721 and WR-151327. *Radiation Research*, **106,** 224–233.

SMOLUK, G. D., FAHEY, R. C., CALABRO-JONES, P. M., AGUILERA, J. A. and WARD, J. F., 1988. Radioprotection of cells in vitro by WR-2721 and derivatives: form of the drug responsible for protection. *Cancer Research*, **48,** 3641–3647.

STEEL, L. K., JACOBS, A. J., GIAMBARRESI, L. J. and JACKSON III, W. E., 1987. Protection of mice against fission neutron irradiation by WR-2721 or WR-151327. *Radiation Research*, **109,** 469–478.

SUZUKI, S., NGO, F. Q. H., KOUMOUNDOUROUS, L., TOURDOT, K. R. and ROBERTS, W. K., 1988. Survival responses and potentially lethal damage repair of normal 10T½ and its transformed TCL15 cells after irradiation with 43-MeV proton-produced neutrons. *Acta Oncologica*, **27,** 281–287.

SUZUKI, Y., LYALL, V., BIBEE, T. C. L. and FORD, G. D., 1990. A modified technique for the measurement of sulfhydryl groups oxidized by reactive oxygen intermediates. *Free Radical Biology and Medicine*, **9,** 479–484.

TERASIMA, T., YUSUKAWA, M. and KIMURA, M., 1985. Nec-

plastic transformation of plateau-phase mouse 10T½ cells following single and fractionated doses of X-rays. *Radiation Research*, **102,** 367–377.

VAN ANKEREN, S. C., MILAS, L. and MURRAY, D., 1989, Protection of cultured Chinese hamster cells by the aminothiol WR-255591 from the lethal and DNA-damaging effects of fast neutrons. *International Journal of Radiation Oncology, Biology and Physics*, **16,** 1205–1208.

ZEMAN, G. H., DOOLEY, M., EAGLESON, D. M., GOODMAN, J., SCHWARTZ, R. B., EISENHAUER, C. M. and MCDONALD, J. C., 1988, Intercomparison of neutron dosimetry techniques at the MERR TRIGA reactor. *Radiation Protection Dosimetry*, **23,** 317–320.

MILITARY MEDICINE, 157, 10:548, 1992

Behavioral Differences of Irradiated Persons Associated with the Kyshtym, Chelyabinsk, and Chernobyl Nuclear Accidents

LTC Daniel L. Collins, USAF

Three nuclear accidents besides Chernobyl have occurred in the former Soviet Union. The accidents occurred around Kyshtym and Chelyabinsk in the Ural Mountains between 1949 and 1967 and contaminated over one-half million people. The health ministries are now interested in the data previously collected on these irradiated populations in order to examine the health (e.g., psychological, hereditary, genome damage, etc.) implications of long-term radiation exposure.

Introduction

In September 1991, 3 weeks after the attempted putsch, I represented the Defense Nuclear Agency/Armed Forces Radiobiology Research Institute (DNA/AFRRI) as part of an official contingent to Moscow and St. Petersburg, Russia. I met numerous scientists who were and are currently involved in all the nuclear accidents that occurred in their country. The majority of the data contained in this report comes from discussions and briefings. In addition, on December 2, 1991, several scientists from the Institute of Biophysics of the USSR Ministry of Health, Chelyabinsk Branch Office, who have studied the Kyshtym and Chelyabinsk nuclear accidents for decades, presented human data that have never before been released to the West. Consequently, the radiation units of measurement reflect those provided by different scientists and vary (sieverts, roentgen, etc.) throughout the paper.

The radiation situations in the area of Kyshtym and Chelyabinsk are unique because over the last 40 years masses of people have been exposed to ^{90}Sr in the food and water chain. Basic dosimetry investigations have focused on the doses of ^{90}Sr. The first estimates of activity were from nuclide measurements taken from the river sediment. These analyses began in 1951, 1.5 years after the accident occurred.

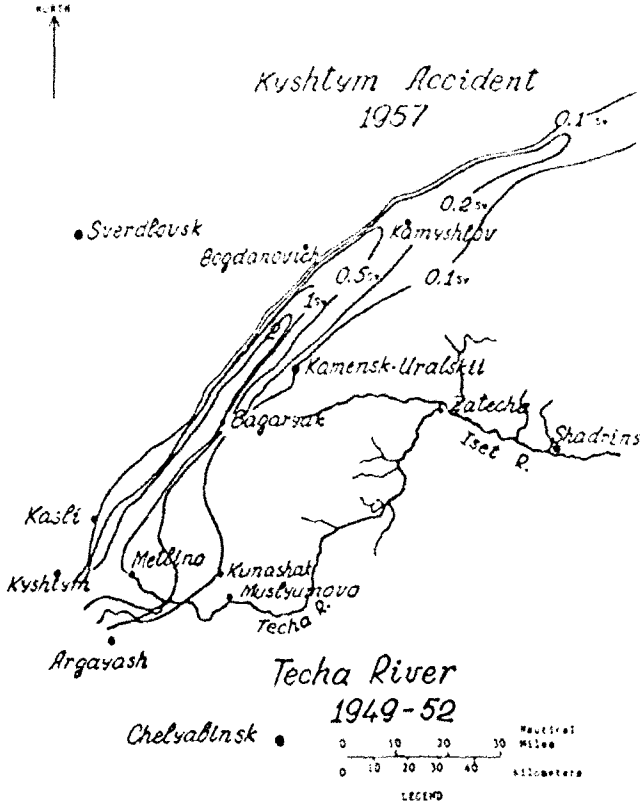

Fig. 1. The Kyshtym/Chelyabinsk region of the FSU.

Nuclear Accidents in the Former Soviet Union (FSU)

In 1948, the USSR began operating a plutonium production plant called Mayak in the Kyshtym/Chelyabinsk region (Fig. 1). In 1949–1951, an accident released 3 million Ci of radiation into the Techa River. A second accident occurred in 1957, southeast of Kyshtym, when improperly ventilated storage tanks exploded, and 20 million Ci of radioactive waste were released into the atmosphere. The storage complex was located 1.5 km from the reprocessing plant and consisted of 60 underground storage tanks. The radionuclide composition of the fallout indicated it was comparatively fresh nuclear waste from reprocessing, stored for not more than 6–7 months, from which not only uranium and plutonium but also cesium had been removed.[1]

Due to the confined nature of the blast, the majority (90%) of the nuclear waste was dispersed near the tanks in the form of a liquid pulp.[2] However, a plume cloud with an activity of 2 million Ci dispersed its radioisotopes over the area shown on the map in Figure 1. The contaminants from the plume cloud were confined to the Chelyabinsk and the Sverdlovsk provinces. Before the accident, more than 28,000 people lived in the 38 villages along the Techa River. Contamination levels of ^{90}Sr exceeded 0.01 Ci/km^2 and were distributed over 23,000 km^2. The highest concentration of ^{90}Sr was located in an area known as Metlino, located near Kyshtym. The doses in the Metlino area averaged 3 Sv/km^2. The dispersion of radioactivity from the plume cloud is shown in Figure 1.

In the spring of 1967, further contamination of the Techa River occurred when a severe drought caused the highly radio-

Armed Forces Radiobiology Research Institute, Bethesda, MD 20889.

This manuscript was received for review in February 1992. The revised manuscript was accepted for publication in June 1992.

active Lake Karachay to recede, which allowed the wind to blow the contaminated silt and sand particles over the Kyshtym, Chelyabinsk, and Techa River areas. This lake is located west of Argayash. A total of 600 Ci ^{137}Cs and ^{90}Sr was released by the air transfer of sand particles from the Lake Karachay beach. Radiation was primarily gamma radiation along the Techa River and reached 5 R/hour. The average activity along the Techa River was 10^{-5} Ci/l of water. A massive 3-month clean-up effort occurred between the summer and autumn of 1967 and resulted in a 10-fold decrease in radiation levels. This occurred because the Soviets removed a considerable amount of the water from the contaminated reservoir located near the Metlino area.

Discussion

In the aftermath of the Kyshtym accident, if a village was found to be radioactive it was scheduled for evacuation as political circumstances dictated. In addition to the area dosimetry, which measured river sediment for contamination, human dosimetry began in the summer of 1951, measuring body excrement and contaminated clothes. It should be noted that during this 1.5-year hiatus between the accident and the beginning of dosimetry measurements, the people were neither informed of the accident nor of their internal or external exposure to any form of ionizing radiation. Consequently, all the food and water consumed during this time period was contaminated with radiation isotopes.

In an attempt to further quantify dosimetry from the Kyshtym and Chelyabinsk accidents, the bones of deceased persons were exhumed during the 1960s and resulted in the creation of a data base that reflected their "lifetime" exposures to ^{90}Sr. In 1974, Soviet scientists created a data base using live subjects to determine their whole-body doses of ^{90}Sr. The methodology used to make these determinations from the living Techa River residents included dosimetric examinations of urine samples and frontal lobes. The urine samples were obtained from 1,500 residents living beside the Techa River. The 12,500 living subjects involved in the frontal lobe study also resided along the Techa River. The teeth of 15,000 living subjects in this area were also examined for ^{90}Sr doses. The location from which these residents were evacuated is known today as the "Post Box Chelyabinsk-40" area.[1]

The dosimetry revealed that 1,000 people living by the Techa River had greater than 1 μCi of ^{90}Sr in their bones. Further analyses showed that those people born in 1932–1933, who were teenagers during the first accident, accumulated three to five times more ^{90}Sr than did those who were adults at the time of the first accident. The maximum reading of 6 μCi per person occurred in those individuals who were teenagers during the time of the first accident. Measuring the metabolism measurements of ^{90}Sr and overlaying them with all three previous accidents provided the following results. The dose levels averaged 0.42 Sv along the Techa River to the southwest, 0.52 Sv along the middle portion of the Techa River, and 2 Sv near Chelyabinsk (Akleev, 1991, personal conversation). The three accidents affected 437,000 people. Of these, 1,200 people obtained 200 rems over a 2-year period. In addition, some people received doses of up to 400 rems to their bone cells.

Relocation of Irradiated Victims

Of the 38 villages along the Techa River before the accident, only 4 are safe to inhabit today. Analyses of the people along the Techa River revealed decreased leukocyte and immune system functioning. This is attributed to the time period when people drank the radioactive water and ate contaminated food daily before their relocation. The time range for relocation spanned 1 week to 11 years for the evacuation of all residents from the 34 contaminated villages along the Techa River.[1] The total number of people relocated during this time exceeded 10,500. After the people were relocated, the villages were incinerated to ensure that no human habitation would occur in this highly radioactive area. However, the heat and smoke created by the incineration process further spread the contamination over the streams, rivers, and lakes, which exacerbated the already contaminated food chain for animals and humans.

Although some of the residents living in the contaminated areas experienced a protracted relocation, others were quickly evacuated out of necessity. Following the Kyshtym accident, 1,154 residents of Kasli, near Kyshtym, were removed 7–10 days after the accident due to extremely high ^{90}Sr levels. People who were removed during this time now have twice the acute myeloid leukemias that the control groups have exhibited.

On a historical note, the construction of the radioactive facilities was conducted between 1945–1948 by approximately 70,000 inmates from the nearby gulag (prison). The Kyshtym location is N 55-44, E 60-35; the Kyshtym restricted area covered 2,700 sq km and contained eight lakes with interconnecting watercourses. The Kyshtym atomic plant was built in a tunnel, which extended beneath a river, with only a smokestack visible from the air or ground. During the construction process, one lake was drained, a building was built on its lakebed with cement, rubber, and lead, and the lake was refilled.[1] During the Cold War, several high-altitude reconnaissance aircraft routinely photographed this area. In 1960, MAJ Francis Gary Powers was shot down by a surface-to-air missile while flying over the Kyshtym and Chelyabinsk atomic facilities.

Control Groups

Two control groups were selected for comparison purposes for this longitudinal field study of irradiated humans. The control groups were located just south of this area and were not exposed to the radiation. The first control group consisted of 34,000 persons of the same socioeconomic status as the victims. They did not have access to the contaminated Techa River and were not contaminated by the plume cloud or the other accidents. The second control group consisted of all nonirradiated people in the greater Chelyabinsk province (i.e., those not living in or near the contaminated city of Chelyabinsk). The control groups within the nonradioactive portions of the Chelyabinsk province consisted of 1.5 million people. The Chelyabinsk Ministry of Health's data base has resulted from an ongoing research project over the last 40 years. The following information is a summary compiled from 33 years of data collection (Akleev, 1991, personal conversation).

Impact of Ionizing Radiation Accidents

Results showed significantly increased death rates along the Techa River over the last 33 years. Coefficients were described in terms of excessive risk per Gy. Stomach cancer rates were found to be two to three times greater than in survivors of Nagasaki and Hiroshima, breast cancer two times greater, and lung and esophageal cancers two to three times greater (Degteva, 1991, personal conversation). Research is in progress that examines the progeny of irradiated mothers for stillborn children, abortions, and miscarriages. Analyses thus far indicate a significantly greater number of birthing complications in the irradiated mothers than in the control groups. Today, near the Kyshtym reservation, where the town of Kasli used to be, the ground surface still contains from 1,000 to 2,000 Ci/km^2 of ^{90}Sr.[1] It was from this area that 1,154 previous residents of Kasli were rapidly evacuated in a 7- to 10-day period following the accident. In the past, several types of military training maneuvers were routinely conducted in these contaminated areas.

In addition to the ionizing radiation doses, the victims of these three radiation accidents received little, if any, humanitarian support. The people also lived on less than a well-balanced diet and received only rudimentary medical care due to a pervasive lack of medical equipment. There were and still are only 50 hospital beds to care for the 500,000 irradiated people from the three irradiation accidents.

Contamination within the Kyshtym and Chelyabinsk Nuclear Facilities

In addition to the radiation exposure to the populace outside the atomic plants, intra-plant contaminations also occurred.[3,4] During these formative years of discovering how to work with radioactive material, several personnel were exposed to varying doses of ionizing radiation. Those individuals primarily at risk were maintenance and reactor personnel. This period was characterized by an operational focus that minimized safety concerns.[3] Several persons manifested the symptoms of acute radiation exposure following the start-up of these atomic facilities. Many persons also suffered symptoms of chronic radiation sickness, which resulted in the creation of a dosimetry program.[4]

The dosimetry programs recorded that numerous persons received 25 rem or more performing routine repair operations. The 25 rem or more doses were received in different time intervals (e.g., day, week, month, or year). Consequently, the rotation of these irradiated persons to other jobs not requiring further exposure resulted in an ever-increasing demand to fill the vacancies created by the safety-mandated transfers. The irradiated populations consist of approximately 6–7,000 persons who worked in these atomic plants before 1958.[4] The irradiated persons were divided into four groups: <25 rem, 25–100 rem, 100–400 rem, and >400 rem.[4] These irradiated individuals have been monitored for the last several decades to detect for the presence of any health anomalies.

One-half the workers at Chelyabinsk routinely received 100 rem during the late 1940s and early 1950s. Of this population, 8–9% of the persons who began work before 1958 and received doses greater than 100 rem died of cancer.[3] Cancer mortality was approximately 88% higher for those who received more than 100 rem than for those persons receiving less than 100 rem.[3,4]

Contamination within the Chernobyl Nuclear Plant

In addition to the early incidents of ionizing radiation exposure at Kyshtym and Chelyabinsk, more information regarding irradiated persons comes from the accident at the Chernobyl nuclear power plant. Following the accident at Unit 4, which occurred on April 26, 1986, the Soviets were faced with decisions that would disrupt and redirect the lives of persons living in the contaminated areas but also those working within the damaged Chernobyl plant. In order to minimize the danger of more contamination to the residents living in the greater Chernobyl area, several thousand persons working within the plant would be exposed to significant doses of ionizing radiation.

In order to remove the highly radioactive debris from the roof of Unit 4, it was necessary to use humans since the mechanical robots ceased to function due to the high radiation levels or became stuck in the radioactive debris scattered across the roof. Consequently, approximately 3,200 humans called "biorobots" were used to run onto the roof and throw the radioactive chunks of debris into the radioactive chasm left by the exploded reactor. The biorobots accomplished this task "by hand" since no other method worked. Their voluntary efforts allowed for access to this area and the sarcophagus construction to proceed.

Clean-up work needed to be carried out in other places that were much closer to the melted reactor core. Workers transited areas that were 3–4 m from the damaged core being protected by existing concrete and lead shielding. These workers were exposed to between 100 and 500 R/hour in the Block 4 area.[5]

Overall, more than 600,000 workers were involved in clean-up activities and the sarcophagus construction. Those involved in consolidating the radioactive waste from the "hot zone" into waterproof trenches were called "liquidators," and worked 2-week (or/off) shifts in the "hot zone."

It is interesting to note that the anticipatory stress of these people was high but so was their motivation and goal orientation. Many willingly and repeatedly exposed themselves to ionizing radiation by being a biorobot, a liquidator, or exploring the damaged reactor to discover the extent of damage and locate the missing core section. When the melted core section was finally located, the solidified mass of radiation resembled an "elephant's foot" and registered 10,000 R/hour.[5] These people had a modicum of control over whether or not they would be exposed (volunteering or not) and could largely regulate their exposure in this manner. The presence of this "perception of control" is very important to the maintenance of goal-oriented behavior. As we will see later on, the absence of this perception of control results in feelings of victimization and the cascade of negative psychological feelings that resulted in heated demonstrations, even though their exposure to ionizing radiation was far less than the Chernobyl workers.

Psychological Aspects of Nuclear Accidents

It is noteworthy that people living in the Kyshtym and Chelyabinsk areas are antinuclear as evidenced by the voluntary shutdown of two nuclear electrical generating reactors during June-July 1989.[1] Also, although billions of rubles (equivalent to millions of U.S. dollars) had been spent on the construction of a breeder reactor, it too was shut down approximately 3 years ago, an aftermath of the Chernobyl accident in 1986.[1] The reason given for shutting down both of these "nuclear" facilities after years of use and construction was the psychological animosity that existed in the people living in this contaminated region. A similar psychologically induced result occurred in Moscow, where a new, ready-to-be-used nuclear power plant was prevented from opening due to the public outcry. In addition, a nuclear power plant approximately 40 km south of St. Petersburg was closed to appease the psychologically upset populace. The impact that individual perceptions of ionizing radiation have on society is now being realized.[6,7]

In other parts of the FSU, specifically around the contaminated Chernobyl region, 35,000 people in the Belorus city of Gomel went on strike on April 26, 1991 to protest the fifth anniversary of the Chernobyl accident. Similarly, 60,000 people waving "nationalist" flags packed the square in front of the Sofia Cathedral in Kiev, the capital of the Ukraine, and demanded punishment for those responsible for the world's worst nuclear accident.[8,9] The Rukh press agency reported similar antinuclear demonstrations in Kiev, the western Ukrainian city of Lvov, and in the Belorus city of Minsk, as well as demonstrations elsewhere in the two republics that were the worst hit by fallout from the accident.[9]

Reasons for the psychological outcry among the Chernobyl victims are numerous.[10,11] The delays caused by scientific and political discussions finally resulted in the evacuation of 40,000 residents from an area where the contamination was 40 Ci/km^2. Furthermore, 10,000 people living in an area contaminated with 15-20 Ci/km^2 and 60,000 people living in an area with 5-15 Ci/km^2 were not allowed to relocate. It has been estimated that the rate of thyroid cancer will be 5 to 10 times the normal rate expected for 1.5 million Soviet citizens, leukemia rates among children in some areas of the Ukraine are 2 to 4 times normal levels, and the death rate for people working in the Chernobyl plant since the accident is 10 times what it was before the accident.[10] Furthermore, the scientific director of the zone surrounding the damaged Chernobyl power station estimated that the disaster has currently claimed many more lives than previously reported.[12] The best estimates to date regarding the Chernobyl death toll is that approximately 321 persons have perished as a direct result of radiation exposure.

Perhaps the worst aspect of these nuclear accidents is the omnipresent invisible threat and the continuing fear that the future is marred by irreversible cancer or genetic defects. This may have increased since the accidents, when radioactive fallout contaminated the environment, animals, and people. An undeniable and continual reminder for the residents is that all the timber in the affected areas is radioactively contaminated and cannot be used for furniture, for construction, or even for firewood.[13]

In addition to the forests, the waters of the Pripyat, Sozh, Nevsich, Iput, Besyoad, Braginka, Kolpita, and Pokot Rivers are carrying radioactive silt into the Dnepr River. The entire grid of power stations on the Dnepr River down to the Black Sea is threatened with 60 million tons of radioactive silt, as are the 60 million people in these regions.[13]

The anticipatory stress of these people is readily apparent and can be easily understood. Interestingly, according to an assessment by 200 scientists from 25 countries and 7 multinational organizations done for the United Nations International Atomic Energy Agency, stress-related illnesses are caused by lack of public information about the disaster and the mass evacuations that follow.[7] The psychological stress that followed in the surrounding areas outside the radioactive hot zones was "wholly disproportionate to the biological significance of the radioactive contamination."[7]

Even when no radiation is released from a nuclear accident, but only threatens, as was the case at Three Mile Island (TMI), the Kemeny Commission,[14] and other documents,[6,7,15,16] concluded that mental stress would be the main effect. The psychological findings could be criticized, if used alone, for their potential self-serving function. To avoid this perception neurochemical analyses that measured individual stress values were employed.[6,16,17] By using this multidisciplinary approach, we further clarified the adverse effects that exposure or potential exposure to ionizing radiation has on humans. Consequently, since increased stress and associated behavioral alterations occur from anticipation as occurred at TMI, and when actual exposure and deaths occur from radiation, the psychological, and behavioral actions of the FSU residents are easily understood.

Thus, the workers within the Kyshtym, Chelyabinsk, and Chernobyl nuclear facilities continued to voluntarily function despite knowing they would receive a significant dose of radiation. Conversely, the populace of the FSU was extremely concerned about being exposed to any dose of radiation, and vociferously demonstrated to close nuclear plants that "threatened" them with potential exposure.

The difference in behaviors between persons who were voluntarily exposed and those threatened with exposure to radiation is unexplainable unless we examine their different psychological "mind sets." The unifying principle to explain the behavioral differences between these two groups is a function of their control-oriented coping strategies when faced with their ionizing radiation stressor. The importance of this coping and control construct was first uncovered at TMI regarding individuals who experienced anticipatory stress to potential exposure to ionizing radiation. (Note: See Collins, 1984 for an indepth doctoral dissertation that describes this "human" control-oriented coping concept). The knowledge obtained about the nuclear accidents in the FSU has extended our understanding of this construct to parsimoniously explain the radically different behaviors of voluntarily irradiated persons from those involuntarily irradiated or experiencing potential radiation exposure.

Conclusion

The compilation of knowledge from this article regarding the different behaviors of irradiation-threatened or -exposed

persons results in wisdom to be used appropriately in the future by mission planners, medical personnel, response team members, special forces personnel, Federal Emergency Management Agency personnel, and others. This psychological and behavioral information can be appropriately used to our advantage in the future to better understand and predict the behaviors of highly trained and goal-oriented persons vs. the behaviors of a population that perceives itself as being victimized by radiation exposures. Failure to properly assimilate and apply these key psychological constructs, which explain otherwise counterintuitive behaviors, especially as they apply to potential nuclear adversaries (e.g., terrorists), will risk the use of these complex aspects of human behavior being used against us.

Consequently, the situation in the FSU is likely to become of major concern in future years as the future of 60 million people is adversely affected by the Chernobyl accident, and another million people (±) are adversely affected by the three accidents in the Kyshtym and Chelyabinsk areas. The psychological, physiological, and epidemiological implications of these disasters require further study.

Acknowledgments

I wish to thank the numerous scientists in the FSU for sharing the historical impact of these nuclear accidents. Thanks go to the AFRRI Director and Scientific Director, CAPT Robert L. Bumgarner, MC USN, and E. John Ainsworth, Ph.D., for funding this international research effort.

References

1. Medvedev Z. Bringing the skeleton out of the closet. Nuclear Engineering International 35:26–32. 1991
2. Burnazyan AI. The results of investigating and the experience of scientific studying the consequences of accidental contamination of territory by radioactive fission products. Moscow: Energoatomizdat (Reprint of a 1974 report previously classified in Russia). 1990
3. Marshall E. Radiation exposure: hot legacy of the Cold War. Science 249:474. 1990
4. Nikiperov BV, Lizlov AF, Koshurnikova NA. Experience with the first Soviet nuclear installation: irradiation doses and personnel health. Priroda February. 1990
5. Nova Series. Films for the Humanities. WGBH, Boston, MA. October 22. 1991
6. Collins DL. Stress at Three Mile Island: altered perceptions, behaviors and societal doctrine values. In: The Medical Basis for Radiation Accident Preparedness III: Psychological Perspectives. Edited by Ricks RC, Berger ME. New York: Elsevier Press. 1991 pp 71–79
7. International Chernobyl Project Technical Report. ISBN 92 0 129191 4. International Atomic Energy Agency. 1991. pp 277–413
8. Bohlen C. Top Chernobyl officials sentenced: nuclear power plant's director, five others sent to labor camp. The Washington Post July 30, 1987. p A1
9. Reuters News Service. Chernobyl rally attended by thousands. The New York Times April 27, 1990. p A6
10. Barringer F. Four years later, Soviets reveal wider scope to Chernobyl horror. The New York Times April 26, 1990. p 1
11. Lee GA. Chernobyl trial opens: accused officials blame design faults. The Washington Post July 8, 1987. p A1
12. Wise MZ. U.N. report blames stress, not radiation, for Chernobyl illnesses. The Washington Post May 22, 1991. p A25
13. Matukovsky N. The lessons of Chernobyl. Izvestia March 26, 1990. p 3
14. Kemeny JG. Report of the President's Commission on the Accident at Three Mile Island: The Need for Change: The Legacy of TMI. Washington. 1979
15. Collins DL. Persistence differences between Three Mile Island residents and a control group. AD-A145567. National Technical Information Service. Springfield, VA. 1984
16. Davidson LM, Baum A, Collins DL. Stress and control related problems at Three Mile Island. J Appl Psychol 12:349–359. 1982
17. Collins DL, Baum A, Singer JE. Coping with chronic stress at Three Mile Island: psychological and biochemical evidence. Health Psychol 2:149–166. 1983

Brain Research, 600 (1993) 106–110

BRES 18617

Involvement of superoxide dismutase and glutathione peroxidase in attenuation of radiation-induced hyperthermia by interleukin-1α in rats

Sathasiva B. Kandasamy [a], K. Sree Kumar [b] and Alan H. Harris [a]

[a] *Behavioral Sciences and* [b] *Radiation Biochemistry Departments, Armed Forces Radiobiology Research Institute, Bethesda, MD 20889-5145 (USA)*

(Accepted 6 October 1992)

Key words: Antioxidant enzyme; Hyperthermia; Hypothalamus; Interleukin; Radiation

Pretreatment with recombinant human interleukin-1α (rhIL-1α) 20 h before irradiation attenuates radiation-induced hyperthermia. Experiments were conducted to determine the role of antioxidant enzymes such as superoxide dismutase (SOD) and glutathione peroxidase (GSHPx) in rhIL-1α-induced attenuation of radiation-induced hyperthermia. Radiation exposure increased SOD and decreased GSHPx levels in the hypothalamus, while treatment with rhIL-1α increased GSHPx levels and had no effect on SOD levels. However, rhIL-1α and irradiation together increased hypothalamic SOD level but prevented the fall in GSHPx level. Our results suggest that attenuation of radiation-induced hyperthermia by rhIL-1α may involve stimulation of SOD and GSHPx because rhIL-1α treatment and irradiation together increased hypothalamic GSHPx and SOD levels, and intracerebroventricular administration of SOD and GSHPx attenuated the radiation-induced hyperthermia.

INTRODUCTION

Exposure of mammals to ionizing radiation causes the development of a complex, dose-dependent series of potentially fatal physiologic and morphologic changes known as acute radiation syndrome. Critical cellular biomolecules are directly damaged by ionizing radiation or indirectly damaged by radicals generated from the radiolysis of cellular water[11]. The free radicals thus produced can further interact among themselves or with cellular oxygen to perpetuate the radiation effects. Protection and/or recovery from the consequences of ionizing radiation have been investigated at different cellular and molecular levels. DNA repair mechanisms and chemical radioprotection afforded by thiol compounds have been studied extensively[8,12]. Radioprotection has also been reported to be conferred by endogenous radioprotective mediators such as interleukin and immunomodulatory radioprotectors that elicit interleukin production[24]. Antioxidant enzymes such as superoxide dismutase (SOD), glutathione peroxidase (GSHPx) and catalase, offer protection against ionizing radiation-induced oxidants[11]. Pretreatment with recombinant human interleukin-1α (rhIL-1α) protects mice from the lethal effects of ionizing radiation and it has been reported that the radioprotectant effect of rhIL-1α may involve induction of endogenous MnSOD[19].

Exposure of rats to ionizing radiation induces hyperthermia[14], and the hyperthermic response appears to be centrally mediated because irradiation of the head alone causes these effects whereas irradiation of the trunk only does not[14]. The hypothalamus is the most important site for thermoregulation. Radiation-induced hyperthermia is mediated by prostaglandin E_2 (PGE_2)[14]. Preliminary experiments demonstrated that when rats were pretreated with rhIL-1α 20 h before radiation exposure, rhIL-1α pretreatment attenuated radiation-induced hyperthermia[15]. Experiments confirmed rhIL-1α attenuation of radiation-induced hyperthermia, and the hypothalamic levels of SOD and GSHPx were then measured to determine if the attenuation is due to the stimulation of these substances.

MATERIALS AND METHODS

Drugs

RhIL-1α was a generous gift from Dr. P. Lomedico of Hoffman-LaRoche (Nutley, NJ) and was diluted to the desired concentration

Correspondence: S.B. Kandasamy, Behavioral Sciences Department, Armed Forces Radiobiology Research Institute, Bethesda, MD 20889-5145, USA. Fax: (1) (301) 2956552

in pyrogen-free saline before injection. PGE$_2$, GSHPx, SOD, and all other chemicals and reagents used were of the highest analytical grade, were obtained from Sigma (St. Louis, MO), and were dissolved in pyrogen-free saline before injection.

Experimental animals

Male Sprague Dawley rats (Crl:CD(SD)BRD; Charles River Breeding Laboratories, Kingston, NY) weighing 200–300 g were quarantined on arrival and screened for evidence of disease by serology and histopathology. The rats were housed individually in polycarbonate Micro-Isolator cages (Lab Products, Maywood, NJ) on autoclaved hardwood contact bedding (Beta Chip, Northeastern Products Corp., Warrensburg, NY) and were provided commercial rodent chow (Wayne Rodent Blok, Continental Grain Co., Chicago, IL) and water ad libitum. Animal holding rooms were kept at 21 ± 1°C with 50 ± 10% relative humidity on a 12-h light:dark cycle with no twilight.

Radiation exposure

Rats were placed in clear plastic well-ventilated containers for approximately 5 min before irradiation or sham irradiation. The animals were unilaterally irradiated (irradiation of rats when the radiation incidents from one side) to a total dose of 10 Gy (midline tissue) of 18.5 MeV (nominal) electrons using a linear accelerator (dose rate: 10 Gy/min; 1.875 pulses/s). Exposure of rats to 1–15 Gy of γ rays or electrons induces hyperthermia and a submaximal dose of 10 Gy was selected to study the mechanisms involved in radiation-induced hyperthermia[14]; therefore, the radiation dose of 10 Gy was selected for this study. Prior to irradiation, the radiation dose rate was measured using a 0.05 cc tissue-equivalent chamber (manufactured by Exradin, Inc) placed at the midline of a 5 cm diameter acrylic rat phantom. Exposure uniformity measurements showed that the dose rate varied by at most ±5% along the length of the phantom. All ionization chambers that were used have calibration factors traceable to the National Institute of Standards and Technology. Dosimetry measurements were performed following the AAPM Task Group 21 Protocol for the Determination of the Absorbed Dose from High-Energy Photon and Electron Beams[30].

The measurement of SOD and GSHPx in hypothalamus

Groups of rats were pretreated ip with 10 μg/kg of rhIL-1α or saline 20 h prior to radiation exposure (the dose of rhIL-1α was chosen from previous data[25] and a pilot study). The rats were decapitated after sham-irradiation or irradiation with high-energy electrons; the brains were removed, and the hypothalamus dissected, frozen, and stored at −70°C. All the tissues were stored for 2 weeks while analyses were in progress. For analysis, the tissues were suspended in 0.25 M sucrose and homogenized using a Potter-Elvehjem homogenizer. The homogenate was centrifuged for 10 min at 700 × *g*, and the supernatant was used for assaying SOD and GSHPx activity. SOD activity was assayed with the xanthine oxidase-cytochrome *c* method[31] and total and selenium-dependent GSHPx activity were determined in a coupled assay with glutathione reductase and NADPH[21].

Central administration of drugs

Rats were anesthetized with 1 ml/kg of a mixture of ketamine (50 mg/kg), xylazine (5 mg/kg), and acepromazine (1 mg/kg) given im and were placed in a stereotaxic apparatus (David Kopf Instruments, No. 320). A single cannula was inserted aseptically into the lateral ventricle according to the coordinates derived from the atlas of Pellegrino et al.[26]: 0.8 mm posterior to bregma, 2.5 mm lateral. The cannula was lowered until cerebrospinal fluid rose in the cannula. Dental acrylic cement was used to secure the cannula. Animals were allowed to recover for 2 days before they were used for experiments. At the end of the experiments, injection sites were verified histologically.

Measurement of body temperature

All experiments were performed at an environmental temperature of 22 ± 1°C, and body temperature was measured as described previously[13]. Briefly, the animals were placed in restraining cages 30 min before starting the experiments, and body temperatures were measured with thermistor probes (YSI series 700, Yellow Springs Co., Inc., Yellow Springs, OH) inserted approximately 6 cm into the rectum and connected to a datalogger (Minitrend 205). All animals were euthanized immediately after experiments with an overdose of carbon dioxide by inhalation.

Miscellaneous methods

Protein content was determined by the method of Bradford[7], using bovine serum albumin as the standard. Statistical evaluations were undertaken using analysis of variance with a significance level of $P < 0.05$. Intergroup comparisons were performed using Tukey's test[9].

RESULTS

When 10 μg/kg of rhIL-1α was administered ip 20h before sham irradiation it increased hypothalamic levels of total and selenium-dependent GSHPx (Fig. 1) and had no effect on SOD (Fig. 2). Radiation exposure alone increased body temperature (Fig. 3), decreased hypothalamic levels of total and selenium-dependent GSHPx (Fig. 1), and increased hypothalamic SOD (Fig. 2). However, rhIL-1α treatment and irradiation together attenuated radiation-induced hyperthermia (Fig. 3) and increased hypothalamic SOD (Fig. 2) but prevented the fall in total and selenium- dependent GSHPx (Fig. 1). When rhIL-1α was administered 1 h before radiation exposure, it had no effect on hypothalamic GSHPx and SOD levels (Table I) and it did not attenuate radiation-induced hyperthermia (Table II). Intrac-

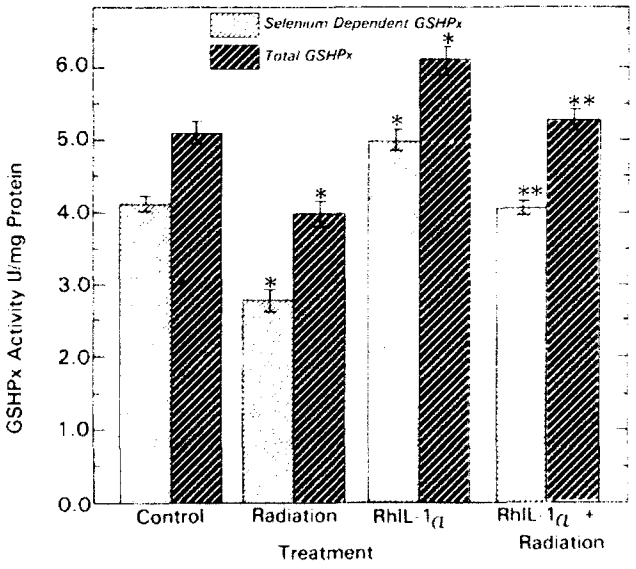

Fig. 1. Effect of 20 h pretreatment with 10 μg/kg of rhIL-1α i.p. alone, in combination with 10 Gy of radiation, or 10 Gy of radiation alone on hypothalamic selenium-dependent and total GSHPx levels. Values are expressed as mean of activity from 6 rats ± S.E.M. * Significantly different from control values: $P < 0.05$. ** Significantly different from irradiated values: $P < 0.05$.

TABLE I

Effect of 1 h i.p. pretreatment with 10 μg / kg of rhIL-1α alone, in combination with 10 Gy of radiation, or 10 Gy of radiation alone on hypothalamic selenium-dependent GSHPx, total GSHPx, and SOD levels (units / mg protein)

Values are expressed as mean of activity from 6 rats ± S.E.M.

Antioxidant enzymes	*Sham radiation*	*Radiation alone*	*RhIL-1α alone*	*RhIL-1α + radiation*
Selenium-dependent GSHPx	4.1 ± 0.10	2.8 ± 0.15 [a]	4.5 ± 0.10	3.0 ± 0.15 [a]
Total GSHPx	5.2 ± 0.10	4.0 ± 0.10 [a]	5.5 ± 0.15	4.3 ± 0.15 [a]
SOD	21.0 ± 0.15	28 ± 0.10 [a]	22 ± 0.15	29 ± 0.10 [a]

[a] Significantly different from sham radiation values: $P < 0.05$.

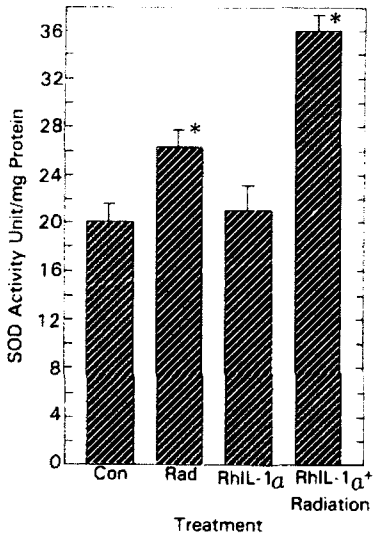

Fig. 2. Effect of 20 h pretreatment with 10 μg/kg of rhIl-1α i.p. alone, in combination with 10 Gy of radiation, or 10 Gy of radiation alone on hypothalamic SOD levels. Values are expressed as mean of activity from 6 rats ± S.E.M. [a] Significantly different from control values: $P < 0.05$. [b] Significantly different from irradiated values: $P < 0.05$.

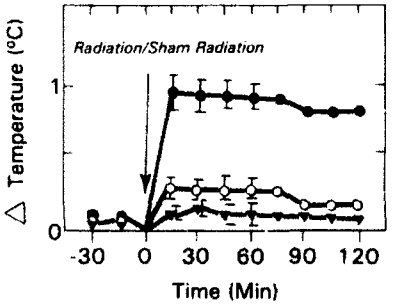

Fig. 3. Effect of 20 h pretreatment with rhIL-1α or saline given i.p. on radiation-induced hyperthermia. 10 Gy of irradiation alone (●), in the presence of 10 μg/kg rhIl-1α (○) or 10 μg/kg rhIL-1α alone (▼). Each point represents mean ± S.E.M. of observation of six animals. Zero on ordinate represents the temperature of (●) 38.3 ± 0.1, (○) 38.1 ± 0.05, and (▲) 38.0 + 0.1 at the time of radiation/sham radiation.

TABLE II

Effect of 1 h i.p. pretreatment with 10 μg / kg of rhIL-1α or saline given i.p. on radiation-induced (10 Gy) hyperthermia

Values are expressed as mean of activity from 6 rats ± S.E.M.

Treatment	*Mean change in temperature (°C ± S.E.M.)*
Saline + radiation	1.1 ± 0.10
RhIL-1α + radiation	1.3 ± 0.15
RhIL-1α + sham radiation	0.3 ± 0.10

erebroventricular administration of 1–5 units of GSHPx (Fig. 4) or 1–5 μg of SOD attenuated radiation-induced hyperthermia (Fig. 5).

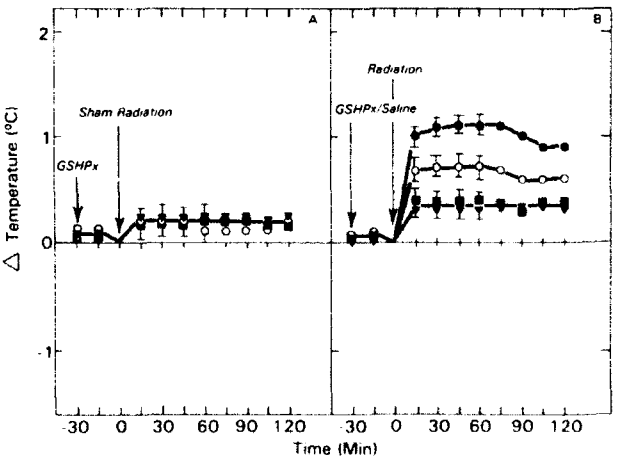

Fig. 4. Effect of GSHPx, ICV on radiation-induced hyperthermia. A: non irradiated controls given 1 unit (○), 3 units (■) or 5 units (▼) of GSHPx. B: 10 Gy of irradiation alone (●), in the presence of 1 unit (○), 3 units (■), or 5 units of GSHPx (▼). Each point represents the mean ± S.E.M. of observation of five animals. Zero on ordinate represents the temperature at the time of second injection (A) (○) 38.0 + 0.10, (■) 38.0 + 0.05, and (▼) 37.9 + 0.10, and at the time of irradiation (B) (●) 38.2 + 0.10, (○) 38.1 + 0.15, (■) 38.0 + 0.10, and (▼) 37.9 + 0.05.

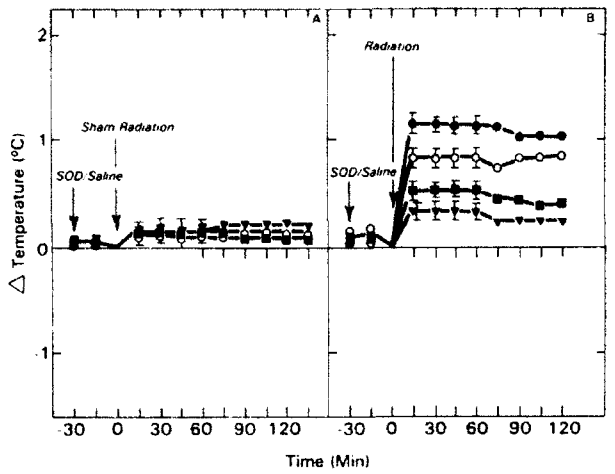

Fig. 5. Effect of SOD, ICV on radiation-induced hyperthermia. A: non-irradiated controls given 1 μg (○), 3 μg (□) or 5 μg (▼) of SOD. B: 10 Gy of irradiation alone (●) in the presence of 1 μg (○), 3 μg (■), or 5 μg of SOD (▼). Each point represents the mean ± S.E.M. of observation of five animals. Zero on ordinate represents the temperature at the time of second injection (A) (○) 38.0 ± 0.05, (■) 37.9 ± 0.10, and (▼) 37.8 ± 0.10, and at the time of irradiation (B) (●) 38.1 ± 0.05, (○) 37.9 ± 0.15, (■) 37.9 ± 0.10, and (▼) 37.9 ± 0.10.

DISCUSSION

Considering the role of free radicals in radiation injury, it is apparent that mechanisms of protection involve detoxification of radicals produced by radiation[20]. Protectors of this type include xenobiotic scavengers of free radicals and inducible endogenous antioxidant defense mechanisms such as antioxidant enzymes[5,2]. Cell damage induced by superoxide radicals and related oxygen species, such as singlet oxygen and hydroxyl radicals, has recently been tentatively connected with the etiology of a number of pathological conditions in the brain[4,6,13,29]. Enzymatic defense against activated oxygen species involves a cooperative action of several enzymes. The major defense against toxicity of superoxide radicals is conferred by SOD. This enzyme catalyses the dismutation of superoxide radicals to hydrogen peroxide and oxygen. Although the resulting hydrogen peroxide is relatively less toxic (scavenged by catalase and GSHPx) a highly toxic hydroxyl radical is produced when hydrogen peroxide reacts with superoxide or with transition metals, such as iron or copper. Therefore, catalase and GSHPx, which scavenge hydrogen peroxide, act in concert with SOD[31].

Radiation exposure increased SOD and decreased GSHPx levels in the hypothalamus. It has been reported that there is an increase in SOD levels in bone marrow of mice 1 h and 24 h and 72 h in rats after irradiation[31,18]. Superoxide radicals and hydroxy radicals are produced by irradiation. SOD reacts promptly to radiation-induced superoxide radical production by increased activity in the hypothalamus, thus providing an efficient quenching of superoxide radicals. At the present time we have no experimental data to explain the decreased GSHPx level after radiation exposure and the failure of rhIL-1α to increase hypothalamic SOD levels when given alone; however, we would like to suggest that GSHPx is utilized to scavenge free radicals caused by radiation exposure, resulting in decreased GSHPx levels. We also do not have the explanation for the failure of 1 h pretreatment with rhIL-1α to attenuate radiation-induced hyperthermia and the changes in GSHPx and SOD levels.

Several mechanisms have been proposed for radioprotection by IL-1. Two of these mechanisms are induction of PGs and acute phase proteins such as ceruloplasmin and metallothionein[24,10,17], which are free radical scavengers. However, experimental evidence does not support mechanisms based on PG or metallothionein induction for radioprotection by IL-1[24]. It has been reported that, in mice, the radioprotectant effect of rhIL-1α may involve induction of endogenous MnSOD in liver, which was confirmed by the induction of MnSOD-mRNA in the liver[19]. SOD might be a naturally occurring compound with a radioprotective effect[1] because the iv administration of SOD provoked an increase in SOD level in various tissues of experimental animals and led to an enhanced resistance to ionizing radiation[27,28].

Although the mechanisms that underlie the attenuation of radiation-induced hyperthermia by rhIL-1α remain speculative, our results suggest that one of the mechanisms of rhIL-1α-induced attenuation of radiation-hyperthermia is stimulation of hypothalamic SOD and GSHPx, because rhIL-1α and irradiation together increased both hypothalamic GSHPx and SOD levels and central administration of SOD and GSHPx attenuated radiation-induced hyperthermia. Hypothalamic PGE_2, corticotropin releasing factor (CRF), and plasma adrenocorticotropic hormone (ACTH) levels are increased after pretreatment with IL-1[7]. CRF and ACTH are antipyretics and have been implicated in thermoregulation[22]. Recent experiments with CRF and ACTH in normal, hypophysectomized, and adrenalectomized rats suggest that the attenuation of radiation-induced hyperthermia by IL-1 is mediated by an increase in CRF and ACTH in addition to the stimulation of antioxidant enzyme levels[16].

REFERENCES

1 Bartosz, G., Leyko, W. and Fried, R., Is superoxide dismutase a physiological radioprotector?, *Experientia*, 35 (1979) 1194.

2 Braglow, J.E., Varnes, M.E., Epp, E.R., Clark, E.P. and Astor, M., Redox enzymes and thiol radicals. In A. Breccia, M.A.J. Rodgers, and G. Semerano (Eds.), *Oxygen and Sulfur Radicals in Chemistry and Medicine*, Lo Scarabeo, Italy, 1986, pp. 89–102.

3 Braford, M.M., A rapid and sensitive method for the quantitation of protein utilizing the principle of protein-dye binding. *Anal. Biochem.*, 72 (1976) 248–254.

4 Cadet, J.B., Lohr, J.B. and Jeste, D.V., Free radicals and tardive dyskinesia, *Trends Neurosci.*, 9 (1986) 108–109.

5 Chapman, J.D., Reuvers, A.P., Borsa, J. and Greenstock, C.L., Chemical radioprotection and radiosensitization of mammalian cells growing in vitro, *Radiat. Res.*, 56 (1973) 291–306.

6 Dexter, D.T., Carter, C.J., Wells, F.R., Javoy-Agid, F. Agid, Y., Lees, A., Jenner, P. and Marsden, C.D., Basal lipid peroxidation in substantia nigra is increased in Parkinson's disease, *J. Neurochem.*, 52 381–389

7 Dinarello, C.A., Biology of interleukin 1, *FASEB J.*, 2 (1988) 108–115.

8 Elkind, M.M., Repair processes in radiation biology, *Radiat. Res.*, 100 (1984) 425–431.

9 Glass, G.V. and Stanley, J.C., In *Statistical Methods in Education and Psychology*, Prentice-Hall, Englewood Cliffs, NJ, 1970.

10 Goldstein, I.M. and Charo, I.F., Ceruloplasmin: An acuto phase reactant and antioxidant. In E. Pick (Ed.), *Lymphokines, Vol. 8*, Academic Press, New York, 1983, pp. 373–411.

11 Hall, E.J., The physics and chemistry of radiation absorption. In E.J. Hall (Ed.), *Radiobiology for the Radiologist*, 3rd edn., Lippincott, Philadelphia, 1988, pp. 1–16.

12 Hall, E.J., Radioprotectors. In E.J. Hall (Ed.), *Radiobiology for the Radiologist*, 3rd edn., Lippinocott, Philadelphia, 1988, pp. 201–209.

13 Hallwell, B. and Gutteridge, J.M., Oxygen radicals and the nervous system. *Trends Neurosci.*, 5 (1985) 22–26.

14 Kandasamy, S.B. and Hunt, W.A., Involvement of prostaglandins and histamine in radiation-induced temperature responses in rats. *Radiat. Res.*, 121 (1990) 84–90.

15 Kandasamy, S.B., Kumar, K.S., Harris, A.H. and Weiss, J.F., Effect of interleukin-1a on radiation-induced hyperthermia in rats. *Soc. Neurosci. Abstr.*, 16 (1990) 496.10.

16 Kandasamy, S.B., Stevens-Blakely, S.A., Dalton, T.K. and Harris, A.H., Mechanisms involved in attenuation of radiation-induced hyperthermia in rats by interleukin, *FASEB J.*, Abstr. 6, Part I, (1992) [Abstract 2296].

17 Karin, M., Metallothioneins: protein in search of function, *Cell*, 41 (1985) 9–10.

18 Krizala, J., Stoklasova, A., Kovarova, W. and Ledvina, M., The effect of γ-irradiation and cystamine on superoxide dismutase activity in the bone marrow and erythrocytes of rats. *Radiat. Res.*, 91 (1982) 507–515.

19 Kumar, K.S., Vaishnav, Y.N., Smith, C. and Clark, E.P., Radiation injury and antioxidant mechanisms of protection. In S. Nigam, K.V. Honn, E.J. Marnett, and F.E. Walden Jr. (Eds.), *Eicosanoids and other Bioactive Lipids in Cancer, Inflammation and Radiation Injury*, Kluwer, Boston, 1992, pp. 333–339.

20 Kumar, K.S., Vaishnav, Y.N. and Weiss, J.F., Radioprotection by antioxidant enzymes and enzyme mimetics, *Pharmacol. Ther.*, 39 (1988) 301–309.

21 Lawrence, R.A. and Burk, R.F., Glutathione peroxidase activity in selenium-deficient rat liver, *Biochem. Biophys. Res. Commun.*, 71 (1976) 952–958.

22 Lipton, J.M. and Clark, W.G., Neurotransmitters in temperature control, *Annu. Rev. Physiol.*, 48 (1986) 613–623.

23 McCord, J.M. and Fridovich, I., Superoxide dismutase. An enzymic function for erythrocuprein (hemocuprein), *J. Biol. Chem.*, 244 (1969) 6049–6055.

24 Neta, R., Oppenheim, J.J., Douches, S.D., Giclas, P.C., Imbra, R.J. and Karin, M., Radioprotection with interleukin-1: Comparison with other cytokines, *Prog. Immunol.*, VI (1986) 900–908.

25 Neta, R., Douches, S. and Oppenheim, J.J., Interleukin 1 is a radioprotector, *J. Immunol.*, 136 (1986) 2483–2485.

26 Pelligrino, L.S., Pelligrino, A.S. and Cushman, A.J., *A Stereotaxic Atlas of the Rat Brain*, Plenum, New York, 1979.

27 Petkau, A., Radiation protection by superoxide dismutase, *Photochem. Photobiol.*, 28 (1978) 765–774.

28 Petkau, A., Chelack, S. and Pleskach, S.D., Protection by superoxide dismutase of white blood cells in x-irradiated mice, *Life Sci.*, 22 (1978) 867–882.

29 Saggu, H., Cooksey, J., Dexter, D., Wells, F.R., Lees, A., Jenner, P. and Marsden, C.D., A selective increase in particulate superoxide dismutase activity in parkinsonian substantia nigra, *J. Neurochem.* 53 (1989) 692–697

30 Task Group 21, Radiation Therapy Committee AAPM, A protocol for the determination of absorbed dose from high energy photon and electron beams, *Med. Phys.*, 10 (1983) 741.

31 Weiss, J.F. and Kumar, K.S., Antioxidant mechanisms in radiation injury and radioprotection. In C.K. Chow (Ed.), *Cellular Antioxidant Defense Mechanisms, Vol. II*, CRC Press, Boca Raton, FL, 1988, pp. 163–189.

In: *The Biology of Nitric Oxide.*
S. Moncada, M.A. Marletta, J.B. Hibbs, Jr., and E.A. Higgs, eds.
Portland Press, London, 1992.

Implication of nitric oxide synthase in radiation-induced decrease in hippocampal noradrenaline release in rats

S. B. Kandasamy, S. A. Stevens-Blakely, T. K. Dalton and A. H. Harris
Behavioral Sciences Department, Armed Forces Radiobiology Research Institute, Bethesda, MD 20889-5145, U.S.A.

Introduction

The hippocampus is important in critical functions such as learning, memory, and motor performance, and these functions are impaired after exposure to ionizing radiation [1]. Noradrenergic systems are important in mediating arousal, food intake and to some extent motor functions; histofluorescence and immunohistochemical techniques have shown noradrenergic pathways in the hippocampus [2]. Several factors can contribute to acute nervous system damage *in vivo*: systemic blood pressure is reduced following exposure to 25–100 Gy γ radiation [3, 4], and cerebral blood flow decreases in a variety of brain regions, including the hippocampus [5]; the ischaemia produced by decreased blood flow is likely to affect neuronal activity [6]; ionizing radiation generates free radicals, and resulting oxygen radicals have been implicated in cell damage following ischaemia; brain ischaemia induces the release of an excessive amount of glutamate in the hippocampus, and glutamate acts on nitric oxide (NO) synthase to form NO through N-methyl-D-aspartate receptors, causing toxic effects [7]. The purpose of this study was to examine the effect of ionizing radiation on hippocampal noradrenaline (NA) release *in vitro*, stimulated by KCl 0.5, 24, 48, and 72 h after irradiation/sham-irradiation and to determine the role of NO synthase in the radiation-induced decrease in NA release.

Methods

Male Sprague–Dawley rats, weighing 200–300 g, were used in these experiments. Rats were killed by decapitation, and brains were removed. The hippocampus was dissected using the method of Glowinski & Iversen [8]. NA was measured by h.p.l.c. coupled with electrochemical detection. Release of hippocampal NA *in vitro* was stimulated by KCl and the irradiation procedures were carried out as described previously [9]. Rats were exposed bilaterally to varying doses of γ rays using a ^{60}Co source at a rate of 10 Gy min^{-1}. Statistical analysis was performed using Student's *t* test. Multiple comparisons with a sham-irradiated control were done by analysis of variance and Dunnett's test. Data were identified as significant if $P < 0.05$.

Table 1

Radiation dose/ sham-irradiation	NA release (pmol mg^{-1} of protein)			
	0.5 h	24 h	48 h	72 h
Sham	15.8±0.3	15.2±0.4	15.5±0.2	15.3±0.4
5 Gy	16.5±0.8	14.5±0.9	12.0±0.5*	12.0±0.2*
10 Gy	16.5±0.6	12.4±0.8	8.4±0.65*	8.0±0.5*
30 Gy	16.7±0.5	12.0±0.4*	8.0±0.85*	8.0±0.6*

Effect of exposure to γ rays (10 Gy min^{-1}) on NA release

*Values are means ± S.E.M. of three separate experiments. * Significantly different from sham-irradiated values; $P < 0.05$.*

Table 2

L-NA concentration (mg/kg)	NA release (pmol mg^{-1} of protein)			
	Sham irradiation	Saline + irradiation	L-NA + sham-irradiation	L-NA + irradiation
0	16.0±0.3	8.4±0.6*	16.9±0.9	8.6±0.4*
3	15.8±0.6	8.0±0.4*	17.5±0.6	12.0±0.4**
5	15.4±0.4	8.2±0.3*	21.5±0.4*	16.5±0.8**
10	15.5±0.65	8.0±0.3*	24.0±0.6*	19.5±0.6**

Effect of pretreatment with L-NA on NA (pmol mg^{-1} of protein) release 48 h after exposure to 10 Gy of γ rays

*Values are means ± S.E.M. of three separate experiments. * Significantly different from sham-irradiation values; $P < 0.05$. ** Significantly different from irradiated values; $P < 0.05$.*

Results

There was no significant difference in NA release between irradiated and sham-irradiated rats when the hippocampal NA concentration was determined 0.5 h after radiation exposure (5–30 Gy at 10 Gy min^{-1}). However, there were significant decreases in hippocampal NA release 48 and 72 h after exposure to 5 and 10 Gy and 24, 48, and 72 h after exposure to 30 Gy of γ rays (Table 1). Based on the above data, a post-irradiation time period of 48 h and a γ-radiation dose of 10 Gy at 10 Gy min^{-1} were chosen for further studies with an NO synthase inhibitor, N^G-nitro-L-arginine (L-NA). Pretreating rats with 1 mg kg^{-1} of L-NA administered i.p. 1 h before irradiation or sham-irradiation had no effect on the radiation-induced decrease in NA (data not shown). However, 3 mg kg^{-1} of L-NA prevented the radiation-induced decrease in NA release, and 5 and 10 mg kg^{-1} L-NA not only prevented the decrease in NA release in irradiated rats but also enhanced NA release in sham-irradiated rats (Table 2). Similar pretreatment with 1–10 mg kg^{-1} of L-arginine before irradiation or sham-irradiation had no effect on either the radiation-induced decrease in NA release or the basal hippocampal NA release (data not shown).

Discussion

This study demonstrates that radiation had no effect on hippocampal NA release 0.5 h after exposure but decreased NA release 24, 48 and 72 h after exposure, depending on the radiation dose. At the present time we have no data to explain the differences in NA release at post-irradiation time intervals. However, it has been suggested that the blood-brain barrier could be disrupted by ionizing radiation [10, 11]. This would allow radiation-released neurotransmitters such as prostaglandins (PGs), histamines, and 5-hydroxytryptamine, as well as other circulating factors, (abnormal) access to neurons that modulate hippocampal NA release [12]. It has been shown that PGs of the E series inhibit the release of NA from sympathetic nerves both in the periphery and the central nervous system; conversely, inhibition of PG synthesis leads to an increase in NA release [13].

Immunochemical localization of NO synthase has been demonstrated in most areas of the rat brain, including the hippocampus. NO synthase forms NO from L-arginine [7]. Pretreatment with L-NA (a selective inhibitor of brain NO synthase) reversed the radiation-induced decrease in NA release, suggesting that NO synthase is involved in this phenomenon. Pretreatment with L-NA also enhanced NA release in sham-irradiated rats, suggesting that NO is involved in the regulation of NA under normal conditions. However, inhibition of PG synthesis by L-NA (thereby increasing NA levels) should not be excluded at this time. Although no results are currently available on the measurement of glutamate release in the hippocampus following exposure to radiation, our results support the hypothesis that toxic overstimulation of glutamate receptors by radiation or excitotoxicity contributes to overproduction of NO that can be toxic to neurons.

In conclusion, these results suggest that ionizing radiation induces a decrease in hippocampal NA release 24, 48 and 72 h after exposure, and NO synthase is implicated in this radiation-induced decrease in NA release.

References

1 Kimeldorf, D. J. & Hunt, E. L. (1965) in Ionizing Radiation: Neural Function and Behavior (Kimeldorf, D. J. & Hunt, E. L., eds.), pp. 166–213, Academic Press, New York
2 Van Dongen, P. A. M. (1981) Prog. Neurobiol. **16**, 117–143
3 Chapman, P. H. & Young, R. J. (1968) Radiat. Res. **35**, 78–85
4 Cockerham, L. G., Cervenv, T. J. & Hampton, J. D. (1986) Aviat. Space Environ. Med. **57**, 578–582
5 Cockerham, L. G., Pautler, E. L. & Hampton, J. D. (1985) Fed. Proc. **44**, 1357
6 Karino, T., Tamura, A. & Sano, K. (1985) Prog. Brain Res. **63**, 39–58
7 Snyder, S. H. & Bredt, D. S. (1991) Trends Pharmacol. Sci. **12**, 125–128
8 Grzywinski, J. & Iversen, L. L. (1966) J. Neurochem. **13**, 655–669
9 Joseph, J. A., Kandasamy, S. B., Hunt, W. A., Dalton, T. K. & Stevens, S. (1988) Pharmacol. Biochem. Behav. **29**, 335–341
10 Griffin, T. W., Rasey, J. S. & Blesser, W. A. (1977) Cancer **40**, 1109–1111
11 Scheitler, T. & Sheafs, C. N. (1970) J. Neurosurg. **32**, 89–94
12 Kandasamy, S. B. & Hunt, W. A. (1990) Radiat. Res. **121**, 84–90
13 Bergstrom, S., Carmeho, L. O. & Fuxe, K. (1973) Eur. J. Pharmacol. **21**, 362–368

Radiation Protection Dosimetry
Vol. 44 No. 1-4 pp. 61-64 (1992)
Nuclear Technology Publishing

ENERGY DEPOSITION IN A SPHERICAL CAVITY OF ARBITRARY SIZE AND COMPOSITION

E. Kearsley
Radiation Biophysics Department
Armed Forces Radiobiology Research Institute
Bethesda, MD 20889-5145, USA

Abstract — The dose distribution inside a spherical cavity is calculated using analytical expressions for both the stopping power and the starting energy distributions for elastically scattered secondary charged particles. Cavity-generated secondaries are treated separately from secondaries generated in the surrounding medium. The result is an analytical expression for the ratio of the dose to the cavity to the dose to the surrounding medium. This expression, sometimes referred to as the 'effective stopping power' is in a form similar to the Burlin general cavity theory for photons.

INTRODUCTION

The energy deposited in a spherical cavity irradiated in a neutron field depends on the composition of the cavity and surrounding medium, the size of the cavity, and the energy of the neutrons. Caswell[1] analysed this problem in terms of 'insiders, starters, stoppers, and crossers', referring to the trajectories of secondary charged particles relative to the volume of the cavity. His objective was to provide a detailed understanding of the pulse height distributions obtained from measurements using tissue-equivalent proportional counters. Rubach and Bichsel[2-4] applied these same techniques to the study of the response of ionisation chambers with a variety of wall–gas combinations and cavity volumes. This approach provides insight into the total energy deposition in a volume but little information about the spatial distribution of the deposited energy, which may be important to our understanding of the biological response of certain tissues of the body after neutron irradiation. This paper describes a calculation of both the dose distribution and the average dose within a spherical cavity of arbitrary size and composition from neutron interactions with both the cavity material and the surrounding medium.

THE CALCULATION

The origin of a spherical coordinate system is placed at a distance, x, from the centre of a sphere of radius, a (Figure 1). The coordinate r may extend to any point inside or outside the cavity volume. The dose at x is the product of the fluence of secondary charged particles and their stopping power. Assuming an isotropic source of secondaries and neglecting any scattering effects at the interface for secondaries generated outside the cavity, the charged particle fluence at x, generated by neutron interactions in a differential volume element, dV, located at a distance, r, from the origin can be written as

$$d\Phi = \frac{N\,dV}{4\pi r^2} \qquad (1)$$

where N is the number of secondary charged particles per unit volume.

If it is assumed that the range of a secondary can be written as $R = A\,E^m$, where A and m are constants that depend on the particle type, then the stopping power for a secondary generated in dV with an initial range, R, after travelling a distance, r, can be written

$$\frac{dE}{dx} = \frac{1}{m}\left(\frac{1}{A}\right)^{1/m}(R - r)^{(1/m)-1} \qquad (2)$$

The contribution to the dose at the origin of the coordinate system is determined by considering the separate contributions from neutron interactions in the cavity material (i.e. the cavity contribution) and in the surrounding wall (i.e. the wall contribution). The complete calculation

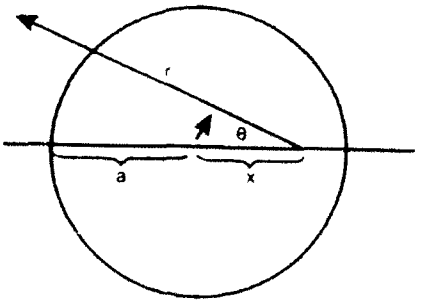

Figure 1. Geometry for the calculation of the response of a spherical cavity in a neutron field. A spherical co-ordinate system is centred at a distance x from the centre of a sphere of radius a.

considers a series of cases that depend on the range of the secondaries and the boundaries of the cavity. Only the case in which the maximum range of the secondary, R_m, is less than the cavity radius, a, will be illustrated in detail.

The cavity contribution

Every point in the region, $O < x < (a - R_m)$, is surrounded by a thickness of cavity material greater than R_m. The dose in this region can be written as

$$D_{c,1}(x) = \int_0^{2\pi} d\phi \int_0^{E_m} dE \int_0^{\pi} d\theta \int_0^{R(E)} dr \frac{N_c}{4\pi\rho_c E_m} \sin\theta \frac{1}{m}\left(\frac{1}{A}\right)^{1/m} (R-r)^{1/m-1} \quad (3)$$

Both ϕ and θ have their usual meanings in a spherical coordinate system. The integrand is the product of the secondary fluence and stopping power, divided by the density of the cavity material. The radial integration is limited by the range of the secondary which depends on its energy. The energy integral is over the starting energy distribution, which is assumed to be a simple step function. The subscript, c, refers to the contributions to the dose to the cavity from neutron interactions within the cavity; the numerical subscript is an index to distinguish between different components of the dose.

For the region $(a-R_m) < x < a$, secondaries generated within the cavity with a range less than (a–x) will contribute

$$D_{c,2}(x) = \int_0^{2\pi} d\Phi \int_0^{E_1} dE \int_0^{\pi} d\theta \int_0^{R(E)} dr\, I(r,E,\theta) \quad (4)$$

where $I(r,E,\theta)$ is the same integrand used in Equation 3. E_1 is the energy for a secondary with a range equal to (a–x):

$$E_1(x) = \left(\frac{a-x}{A}\right)^{1/m} \quad (5)$$

For a secondary with a range greater than (a–x), the integral becomes

$$D_{c,3}(x) = \int_0^{2\pi} d\Phi \int_{E_1}^{E_m} dE \int_0^{\theta_m} d\theta \int_0^{R(E)} dr\, I(r,E,\theta) + \int_0^{2\pi} d\Phi \int_{E_1}^{E_m} dE \int_{\theta_m}^{\pi} d\theta \int_0^{r_s} dr\, I(r,E,\theta) \quad (6)$$

where r_s is the distance between the origin and the boundary of the cavity at a given angle θ; θ_m is the azimuthal angle at which the range of a secondary is equal to r_s. The sum of Equations 3, 4, and 6 represents the total dose to the cavity from interactions with the cavity material producing secondaries with ranges less than the cavity radius.

The wall contribution

To account for the fact that some fraction of the path of the secondary is in the wall, the residual range appearing in the stopping power becomes

$$(R - r) \rightarrow R - \tilde{n}(r - r_s) - r_s \quad (7)$$

where $\tilde{n}$ is the ratio of the range in the cavity to the range in the wall material. The dose at x from secondaries produced from the wall can then be written

$$D_{w,1}(x) = \int_0^{2\pi} d\Phi \int_{E_1}^{E_m} dE \int_{\theta_m}^{\pi} d\theta \int_{r_s}^{r_{max}} dr \frac{N_w}{4\pi\rho_c E_m} \sin\theta \frac{1}{m}\left(\frac{1}{A}\right)^{1/m} [R-\tilde{n}(r-r_s)-r_s]^{1/m-1} \quad (8)$$

where r_{max} is the maximum range of a secondary starting in the wall at an angle θ, correcting for the range differences in the two materials. That is,

$$r_{max} = r_s + \frac{R_c - r_s}{\tilde{n}} \quad (9)$$

The Brass simplification

For the special case in which the cavity and wall material are identical, the sum of the cavity contribution and the wall contribution at any point x within the cavity must be equal to the equilibrium dose to the material:

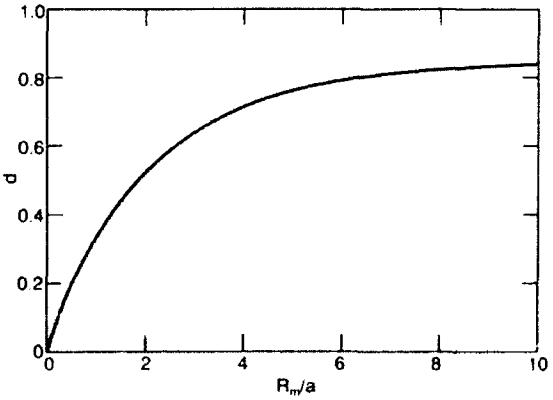

Figure 2. A plot of d as a function of R_m/a for a value of m = 1.75 (appropriate for protons).

$$D_c(x) + D_w(x)|_{w\to c} = \frac{N_c E_m}{2\rho_c} \qquad (10)$$

Therefore, the cavity contribution can be determined from the wall contribution and the total dose at any point x within the cavity can be written:

$$D_T(x) = D_c(x) + D_w(x) = \frac{N_c E_m}{2\rho_c} - D_w(x)|_{w\to c} + D_w(x) \qquad (11)$$

This procedure, first suggested by Bragg[5], is useful because the expression for the wall contribution, $D_w(x)$, is always much simpler to derive than the cavity contribution, $D_c(x)$. The average dose to the cavity can then be determined by integrating over all values of x. The result can be put into the simple form:

$$\langle D_T \rangle = \frac{N_w E_m}{2\rho c\tilde{n}}\, d + \frac{N_c E_m}{2\rho_c}\,(1-d) \qquad (12)$$

where $d = d(R_m,a,m)$

Dividing both sides of this expression by the equilibrium dose to the wall of the cavity, we obtain an expression for what is sometimes referred to as the 'effective stopping power'

$$f_w^c = \frac{\rho_w}{\rho_c\tilde{n}}\, d + \frac{N_c E_m \rho_w}{N_w E_m \rho_c}\,(1-d) \qquad (13)$$

Note that this is in the form of the Burlin general cavity theory for photons[6]. The first term is effectively the mass stopping power ratio for the secondaries multiplied by $d(R_m,a,m)$. The second term is effectively the neutron kerma factor ratio (equivalent to the ratio of the mass energy absorption coefficients in the Burlin theory) multiplied by (1–d).

The function $d(R_m,a,m)$ is illustrated in Figure 2 for recoil protons (m=1.75). The exact expression for $d(R_m,a,m)$ is a complicated, multi-termed function. Space limitations do not permit a full listing of the analytical expression for $d(R_m,a,m)$. However, an approximate expression that can be used to determine values of $d(R_m,a,m)$ to within 1% of the exact value is

$$d(R_m,a) = 1 - \left[\alpha \left(\frac{R_m}{a}\right)^2 + \beta \left(\frac{R_m}{a}\right) + \gamma\right]^{-1} \qquad (14)$$

Recommended values for α, β, and γ are provided in Table 1. For a practical calculation involving complex materials such as muscle tissue or A–150 plastic, the contribution of each secondary must be calculated and summed to determine either the dose at x as in Equation 11 or the average dose to the cavity, Equation 12.

Table 1. Recommended parameters for Equation 14.

$R_m/a < 2$

m	α	β	γ
0.868 (ions)	0.07724	0.2359	1
1.500 (alphas)	0.08511	0.2511	1
1.750 (protons)	0.08117	0.2501	1

$R_m/a > 2$

m	α	β	γ
0.868 (ions)	–0.000902	0.6257	0.5298
1.500 (alphas)	–0.001315	0.6151	0.6202
1.750 (protons)	–0.002566	0.5727	0.6908

DISCUSSION

The calculation rests on several assumptions. First, it is assumed that the secondaries generated by neutron interactions either inside or outside the cavity are produced isotropically. This assumption restricts the use of the model to obtain dose distribution information to cases in which the neutron fields can be considered to be isotropic. However, relations involving the average dose to the cavity such as Equation 12 or Equation 13, are general for any neutron field because of the spherical symmetry of the cavity. Second, the simple parameterised form for the range–energy relationship and therefore the stopping power, Equation 2, is not strictly correct at the end of the track of the secondary. As before, this simplification has little effect on the total energy deposited in the cavity as long as very little of the total energy of the secondary is involved. This simplification will have a greater impact on the dose distribution, because the stopping power at the end of the track will be underestimated. Third, it is assumed that the secondary energy distribution is a simple step function appropriate for secondaries generated via elastic scattering interactions. At high neutron energies, this can introduce substantial errors in the calculation. Fourth, it is assumed that the ratio of ranges for a particular secondary in two different media is independent of the energy. This is approximately correct over a wide range of energies.

The results of this calculation have been compared with the calculations by Rubach and Bichsel[3,4]for a wide range of neutron energies (0.760 – 14 MeV), three cavity–wall combinations

(TE–TE, TE–air, and C–CO_2) and four decades of gas-filled cavity volumes (0.01 – 10 cm^3). At 2 MeV and below, the maximum difference between the ratio of the dose to the cavity to the equilibrium wall dose was less than 3%. At higher energies, the differences between the two calculations are much larger, probably as a result of the assumed shape of the secondary starting energy distribution (i.e. neutron interactions are no longer dominated by elastic scattering).

CONCLUSION

An expression has been derived for the dose distribution within a spherical cavity of arbitrary size and composition surrounded by a medium of arbitrary composition. The expression was averaged over the cavity volume to determine the ratio of the total dose to the cavity to the equilibrium dose to the surrounding medium. The form for the latter expression is identical to the form of the Burlin general cavity theory for photons.

ACKNOWLEDGEMENT

This work was supported by the Armed Forces Radiobiology Research Institute, Defense Nuclear Agency, under Work Unit 4610.

REFERENCES

1. Caswell, R. S. *Deposition of Energy by Neutrons in Spherical Cavities.* Radiat. Res. **27,** 92–107 (1966).
2. Rubach, A. and Bichsel, H. *Neutron Dosimetry with Spherical Ionization Chambers I. Theory of the Dose Conversion Factors r and W_n.* Phys. Med. Biol. **27,** 893–904 (1982).
3. Rubach, A. and Bichsel, H. *Neutron Dosimetry with Spherical Ionization Chambers III. Calculated Results for Tissue–equivalent Chambers.* Phys. Med. Biol. **27,** 1231–1243 (1982).
4. Rubach, A. and Bichsel, H. *Neutron Dosimetry with Spherical Ionization Chambers IV. Neutron Sensitivities for C/CO_2* and Tissue–equivalent Chambers. Phys. Med. Biol. **27,** 1455–1463 (1982).
5. Bragg, W. H. *Studies in Radioactivity* (London: Macmillan) (1912).
6. Burlin, T. E. *A General Theory of Cavity Ionization.* Br. J. Radiol. **39,** 727–734 (1966).

Inhibition of c-*kit* Ligand/Steel Factor by Antibodies Reduces Survival of Lethally Irradiated Mice

By Ruth Neta, Douglas Williams, Faith Selzer, and John Abrams

Survival after irradiation with $LD_{100/30}$ (radiation dose lethal to 100% of mice in 30 days) is based on recovery of impaired hematopoietic function. Our previous studies using antibodies to interleukin-1 receptor (IL-1R), tumor necrosis factor (TNF), and IL-6 demonstrated that endogenous production of these three cytokines is required for untreated mice as well as mice protected with lipopolysaccharide (LPS), IL-1, or TNF to survive lethal irradiation. In this report we show that anti–c-*kit* ligand/steel factor (SIF) antibody similarly abrogates LPS- and IL-1–induced radioprotection. Furthermore, administration of this antibody to unmanipulated mice increased $LD_{50/30}$ radiation lethality from 50% to 100%. Such an effect was not obtained using anti–IL-3, anti–IL-4, or anti–granulocyte-macrophage colony-stimulating factor antibody. Thus, like IL-1, TNF, and IL-6, SIF is required for survival from lethal irradiation.

RADIATION-INDUCED destruction of the hematopoietic system was documented to be the primary cause of septicemia and death based on the findings that transfer of normal bone marrow cells prevents death from lethal irradiation (with $LD_{100/30}$, a dose that causes death of 100% of animals within 30 days). Transplantation of bone marrow can be replaced in part by the administration of inflammatory bacterial lipopolysaccharide (LPS) as well as the proinflammatory cytokines, interleukin-1 (IL-1) and tumor necrosis factor (TNF), which when administered before lethal irradiation enhance the percentage of surviving mice by accelerating the recovery of the hematopoietic system.[1,2] This effect is attributed in part to the ability of these agents to stimulate the production of hematopoietic growth factors (HGFs), including IL-6, granulocyte-macrophage colony-stimulating factor (GM-CSF), granulocyte-CSF (G-CSF), and macrophage-CSF (M-CSF).[3] Several additional cytokines are thought to contribute to the growth and differentiation of cells of the hematopoietic lineages. These cytokines include T-cell–derived pluripotent IL-3[4] and IL-4[5] and the more recently cloned, stromal cell-derived, steel factor (SIF).[6,7]

Identification of the HGFs that are essential for the restoration of sufficient hematopoiesis to result in survival after lethal irradiation may be achieved using neutralizing antibodies to these cytokines. Indeed, we have previously demonstrated that antibodies to IL-1 and TNF abrogate the radioprotective effect of LPS.[8] This indicates that the ability of LPS to enhance survival of mice depends entirely on its ability to induce IL-1 and TNF. The radioprotective effects of IL-1 and TNF, in turn, depend on their induction and interaction with IL-6, because antibody to IL-6 blocked the radioprotective effects of IL-1 and TNF.[9] These results suggest that interaction of all three cytokines is required for radioprotection.

In this study, we evaluated antibodies to SIF, IL-3, IL-4, and GM-CSF to assess the relative contribution of these HGFs to radioprotection with LPS and IL-1 and to innate resistance of untreated mice to radiation. The results indicate that SIF is absolutely necessary for innate as well as LPS- and IL-1–induced protection from the lethal effects of radiation.

MATERIALS AND METHODS

Mice. CD2F1 female mice, 8 to 10 weeks old, were purchased from the Animal Genetics and Production Branch, National Cancer Institute, National Institutes of Health (Frederick, MD). B6D2F1 female mice, 8 to 10 weeks old, were purchased from Jackson Laboratories (Bar Harbor, ME). Mice were handled as previously described.[2]

Antibodies. A rat monoclonal IgG1, anti–IL-1 receptor antibody (35F5), was previously described.[10] A rat monoclonal antibody (MoAb) to β-galactosidase (GL113) was used as a control. Chromatographically purified rat IgG (Sigma, St Louis, MO) was used as an additional control. Polyclonal anti-SIF antibody (P2) was raised in rabbit against purified recombinant yeast-derived murine SIF as described.[6] This antibody at 1:40 dilution neutralized 1.25 μg of recombinant murine SIF in an MC 6 cell proliferation assay. As a control, equivalent concentrations of normal rabbit serum or preimmune serum was used. Rat monoclonal antimouse IL-4 (11B11) was prepared as described.[11] One nanogram of this antibody neutralizes 15 pg of IL-4. Antimouse GM-CSF (22E9.11) was prepared as described.[12] Twenty micrograms of this antibody completely neutralized 44 U of GM-CSF in the BCL1 proliferation assay.[12] Rat monoclonal anti–IL-3 antibody (8F8.11) was prepared as described.[13]

Treatment. Recombinant human IL-1 (rHuIL-1α; 117-271 Ro 24-5008, lot IL-1 2/88; activity, 3×10^8 U/mg) was kindly provided by Dr Peter Lomedico (Hoffmann-La Roche, Nutley, NJ). Bacterial, protein free LPS, prepared from *Escherichia coli* K235 by the phenol-water extraction method, was kindly provided by Dr Stefanie Vogel (Uniformed Services University for the Health Sciences, Bethesda, MD). The antibodies and recombinant cytokines were diluted in pyrogen-free saline on the day of injection. Antibodies or control Ig were administered intraperitoneally (IP) 6 to 20 hours before IP injection of 100 ng/mouse of IL-1 or 1 μg/mouse of LPS. Mice were irradiated 18 to 20 hours after IL-1 or LPS treatment. In an additional series of experiments, untreated mice were first irradiated and 1 to 2 hours later received IP injections of antibody, control protein, or vehicle. In each case, the inoculum was 0.5 mL/mouse.

Bone marrow cellularity, colony-forming units (CFUs) assay, and CSF assay. Bone marrow cells were obtained from groups of mice irradiated with $LD_{50/30}$ and $LD_{100/30}$ doses 8 days after irradiation (3 mice/group) in two separate experiments and counted in hemacytometer. For CFUs determination, bone marrow cells from unirra-

From the Department of Experimental Hematology, Armed Forces Radiobiology Research Institute, Bethesda, MD; the Department of Experimental Hematology, Immunex Corp, Seattle, WA; and the Department of Immunology, DNAX Research Institute, Palo Alto, CA.

Submitted May 11, 1992; accepted September 10, 1992.

Address reprint requests to Ruth Neta, PhD, Department of Experimental Hematology, Armed Forces Radiobiology Research Institute, Bldg 42, NNMC, Bethesda, MD 20889.

The publication costs of this article were defrayed in part by page charge payment. This article must therefore be hereby marked "advertisement" in accordance with 18 U.S.C. section 1734 solely to indicate this fact.

0006-4971/93/8102-0007$0.00/0

diated mice (donors) treated with saline only, anti-SIF antibody, or control rabbit serum 20 hours before killing were obtained and 5×10^4 cells were injected intravenously to lethally (1,050 rad) irradiated recipients (5 mice/group). Splenic colonies were evaluated 8 days later. CSF levels in the serum of mice receiving anti-SIF antibody or rabbit control serum and subsequently treated with IL-1 were determined as previously described.[14]

Irradiation. Mice were randomized, placed in Plexiglass containers, and received whole-body radiation at 40 cGy/min midline tissue dose by bilaterally positioned ^{60}Co elements. The radiation field was uniform within ±2%. The number of surviving mice was recorded daily for 30 days.

Statistical analysis of the results was performed using a contingency table analysis.

RESULTS

The effect of anticytokine antibody on LPS- and IL-1–induced radioprotection. To assess the contribution of GM-CSF, IL-3, IL-4, and SIF to IL-1– and LPS-enhanced survival from lethal irradiation, mice were treated with the antibodies or control proteins before administration of LPS or IL-1 and $LD_{85/30}$ irradiation. The results (Table 1) indicate that, as with anti–IL-1R antibody, anti-SIF antibody blocked IL-1–induced protection from radiation lethality. Furthermore, this antibody also completely blocked LPS-induced radioprotection. In contrast, 800 μg doses of anti–IL-3, anti–IL-4, or anti–GM-CSF antibody had no effect on IL-1– or LPS-induced radioprotection. Thus, SIF is critical to protection from radiation induced lethality by IL-1 and LPS.

The effect of anticytokine antibody on innate resistance to radiation. The antibodies were next administered to mice that were otherwise unmanipulated to test for the effect of the treatment on survival from irradiation. The results in Table 2 indicate that treatment with anti-SIF antibody, as with anti–IL-1R antibody, increased the incidence of mortality of $LD_{50/30}$ irradiated mice. Furthermore, the mean survival time of anti-SIF antibody treated mice was 13.0 ± 1.2 days versus 16.5 ± 2.8 days for control mice. In contrast, treatment with anti–IL-3, anti–IL-4, or anti–GM-CSF antibody did not affect the survival of mice. Therefore, in addition to its critical role in survival of LPS- and IL-1–treated mice, SIF is required for survival of untreated, lethally irradiated mice.

Table 1. The Effect of Anti-HGF Antibodies on Survival of Mice Radioprotected With LPS or IL-1

Treatment		LPS		IL-1	
		Dead/ Total	% Survival	Dead/ Total	% Survival
Saline	–	25/30	17	34/40	15
Rat Ig	+	8/20	60	12/28	58
Control antibody	+	1/20	95	13/44	70
Anti–IL-1R	+	15/20	25*	35/40	12.5*
Anti–SIF	+	19/20	5*	27/30	10*
Rabbit Ig	+	—	—	5/30	83
Anti–GM-CSF	+	7/19	63	6/20	70
Anti–IL-4	+	6/20	70	4/20	80
Anti–IL-3	+	5/20	75	2/15	87

CD2F1 or B6D2F1 mice received IP 100 μg of anti–IL-1R antibody, 1:10 dilution of polyclonal rabbit anti-SIF serum, or preimmunized rabbit serum; 800 μg of anti–GM-CSF, anti–IL-3, or anti–IL-4 antibody; 800 μg GL 113 or rat Ig; or saline in 0.5 mL total volume. Six to 20 hours later, mice received 100 ng of IL-1 or 1 μg of LPS IP, and 1 day later received 950 cGy gamma radiation.

* Different ($P < .05$) from the treatment groups, but not different from the control, saline-only–treated mice.

Table 2. Effect of Anti-HGF Antibodies on Survival of $LD_{50/30}$ Irradiated Mice

Treatment	Dead/Total	% Survival
Saline	28/60	53
Anti–IL-1R (100 μg)	19/20	5*
Anti–SIF (1:10)	40/40	0*
rIg (800 μg)	10/20	50
Anti–IL-3 (400 μg)	4/18	78
Anti–IL-3 (800 μg)	5/18	72
Anti–GM-CSF (800 μg)	6/18	66
Anti–IL-4 (400 μg)	11/28	60
Anti–IL-4 (800 μg)	14/28	50

CD2F1 mice received 825 cGy radiation followed by IP administration of saline, antibody, or control Ig in doses as specified in 0.5 mL total volume.

* Different ($P < .05$) from the control, saline-treated mice

Assessment of biologic effects of anti-SIF antibody. We have tested the anti-SIF antibody in unirradiated as well as irradiated, untreated, and IL-1–radioprotected mice for their effect on bone marrow cells. Mice received a single injection of 1:10 dilution of anti-SIF antibody or control rabbit serum and their bone marrow cells were examined for CFUs in lethally irradiated recipients. Whereas 5×10^4 bone marrow cells from saline alone treated mice yielded 17.2 ± 2.8 splenic colonies, the same number of cells from anti-SIF–treated or control rabbit serum-treated mice yielded 14.6 ± 1.4 and 13.4 ± 4.4 colonies, respectively. Thus, a single dose of the antibody in normal mice did not reduce the number of hematopoietic progenitor cells.

However, similar treatment followed by irradiation resulted in a reduced number of recovering bone marrow cells. Thus, mice receiving $LD_{50/30}$ irradiation and anti-SIF antibody had 2.2×10^6 bone marrow cells/femur at 8 days postirradiation, whereas the control antibody receiving mice had 4.5×10^6 cells/femur. Similarly, after $LD_{100/30}$ irradiation, mice that had received IL-1 had 2.4×10^6 cells/femur, mice receiving control antibody and IL-1 had 1.8×10^6 cells/femur, and mice receiving anti-SIF antibody and IL-1 had 1.0×10^6 cells/femur. Additional assays showed that anti-SIF serum in normal mice did not affect the titers of IL-1–induced CSF in the serum.

DISCUSSION

These results represent the first demonstration that endogenously produced SIF is absolutely necessary for survival from lethal irradiation of unmanipulated mice as well as LPS- and IL-1–radioprotected mice. SIF has been reported to act as a most potent comitogen, in combination with IL-6, IL-3, or IL-1, for hematopoietic stem cells (HSCs).[7,15] Although

treatment of mice with antibody to c-*kit*/SIF receptor resulted in elimination of hematopoietic progenitor cells,[16] the requirement for c-*kit* ligand/SIF for fetal hematopoiesis was questioned by a recent report showing that absolute numbers of hematopoietic progenitor cells nevertheless still increase in SIF-deficient S1/S1 mice.[17]

Our results showing that untreated, as well as IL-1– and LPS-radioprotected mice, do not survive lethal irradiation after receiving SIF neutralizing antibody suggest that the capacity of an animal to survive lethal hematopoietic syndrome depends on the availability of SIF. The question of whether SIF is also required for constitutive hematopoiesis remains to be addressed. Constitutive expression of messenger RNA (mRNA) for SIF was detected in the bone marrow of unmanipulated normal adult mice and was further upregulated in the bone marrow of 5-FU–treated mice (D.W., unpublished results), suggesting that, indeed, constitutive and emergency hematopoiesis may depend on the supply of SIF. The administration of the anti-SIF antibody to IL-1–treated, unirradiated mice did not affect the levels of serum CSF and the numbers of CFUs, but significantly reduced the recovery of bone marrow cells in IL-1–treated, as well as untreated, lethally irradiated mice. These results suggest that SIF may be required for emergency hematopoiesis.

The requirement for SIF is similar to the previously observed requirement for IL-1 and TNF, because antibody to IL-1R and TNF, each administered separately, abrogated radioprotection by IL-1, TNF, or LPS and also enhanced the rate of mortality of unmanipulated mice.[8] Similarly, anti–IL-6 antibody blocked IL-1– and TNF-induced radioprotection and increased the numbers of unmanipulated mice dying after $LD_{50/30}$ irradiation.[9] Taken together, our results indicate that the presence of each of four cytokines (IL-1, TNF, IL-6, and SIF) is absolutely required for hematopoietic recovery from the lethal effects of radiation.

In contrast, systemic administration of antibodies to each of the cytokines (GM-CSF, IL-3, and IL-4) did not reduce the number of surviving mice, although these three cytokines are known stimulators of hematopoietic cells. Repeated administration of GM-CSF, IL-3, and IL-4 after irradiation with less than $LD_{95/30}$ doses increases the number of surviving animals.[18-20] There is an apparent inconsistency between the two sets of observations above. However, because the effects of these three cytokines on early progenitor cells may overlap, treatment with a single antibody may be insufficient to counteract the effect of the remaining cytokines. Alternatively, GM-CSF, IL-3, and IL-4 may be produced in amounts too high to be neutralized by the amount of antibodies used in this study. However, in vivo treatment with 0.5 mg/mouse of anti–GM-CSF antibody significantly reduced the survival of *C neoformans*-infected mice,[21] suggesting that the quantity of the antibody used in our experiments (0.8 mg/mouse) should have been sufficient. Of the three cytokines (IL-3, IL-4, and GM-CSF), GM-CSF is likely to be more prevalent, because it is produced by many cell types, including T cells, monocytes, fibroblasts, and endothelial cells, and is also present in circulation after challenge with LPS or IL-1.[14] In contrast, IL-3 and IL-4 are T-cell products and may be less readily available in the bone marrow. Perhaps local cell-to-cell interaction in a tissue such as spleen allows for utilization of IL-3 and IL-4 in hematopoiesis. However, such a local effect might reduce the accessibility of the cytokine to the neutralizing antibody.

Thus, our results indicate that SIF is critical for survival from lethal irradiation and is generated in limiting quantities, because a single dose of only 0.05 mL/mouse of immune serum precluded recovery.

ACKNOWLEDGMENT

We thank William Jackson for statistical analysis of the results and Drs Joost Oppenheim, David Ledney, and Dov Pluznik for critical comments on this manuscript.

REFERENCES

1. Ainsworth EJ, Hatch MH: Decreased x-ray mortality in endotoxin-treated mice. Radiat Res 9:96, 1958

2. Neta R, Oppenheim JJ, Douches SD: Interdependence of the radioprotective effects of human recombinant IL-1, TNF, G-CSF, and murine recombinant G-CSF. J Immunol 140:108, 1988

3. Neta R, Sayers T, Oppenheim JJ: Relationship of tumor necrosis factor to interleukins, in Vilcek J, Aggarwal B (eds): Tumor Necrosis Factor: Structure, Function and Mechanism of Action. New York, NY, Marcel Dekker, 1991, p 499

4. Metcalf D: The multipotential colony-stimulating factor, multi-CSF (IL 3). Lymphokines 15:183, 1988

5. Peschel C, Paul WE, Ohara J, Green I: Effects of B-cell stimulatory factor-1/interleukin-4 on hematopoietic progenitor cells. Blood 70:254, 1987

6. Williams DE, Eisenman J, Baird A, Rauch C, Ness KV, March CJ, Park LS, Martin U, Mochizuki DY, Boswell HS, Burgess GS, Cosman D, Lyman SD: Identification of the ligand for the c-kit proto-oncogene. Cell 63:167, 1990

7. de Vries P, Brasel KA, Eisenman JR, Alpert AR, Williams DE: The effect of recombinant mast cell growth factor on purified murine hematopoietic stem cells. J Exp Med 173:1205, 1991

8. Neta R, Oppenheim JJ, Schreiber RD, Chizzonite R, Ledney GD, MacVittie TJ: Role of cytokines (interleukin 1, tumor necrosis factor, and transforming growth factor b) in natural and lipopolysaccharide-enhanced radioresistance. J Exp Med 173:1177, 1991

9. Neta R, Perlstein R, Vogel SN, Ledney GD, Abrams J: Role of IL 6 in protection from lethal irradiation and in endocrine responses to IL 1 and TNF. J Exp Med 175:689, 1992

10. Chizonetti R, Truitt T, Kilian PL, Stern AS, Nunes P, Parker KP, Kaffka KL, Chua AO, Lugg DK, Gubler U: Two high-affinity interleukin-1 receptors represent separate gene products. Proc Natl Acad Sci USA 86:8029, 1989

11. Finkelman FD, Katona IM, Urban JF, Holmes J, Ohara J, Tung AS, Sample JG, Paul WE: IL 4 is required to generate and sustain in vivo IgE responses. J Immunol 141:2335, 1988

12. O'Garra A, Barbis D, Wu J, Hodgkin PD, Abrams J, Howard M: The BCL1 B lymphoma responds to IL 4, IL 5 and GM CSF. Cell Immunol 123:189, 1989

13. Abrams JS, Pearce MK: Development of rat anti-mouse interleukin 3 monoclonal antibodies which neutralize bioactivity in vitro. J Immunol 140:131, 1988

14. Vogel SN, Douches SD, Kaufman EN, Neta R: Induction of colony stimulating factor in vivo by recombinant interleukin-1 α and recombinant tumor necrosis factor α. J Immunol 138:2143, 1987

15. Metcalf D, Nicola NA: Direct proliferative actions of stem cell factor on murine bone marrow cells in vitro: Effects of combi-

nation with colony-stimulating factors. Proc Natl Acad Sci USA 88: 6239, 1991

16. Ogawa M, Matsuzaki Y, Nishikawa S, Hayashi SI, Kunisada T, Sudo T, Kina T, Nakauchi H, Nishikawa SI: Expression and function of c-kit in hematopoietic progenitor cells. J Exp Med 174:63, 1991

17. Ikuta K, Weissman IL: Evidence that hematopoietic stem cells express mouse c-kit but do not depend on steel factor for their generation. Proc Natl Acad Sci USA 89:1502, 1992

18. Kindler V, Thorens B, De Kossodo S, Allet B, Eliason JF, Thacher D, Farber N, Vassalli P: Stimulation of hematopoiesis in vivo by recombinant bacterial murine interleukin 3. Proc Natl Acad Sci USA 83:1001, 1986

19. Neta R, Wong GHW, Pilcher M: LIF and IL 4 used after lethal irradiation protect mice from death. Lymphokine Res 9:568, 1990

20. Monroy RI, Skelly RR, MacVittie TJ, Davis IA, Sauber JJ, Clark SC, Donahue RE: The effect of recombinant GM-CSF on the recovery of monkeys transplanted with autologous bone marrow. Blood 70:1696, 1987

21. Collins HL, Bancroft GJ: Cytokine enhancement of complement-dependent phagocytosis by macrophages. Synergy of tumor necrosis factor-α and granulocyte-macrophage colony-stimulating factor for phagocytosis of Cryptococcus neoformans. Eur J Immunol 22:1447, 1992

Experimental Hematology 21:338–344 (1993)

Experimental Hematology

Effects of combined administration of interleukin-6 and granulocyte colony-stimulating factor on recovery from radiation-induced hemopoietic aplasia

M.L. Patchen, R. Fischer, T.J. MacVittie
Department of Experimental Hematology, Armed Forces Radiobiology Research Institute, Bethesda, MD
Offprint requests to: Myra L. Patchen, PhD, Department of Experimental Hematology, Armed Forces Radiobiology Research Institute, Building 42, NNMC, Bethesda, MD 20889-5145
(Received 22 May 1992; in revised form 1 September 1992; accepted 14 September 1992)

Abstract. Hemopoietic aplasia is the primary limitation of drug and radiation cancer therapies. We have previously demonstrated that, individually, both interleukin-6 (IL-6) and granulocyte colony-stimulating factor (G-CSF) can accelerate recovery from radiation-induced hemopoietic aplasia. In vitro studies suggest that IL-6 affects cells early in the hemopoietic hierarchy, while G-CSF affects more committed progenitor cells. Because these cytokines may also affect different cell populations in vivo, we hypothesized that the use of these agents in combination may further enhance recovery from hemopoietic aplasia. Female B6D2F1 mice were exposed to a high sublethal 7.75 Gy dose of ^{60}Co radiation. Following irradiation, mice were administered subcutaneous injections of either saline, 500 μg/kg of recombinant human IL-6 once daily on days 1-6, 125 μg/kg of recombinant human G-CSF once daily on days 1–17, or both cytokines as described. Peripheral white blood cell (WBC), red blood cell (RBC), and platelet (PLT) counts, as well as femoral and splenic granulocyte-macrophage colony-forming cell (GM-CFC) and day-12 spleen colony-forming unit (CFU-S) contents were evaluated on days 7, 10, 14, 17 and 21 postirradiation. IL-6 treatment alone slightly accelerated postirradiation recovery of most hemopoietic parameters, while G-CSF treatment dramatically enhanced recovery of all hemopoietic parameters evaluated. Co-administration of IL-6 and G-CSF further enhanced the hemopoietic recovery. The most notable effects in combination-treated mice were on recoveries of bone marrow and splenic CFU-S, which were significantly enhanced above those in G-CSF-treated irradiated mice as early as day 10 postirradiation. Although by day 14 postirradiation, splenic GM-CFC and CFU-S recoveries in both G-CSF- and combination-treated mice had surpassed unirradiated control values, combination-treated mice exhibited a greater overshoot. These studies demonstrate the ability of IL-6 treatment to enhance G-CSF-mediated acceleration of multilineage recovery following radiation-induced hemopoietic aplasia.

Key words: IL-6—G-CSF—Radiation—Myelosuppression—Therapy

Introduction. Hemopoietic stem and progenitor cell injury and the resulting depletion of functional white blood cells and platelets are critical problems associated with both chemotherapy and radiation exposure [1-3]. Sustained hemopoietic recovery following chemotherapy or radiation exposure requires surviving pluripotent stem cells to self-renew as well as to differentiate into multipotent and committed progenitors capable of giving rise to functional mature cells [4-7].

IL-6 and G-CSF are two cytokines that, individually, stimulate hemopoiesis in vivo in normal animals [8-15] and enhance hemopoietic recovery when administered after radiation-induced hemopoietic injury [11,16-19]. While G-CSF has been shown to selectively stimulate the proliferation of progenitor cells committed to myeloid differentiation [6,7], IL-6 has been reported to elicit numerous effects [8,20-26], including the production of platelets [9-11]. As opposed to acting on committed progenitor cells, IL-6 appears to act on multipotential cells more proximal to the hemopoietic stem cells, synergistically enhancing the responsiveness of these cells to additional hemopoietic cytokines. In vitro data suggest that IL-6 accomplishes this by shifting uncommitted cells from the G0 to the G1 stage of the cell cycle where they become more responsive to additional hemopoietic factors [20-24], perhaps, via cytokine receptor upregulation. Because IL-6 and G-CSF appear to affect hemopoiesis at distinct levels within the hemopoietic heirachy, we hypothesized that the use of these agents in combination may be more effective at enhancing hemopoietic recovery in myelosuppressed animals than the use of these agents individually. In these studies, we have evaluated the ability of IL-6 plus G-CSF therapy to enhance recovery from radiation-induced hemopoietic injury.

Materials and methods

Mice. B6D2F1 female mice (~20 g) were purchased from Jackson Laboratories (Bar Harbor, ME). Mice were maintained in an accredited AAALAC (American Association for Accreditation of Laboratory Animal Care) facility in Micro-Isolator cages on hardwood-chip, contact bedding and were provided commercial rodent chow and acidified water (pH 2.5) ad libitum. Animal rooms were equipped with full-spectrum light from 0600 to 1800 hours and were maintained at 21°C ± 1°C and 50% ± 10% relative humidity with at least 10 air changes per hour of 100% conditioned fresh air. Upon arrival, all mice were tested for *Pseudomonas* and quarantined until test results were obtained. Only healthy mice were released for experimentation. All animal experiments were approved by the Institute Animal Care and Use Committee prior to performance.

IL-6 and G-CSF. Recombinant human IL-6 and recombinant human G-CSF were provided by Amgen (Thousand Oaks, CA). IL-6 (lot #012789) had a specific activity of 1.52×10^7 U/mg and G-CSF (lot #600) had a specific activity of 10^8 U/mg. Endotoxin contamination was less than 0.5 ng/mg protein based on the limulus amebocyte lysate assay.

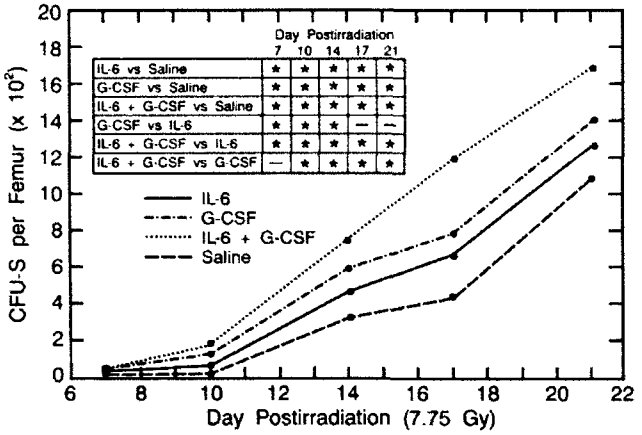

Fig. 1. Effect of IL-6, G-CSF, and IL-6 plus G-CSF on bone marrow CFU-S recovery in irradiated B6D2F1 mice. Mice were exposed to 7.75 Gy ^{60}Co and subcutaneously administered either saline, IL-6 (500 μg/kg/day on days 1-6), G-CSF (125 μg/kg/d on days 1-17), or IL-6 plus G-CSF. Data represent the means of values obtained from 3 experiments. CFU-S values in nonirradiated control mice were 6837 ± 198 per femur. *p<0.05.

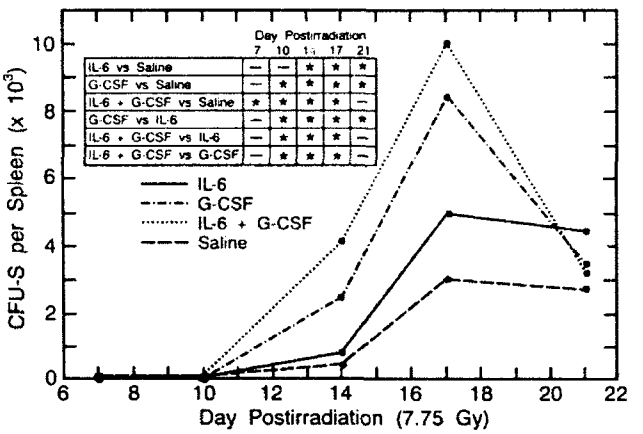

Fig. 2. Effect of IL-6, G-CSF, and IL-6 plus G-CSF on splenic CFU-S recovery in irradiated B6D2F1 mice. Mice were exposed to 7.75 Gy ^{60}Co and subcutaneously administered either saline, IL-6, G-CSF, or IL-6 plus G-CSF as described in Figure 1. Data represent the means of values obtained from 3 experiments. CFU-S values in nonirradiated control mice were 2378 ± 197 per spleen. *p<0.05.

Irradiation. The ^{60}Co source at the Armed Forces Radiobiology Research Institute (AFRRI) was used to administer bilateral total-body ^{60}Co gamma radiation. Mice were placed in ventilated Plexiglas containers and irradiated at a dose rate of 0.4 Gy/min. Dosimetry was performed using ionization chambers as previously described [27], with calibration factors traceable to the National Institute of Standards and Technology. Before experiments were initiated, the dose rate at the midline of an acrylic mouse phantom was measured with a 0.5 cm^3 tissue-equivalent ionization chamber manufactured by Exradin (Lisle, IL). Before each experimental irradiation, the dose rate at the same location with the phantom removed was measured with a 50 cm^3 ionization chamber fabricated at AFRRI. The ratio of these 2 dose rates, the tissue-air ratio (TAR), was then used to ensure delivery of the midline dose desired for each animal exposure. The TAR in these experiments was 1.001.

Cell suspensions. The cell suspensions used for each assay represented tissues from 3 normal, irradiated, or cytokine-treated and irradiated mice at each time point. Cells were flushed from femurs with 3.0 mL of McCoy's 5A medium (Flow Labs, McLean, VA) containing 10% heat-inactivated fetal bovine serum (Hyclone Labs, Logan, UT). Spleens were pressed through a stainless steel mesh screen, and the cells were washed from the screen with 6.0 mL medium. The number of nucleated cells in the suspensions was determined by Coulter counter. Femurs and spleens were removed from mice euthanized by cervical dislocation.

Spleen colony-forming unit assay. Exogenous spleen colony-forming units (CFU-S) were evaluated by the method of Till and McCulloch [28]. Recipient mice were exposed to 9.25 Gy of total-body radiation to eradicate endogenous hemopoietic stem cells. Three to 5 hours later, bone marrow or spleen cells were intravenously (IV) injected into the irradiated recipients. Twelve days after transplantation, the recipients were euthanized by cervical dislocation and their spleens were removed. The spleens were fixed in Bouin's solution, and the grossly visible spleen colonies were counted. Each treatment group consisted of 5 mice and experiments were repeated 3 times.

Granulocyte-macrophage colony-forming cell assay. Hemopoietic progenitor cells committed to granulocyte and/or macrophage development were assayed using a double-layer agar granulocyte-macrophage colony-forming cell (GM-CFC) assay [29]. Mouse endotoxin serum (5% v/v) was added to feeder layers as a source of colony-stimulating factors. Colonies (>50 cells) were counted after 10 days of incubation in a 37°C humidified environment containing 5% CO_2. Triplicate plates were cultured for each cell suspension, and experiments were repeated 3 times.

Peripheral blood cell counts. Blood was obtained from halothane-anesthetized mice by cardiac puncture using a heparinized syringe attached to a 20-gauge needle. White blood cell (WBC), red blood cell (RBC) and platelet (PLT) counts were performed with a Coulter counter.

Statistics. Results of replicate experiments were pooled and the means ± standard errors of pooled data were calculated. Student's *t*-test was used to determine statistical differences. Significance level was set at p<0.05, and statistical differences between treatment groups are indicated on the figures.

Experimental design. Mice were exposed to 7.75 Gy of whole-body ^{60}Co radiation. Postirradiation, cytokines were administered subcutaneously (s.c.) in a 0.1 mL volume at 500 μg/kg/d for IL-6 and at 125 μg/kg/d for G-CSF. G-CSF was administered on days 1 through 17 postirradiation. IL-6 was generally administered only on days 1 through 6 postirradiation for fear that prolonged treatment with this cytokine (which is known to act on early hemopoietic stem cells) might result in stem cell "burnout." In one experiment (Table 1), however,

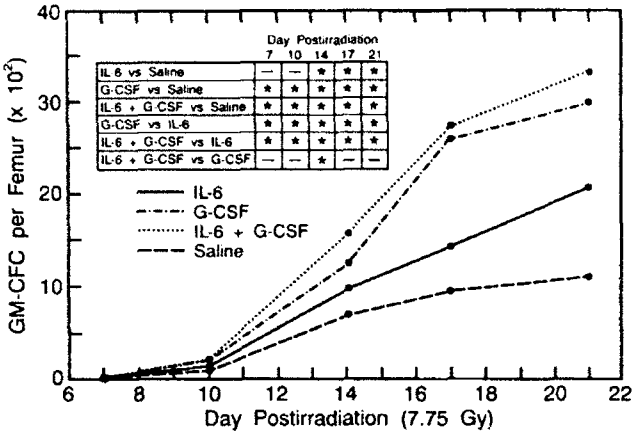

Fig. 3. Effect of IL-6, G-CSF, and IL-6 plus G-CSF on bone marrow GM-CFC recovery in irradiated B6D2F1 mice. Mice were exposed to 7.75 Gy ^{60}Co and subcutaneously administered either saline, IL-6, G-CSF, or IL-6 plus G-CSF as described in Figure 1. Data represent the means of values obtained from 3 experiments. GM-CFC values in nonirradiated control mice were 11,478 ± 406 per femur. *p<0.05.

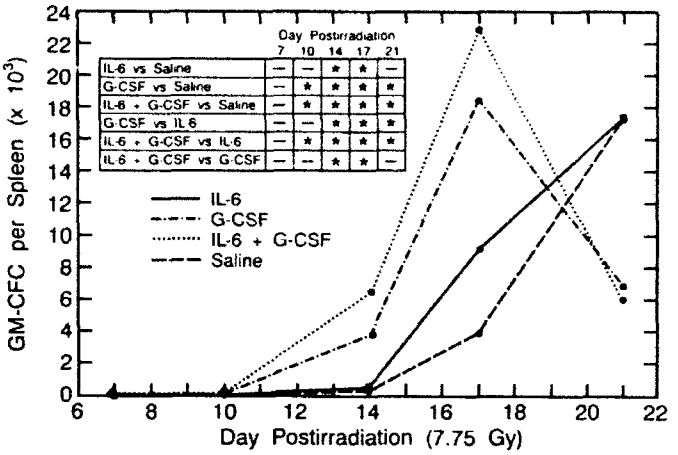

Fig. 4. Effect of IL-6, G-CSF, and IL-6 plus G-CSF on splenic GM-CFC recovery in irradiated B6D2F1 mice. Mice were exposed to 7.75 Gy ^{60}Co and subcutaneously administered either saline, IL-6, G-CSF, or IL-6 plus G-CSF as described in Figure 1. Data represent the means of values obtained from 3 experiments. GM-CFC values in nonirradiated control mice were 3036 ± 180 per spleen. *p<0.05.

mice were administered IL-6 on days 1 through 17. Irradiated mice received either saline, IL-6, G-CSF, or IL-6 plus G-CSF. On days 7, 10, 14, 17 and 21 postirradiation, 3 mice from each treatment group were euthanized to evaluate hemopoietic recovery based on bone marrow and splenic CFU-S and GM-CFC content and on peripheral blood WBC, RBC and PLT numbers. Nonirradiated mice (normal controls) were also evaluated at each time point.

Results

Effects on stem cell repopulation. The ability of IL-6, G-CSF, and IL-6 plus G-CSF therapies to accelerate bone marrow and splenic CFU-S recovery in irradiated mice is illustrated in Figures 1 and 2, respectively. As early as day 7 postirradiation, bone marrow CFU-S numbers in all cytokine-treated mice were significantly greater than in saline-treated mice. In general, G-CSF therapy was more effective than IL-6 therapy, and combination therapy was more effective than G-CSF therapy. Combination therapy produced significantly greater bone marrow CFU-S recovery than either IL-6 or G-CSF therapy on days 10, 14, 17 and 21 postirradiation.

In the spleen, only the combination therapy statistically enhanced CFU-S recovery within 7 days postirradiation. At later times, significantly enhanced splenic CFU-S recovery was observed in all cytokine-treated mice, with combination therapy again being significantly more effective than G-CSF therapy, and G-CSF therapy being significantly more effective than IL-6 therapy. In contrast to the gradual cytokine-induced CFU-S recovery observed in the bone marrow, splenic CFU-S recovery in all cytokine-treated mice exceeded that in nonirradiated mice by day 17 postirradiation. At this time, IL-6-, G-CSF- and combination-treated mice, respectively, exhibited 206%, 354% and 422% of number of normal control splenic CFU-S. By day 21 postirradiation, however, the number of splenic CFU-S in cytokine-treated mice decreased toward normal levels.

Effects on granulocyte-macrophage progenitor cell repopulation. In comparison to saline treatment, all cytokine treatments accelerated bone marrow (Fig. 3) and splenic (Fig. 4) GM-CFC recovery. G-CSF therapy was again significantly more effective than IL-6 therapy. Combination therapy, although it again appeared to be more effective than G-CSF therapy, statistically offered an advantage over G-CSF therapy only at day 14 postirradiation. In spite of initial recovery delays, splenic GM-CFC numbers in all cytokine-treated mice dramatically overshot splenic GM-CFC numbers in normal (nonirradiated) control mice. By day 17 postirradiation, GM-CFC numbers in combination-, G-CSF- and IL-6-treated mice were, respectively, 758%, 614% and 302% of normal control values.

Effects on mature peripheral blood cell repopulation. The reappearance of peripheral WBCs, RBCs and PLTs indicated that all 3 cytokine treatments could facilitate multilineage hemopoietic repopulation (Figs. 5-7). Combination- and G-CSF-treatment led to production of WBCs within 14 days postirradiaton, and production of RBCs and PLTs within 17 days postirradiation. Although evidence of RBC recovery in IL-6-treated mice also occurred on day 17 postirradiation, elevated WBC and PLT recovery was not observed until day 21 postirradiation.

Effects of prolonged IL-6 administration on hemopoietic repopulation. In our final experiment, additional groups of mice were incorporated to evaluate the hemopoietic effects of 6-day vs. 17-day IL-6 treatment. In this experiment, deaths were observed in mice treated long-term with IL-6 alone such that, by day 21 postirradiation, no IL-6-treated mice remained alive to be evaluated. Although mice receiving IL-6 for 17 days plus G-CSF survived better than mice receiving the 17-day IL-6 treatment alone, these mice exhibited less CFU-S and GM-CFC recovery than mice receiving only the 6-day IL-6 treatment combined with G-CSF treatment (Table 1). Peripheral blood values also reflected the suppressed progenitor cell effects. At 21 days postirradiation, peripheral WBC, RBC and

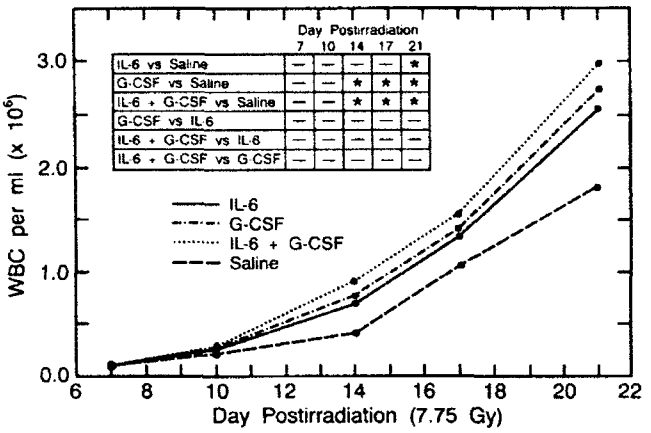

Fig. 5. Effect of IL-6, G-CSF, and IL-6 plus G-CSF on white blood cell recovery in irradiated B6D2F1 mice. Mice were exposed to 7.75 Gy ^{60}Co and subcutaneously administered either saline, IL-6, G-CSF, or IL-6 plus G-CSF as described in Figure 1. Data represent the means of values obtained from 3 experiments. WBC values in nonirradiated control mice were $5.39 \pm 0.35 \times 10^6$ per mL. *p<0.05.

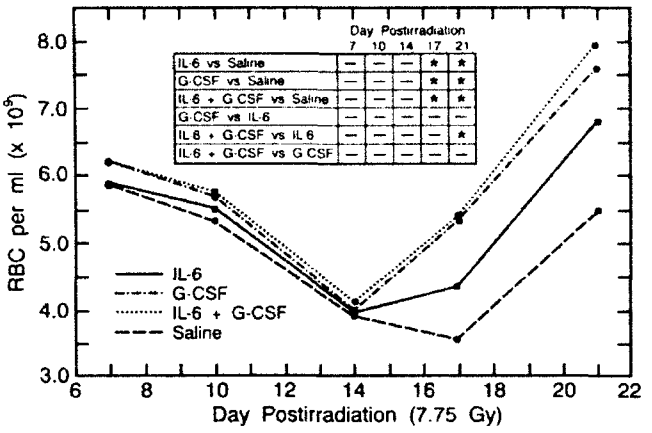

Fig. 6. Effect of IL-6, G-CSF, and IL-6 plus G-CSF on red blood cell recovery in irradiated B6D2F1 mice. Mice were exposed to 7.75 Gy ^{60}Co and subcutaneously administered either saline, IL-6, G-CSF, or IL-6 plus G-CSF as described in Figure 1. Data represent the means of values obtained from 3 experiments. RBC values in nonirradiated control mice were $9.06 \pm 0.12 \times 10^9$ per mL. *p<0.05.

PLT numbers in 6-day IL-6-treated mice, respectively, were 3.90×10^6/mL, 8.16×10^9/mL and 522×10^6/mL, while WBC, RBC and PLT numbers in 17-day IL-6-treated mice, respectively, were only 1.90×10^6/mL, 5.94×10^9/mL and 244×10^6/mL.

Discussion

Morbidity and mortality associated with high-level chemotherapy or radiation exposures can be directly attributed to infectious and hemorrhagic complications resulting from therapy-induced neutropenia and thrombocytopenia. Recovery from potentially lethal effects of hemopoietic depletion requires both the generation of functional granulocytes and platelets that will prevent sepsis and hemorrhage, and the self-renewal of pluripotent and multipotent stem cells that will lead to long-term reconstitution of the hemopoietic system.

In recent years, at least 5 cytokines (G-CSF, GM-CSF, IL-1, IL-3 and IL-6) have been evaluated for the ability to stimulate hemopoietic regeneration following radiation- or chemotherapy-induced myelosuppression [11,14,16-19,30-37]. The lineage-specific cytokine G-CSF, particularly, has shown promise [14,16-19,30,35-37]. In preclinical studies involving irradiated canines, G-CSF dramatically accelerated granulocytic recovery and reduced infections; however, platelet recovery was unaffected, and without platelet transfusions, irradiated animals remained at risk for spontaneous hemorrhage. Promise of treatment for thrombocytopenia has recently come from studies demonstrating the ability of IL-6 to enhance platelet recovery following suppressive radiation or chemotherapy in mice [11,31]. Based on these effects, we hypothesized that combinations of cytokines capable of inducing the production of multiple cell types necessary for survival following chemotherapy and radiation exposures might be more beneficial than individual agents. The combination IL-6 plus G-CSF was chosen for evaluation not only because of the desirable effects each agent induced on granulocyte and platelet production but also because in vitro data indicated an ability of IL-6 to synergize with G-CSF to expand progenitor cell populations committed to granulocytic differentiation [22].

Data presented in this paper confirm previous data describing the abilities of IL-6 and G-CSF, individually, to accelerate hemopoietic recovery in myelosuppressed mice. In this study, IL-6 and G-CSF induced regeneration of multiple hemopoietic cell lineages, including WBCs, RBCs and PLTs, presumably, via the ability of each to enhance regeneration of multipotent CFU-S as well as committed GM-CFC progenitor cells. G-CSF was generally more effective at enhancing recovery than was IL-6. The differences in effectiveness may have occurred because IL-6 was administered for only 6 days postirradiation, while G-CSF was administered for 17 days postirradiation. This is unlikely, however, since we have observed that 17-day IL-6 treatment is not as effective as 6-day IL-6 treatment in stimulating hemopoietic recovery in irradiated mice.

Based on the fact that G-CSF in vitro has been shown to selectively induce granulocytic proliferation and differentiation 16,17], the multilineage effects we observed in vivo following G-CSF administration might seem unusual. It is interesting to note, however, that recently multilineage (granulocyte, erythrocyte and platelet) effects have also been observed in some myelodysplastic patients following G-CSF administration [38,39]. The discrepancy between in vitro and in vivo effects of G-CSF suggests that some in vivo effects may be indirectly mediated, possibly through the induction of additional hemopoietic cytokines (as has been shown for GM-CSF) [40,41], or through the regulation of cytokine receptor expression. Although no direct evidence of G-CSF-induced hemopoietic cytokine production has yet been reported, G-CSF has been demonstrated to increase IL-1 receptor expression on bone marrow cells both in vitro and in vivo [42]. Since IL-1 is known to be a potent hemopoietic regulator in combination with G-CSF (34), an alteration of IL-1 receptor expression may contribute to the hemopoietic effects observed following G-CSF administration in irradiated mice.

Based on in vitro data [20-22,24-26], the multilineage effects observed following IL-6 administration were not sur-

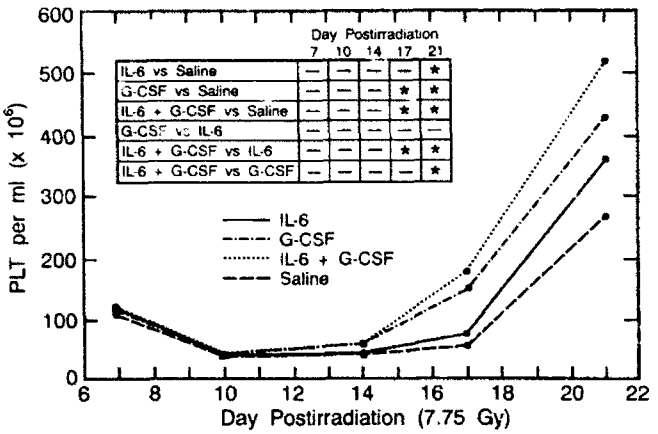

Fig. 7. Effect of IL-6, G-CSF, and IL-6 plus G-CSF on peripheral blood platelet recovery in irradiated B6D2F1 mice. Mice were exposed to 7.75 Gy ^{60}Co and subcutaneously administered either saline, IL-6, G-CSF, or IL-6 plus G-CSF as described for Figure 1. Data represent the means of values obtained from 3 experiments. PLT values in nonirradiated control mice were 904 +/-38x10^6 per mL. *p<0.05.

prising. Of particular interest, however, was the ability of IL-6 to stimulate RBC regeneration. Previous studies have demonstrated anemia following IL-6 administration [10,43]. These studies, however, were performed in normal mice and primates. We can only speculate that the mechanisms regulating lineage commitment may be very different in normal vs. hemopoietically depleted animals. In fact, recent studies in our laboratory [44,45] have demonstrated that messenger ribonucleic acid (mRNA) expression for a variety of hemopoietic cytokines is increased in hemopoietic tissues following a radiation exposure such as the one used in the studies presented here. In particular, bone marrow and splenic IL-1, GM-CSF, and *c-kit* ligand expression have been observed to be dramatically increased; depending on the specific cytokine and tissue, increases can be observed as early as 6 hours postexposure and persist for up to 10 days postexposure. Hence, it is also possible that in vivo IL-6 and G-CSF may interact with additional cytokines being endogenously produced in the irradiated animal to induce the multiple hemopoietic responses observed.

Because IL-6 is known to act on early multipotent progenitor cells [20-26], IL-6 treatment was intentionally restricted in length for fear that continual IL-6 administration, especially in combination with simultaneous G-CSF administration, might induce multipotential cells to differentiate at the expense of self-renewal and result in "stem cell burnout." Although this did not appear to be a problem with the 6-day IL-6 protocol used in our studies, the detrimental effects observed following prolonged IL-6 treatment alone or in combination with G-CSF, suggest that further cautious investigation of this issue is warranted to determine whether these effects reflect IL-6 toxicity or stem cell burnout.

In addition to individual effects, data presented in this paper provide evidence of the ability of IL-6 and G-CSF to interact in vivo to further enhance multilineage hemopoietic regeneration in irradiated mice above that induced by IL-6 or G-CSF individually. Simultaneous IL-6 and G-CSF administration was chosen for evaluation instead of sequential administration based on Rennick's data demonstrating that simultaneous factors were necessary for in vitro synergy [22], and on our experience with in vivo combinations of IL-3 and GM-CSF, where simultaneous administration proved superior to sequential administration in myelosuppressed animals (MacVittie et al. unpublished). The IL-6 plus G-CSF therapy accelerated hemopoietic recovery more than G-CSF therapy (the next best treatment) based on all parameters evaluated (i.e., femoral and splenic CFU-S and GM-CFC values as well as WBC, RBC and PLT values). The earliest and most striking effects were observed on CFU-S recovery, which was evident 3 to 4 days earlier in combination-treated mice than in G-CSF-treated mice. Interestingly, peripheral blood parameters revealed the least significant effects. Because the generation of mature functional end cells from progenitor cells may take several days, it is possible that effects on recovery of peripheral blood elements may have been more apparent later than day 21 postirradiation, which was the last time point evaluated in our studies.

Recent studies evaluating *c-kit* ligand used in combination with G-CSF have demonstrated synergistic interactions in the production of blast-cell colonies [46] and in vitro expanded CFU-S [47]. In addition, *c-kit* ligand in combination with G-CSF has been shown to synergistically enhance granulopoiesis in vivo [48, 49]. Our studies have demonstrated that IL-6 plus G-CSF produces a similar in vivo effect. Since *c-kit* ligand, like IL-6, has been reported to be capable of shifting multipotent progenitor cells from G_0 to G_1 of the cell cycle, where they become more responsive to additional cytokines [46], similarities observed following treatment with these two cytokine combinations may be related to a common mechanism.

In conclusion, we have demonstrated the ability of therapeutically administered IL-6 plus G-CSF to enhance CFU-S and GM-CFC repopulation and to accelerate the production of mature WBCs, RBCs and PLTs in radiation-injured mice more effectively than IL-6 or G-CSF alone. Whether these effects are directly or indirectly mediated following in vivo IL-6 and G-CSF administration remains to be determined.

Acknowledgments

The authors are grateful to Ms. Ruth Seemann for technical assistance, to Ms. Donna Solyan for editorial assistance and to Dr. Larry Souza and Amgen for providing the IL-6 and G-CSF used in these studies. This work was supported by the Armed Forces Radiobiology Research Institute, Defense Nuclear Agency, under Research Work Unit 00132. Research was conducted according to the principles enunciated in the Guide for the Care and Use of Laboratory Animals prepared by the Institute of Laboratory Animal Resources, National Research Council.

References

1. Benacerraf B (1960) Influence of irradiation on resistance to infection. Bacteriol Rev 24:35
2. Hammond CW, Tompkins M, Miller CP (1954) Studies on susceptibility to infection following ionizing radiation: time of onset and duration of endogenous bacteremias in mice. J Exp Med 99:405
3. Durack DT (1982) Infection in compromised hosts. In: Lachmann PJ, Peters DK (eds) Clinical Aspects of Immunology. Oxford: Blackwell Scientific Publishers, 1713
4. Metcalf D (ed) (1977) Hemopoietic colonies. New York: Springer Verlag
5. Golde DW, Cline MJ, Metcalf D, Fox CF (eds) (1978) Hemopoietic cell differentiation. New York: Academic

Table 1. Hemopoietic regeneration following 6-day and 17-day IL-6 treatment combined with G-CSF treatment (day 21 postirradiation)

IL-6 treatment	CFU-S per femur	CFU-S per spleen	GM-CFC per femur	GM-CFC per spleen
6-day	1800±124	3338±288	3055±282	6251±563
17-Day	458±32*	1516±136*	603±55*	2842±316*

*$p<0.05$ with respect to 6-day values

Press

6. Robinson BE, Quesenberry P (1990) Review: Hemopoietic growth factors: overview and clinical applications, part I. Am J Med Sci 300:163
7. Robinson BE, Quesenberry P (1990) Review: Hemopoietic growth factors: overview and clinical applications, part II. Am J Med Sci 300:237
8. Suzuki C, Okano A, Takatsuki F, Miyasaka Y, Hirano T, Kishimoto T, Ejima D, Akiyama Y (1989) Continuous perfusion with interleukin-6 (IL-6) enhances production of hematopoietic stem cells (CFU-S). Biochem Biophys Res Commun 159:933
9. Ishibashi T, Kimura H, Shikama Y, Uchida T, Kariyone S, Hirano T, Kishimoto T, Takatsuki F, Akiyama Y (1989) Interleukin-6 is a potent thrombopoietic factor in vivo in mice. Blood 74:1241
10. Asano S, Okano A, Ozawa K, Nakahata T, Ishibashi T, Koike K, Kimura H, Tanioka Y, Shibuya A, Hirano T, Kishimoto T, Takaku F, Akiyama Y (1990) In vivo effects of recombinant human interleukin-6 in primates: stimulated production of platelets. Blood 75:1602
11. Patchen ML, MacVittie TJ, Williams JL, Schwartz GN, Souza LM (1991) Administration of interleukin-6 stimulates multilineage hematopoiesis and accelerates recovery from radiation-induced hematopoietic depression. Blood 77:472
12. Cohen AM, Zsebo KM, Inoue H, Hines D, Boone TC, Chazin VR, Tsai L, Ritch T, Souza LM (1987) In vivo stimulation of granulopoiesis by recombinant human granulocyte colony-stimulating factor. Proc Natl Acad Sci USA 84:2484
13. Fujisawa M, Kobayashi Y, Okabe T, Takaku F, Komatsu Y, Itoh S (1986) Recombinant human granulocyte colony-stimulating factor induces granulocytosis in vivo. Jpn J Cancer Res 77:866
14. Welte K, Bonilla MA, Gillio AP, Boone TC, Potter GK, Gabrilove JL, Moore MAS, O'Reilly RT, Souza LM (1987) Recombinant human granulocyte colony-stimulating factor: effects on hematopoiesis in normal and cyclophosphamide-treated primates. J Exp Med 165:941
15. Fujisawa M, Kobayashi Y, Okabe T, Takaku F, Komatsu Y, Itoh S (1986) Recombinant human granulocyte colony-stimulating factor induces granulocytopoiesis in vivo. JPN J Cancer Res 77:866
16. Patchen ML, MacVittie TJ, Solberg BD, Souza LM (1990) Therapeutic administration of recombinant human granulocyte colony-stimulating factor accelerates hemopoietic regeneration and enhances survival in a murine model of radiation-induced myelosuppression. Int J Cell Cloning 8:107
17. Kobayashi Y, Okabe T, Urabe A, Suzuki N, Takaku F (1987) Human granulocyte colony-stimulating factor produced by *Escherichia coli* shortens the period of granulocytopenia induced by irradiation in mice. JPN J Cancer Res 78:63
18. MacVittie TJ, Monroy RL, Patchen ML, Souza LM (1990) Therapeutic use of recombinant human G-CSF (rhG-CSF) in a canine model of sublethal and lethal whole-body irradiation. Int J Radiat Biol 57:723
19. Tanikawa S, Nakao I, Tsuneoka K, Nara N (1989) Effects of recombinant granulocyte colony-stimulating factor (rG-CSF) and recombinant granulocyte-macrophage colony-stimulating factor (rGM-CSF) on acute radiation hemopoietic injury in mice. Exp Hematol 17:883
20. Ikebuchi K, Wong GG, Clark SC, Ihle JN, Hirai Y, Ogawa M (1987) Interleukin-6 enhancement of interleukin-3-dependent proliferation of multipotential hemopoietic progenitors. Proc Natl Acad Sci USA 84:9035
21. Leary AG, Ikebuchi K, Hirai Y, Wong GG, Yang YC, Clark SC, Ogawa M (1988) Synergism between interleukin-6 and interleukin-3 in supporting proliferation of human hematopoietic stem cells: comparison with interleukin-1 alpha. Blood 71:1759
22. Rennick D, Jackson J, Yang G, Wideman J, Lee F, Hudak S (1989) Interleukin-6 interacts with interleukin-4 and other hematopoietic growth factors to selectively enhance the growth of megakaryocytic, erythroid, myeloid, and multipotential progenitor cells. Blood 73:1828
23. Bruno E, Hoffman R (1989) Effect of interleukin-6 on in vitro human megakaryocytopoiesis: its interaction with other cytokines. Exp Hematol 17:1038
24. Okano A, Suzuki C, Takatsuki F, Akiyama Y, Koike K, Ozawa K, Hirano T, Kishimoto T, Nakahata T, Asano S (1989) In vitro expansion of the murine pluripotent hemopoietic stem cell population in response to interleukin-3 and interleukin-6: application to bone marrow transplantation. Transplantation 48:495
25. Wong GG, Witek-Giannotti JS, Temple PA, Kriz R, Ferenz C, Hewick RM, Clark SC, Ikebuchi K, Ogawa M (1988) Stimulation of murine hemopoietic colony formation by human IL-6. J Immunol 140:3040
26. Suda T, Yamaguchi Y, Suda J, Miura Y, Okano A, Akiyama Y (1988) Effect of interleukin-6 (IL-6) on the differentiation and proliferation of murine and human hemopoietic progenitors. Exp Hematol 16:891
27. Schulz J, Almond PR, Cunningham JR, Holt JG, Loevinger R, Suntharalingam N, Wright KA, Nath R, Lempert D (1983) A protocol for the determination of absorbed dose for high-energy photon and electron beams. Med Physiol 10:741
28. Till JE, McCulloch EA (1961) A direct measurement of the radiation sensitivity of normal mouse bone marrow cells. Radiat Res 14:213
29. Patchen ML, MacVittie TJ (1986) Hemopoietic effects of intravenous soluble glucan administration. J Immunopharmacol 8:407
30. Matsumoto M, Matsubara S, Matsuno T, Tamura M, Hattori K, Nomura H, Ono M, Yokota F (1987) Protective effect of human granulocyte colony-stimulating factor on

microbial infection in neutropenic mice. Infect Immunity 55:2715

31. Takatsuki F, Okano A, Suzuki C, Miyasaka Y, Hirano T, Kishimoto T, Ejima D, Akiyama Y (1990) Interleukin-6 perfusion stimulates reconstitution of the immune and hemopoietic systems after 5-fluorouracil treatment. Cancer Res 50:2885

32. Kindler V, Thornes B, DeKossodo S, Allet B, Eliason JF, Thatcher D, Farber N, Vassalli P (1986) Stimulation of hemopoiesis in vivo by recombinant bacterial murine interleukin-3. Proc Natl Acad Sci USA 83:1001

33. Monroy RL, Skelly RR, Taylor P, Duboid A, Donahue RE, MacVittie TJ (1988) Recovery from severe hemopoietic suppression using recombinant human granulocyte-macrophage colony-stimulating factor. Exp Hematol 16:344

34. Moore MA, Warren DJ (1987) Synergy of interleukin-1 and granulocyte colony-stimulating factor: in vivo stimulation of stem-cell recovery and hematopoietic regeneration following 5-fluorouracil treatment of mice. Proc Natl Acad Sci USA 84:7134

35. Shimamura M, Kobayashi Y, Yuo A, Urabe A, Okabe T, Komatsu Y, Itoh S, Takaku F (1987) Effect of human recombinant granulocyte colony-stimulating factor on hematopoietic injury in mice induced by 5-fluorouracil. Blood 69:353

36. Morstyn G, Campbell L, Souza LM, Alton NK, Keech J, Green M, Sheridan W, Metcalf D, Fox R (1988) Effect of granulocyte colony-stimulating factor on neutropenia induced by cytotoxic chemotherapy. Lancet 1:667

37. Gabrilove JL, Jakubowski A, Scher H, Sternberg C, Wong G, Grous J, Yagoda A, Fain K, Moore MAS, Clarkson B, Oettgen H F, Alton K, Welte K, Souza LM (1988) Effect of a granulocyte colony-stimulating factor on neutropenia and associated morbidity due to chemotherapy for transitional-cell carcinoma of the urothelium. N Engl J Med 318:1414

38. Greenberg PL, Negrin R, Nagler A (1990) The use of haemopoietic growth factor in the treatment of myelodysplastic syndromes. Cancer Surv 9:199

39. Washizuka T, Koike T, Toba K, Nagai K, Takahashi M, Shibata A (1992) A rise of erythrocytes and platelets in a patient with myelodysplastic syndrome during administration of G-CSF. Am J Hematol 39:153

40. Lindemann A, Riedel D, Oster W, Meuer SC, Blohm D, Mertelsmann RH, Herrmann F (1988) Granulocyte-macrophage colony-stimulating factor induces interleukin-1 production by human polymorphonuclear neutrophils. J Immunol 140:837

41. Moore RN, Oppenheim JJ, Farrar JJ, Carter CS, Waheed A, Shadduck RK (1980) Production of lymphocyte-activating factor (interleukin-1) by macrophages activated with colony-stimulating factors. J Immunol 125:1302

42. Shieh JH, Peterson RH, Moore MA (1991) Granulocyte colony-stimulating factor moderation of cytokine receptors on murine bone marrow cells: in vivo and in vitro studies. J Immunol 147:2984

43. McDonald TP, Cottrell MB, Swearingen CJ, Clift RE (1991) Comparative effects of thrombopoietin and interleukin-6 on murine megakaryopoiesis and platelet production. Blood 77:735

44. Baker WH, Limanni A, Chang CM, Wilhams JL, Patchen ML (1992) Comparison of interleukin-1 alpha gene expression in murine spleen after lethal and sublethal cobalt-60 irradiation. Exp Hematol 20:771

45. Chang CM, Baker WH, Limanni A, Williams JL, Fragoso L, Patchen ML (1992) In vivo gene expression of interleukin-3, granulocyte/macrophage colony-stimulating factor, and *c-kit* ligand in murine bone marrow and spleen after sublethal irradiation. Exp Hematol 20:775

46. Tsuji K, Zsebo K, Ogawa M (1991) Enhancement of murine blast cell colony formation in culture by recombinant rat stem cell factor, ligand for *c-kit*. Blood 78:1223

47. Bodine DM, Orlic D, Birkett NC, Seidel NE, Zsebo KM (1992) Stem cell factor increases colony-forming unit spleen colony numbers in vitro in synergy with interleukin-6, and in vivo in Sl/Sl^d mice as a single factor. Blood 79:913

48. Ulrich TR, DelCastillo J, McNiece IK, Yi ES, Alzona CP, Yin S, Zsebo KM (1991) Stem cell factor in combination with granulocyte colony-stimulating factor (CSF) or granulocyte-macrophage CSF synergistically increases granulopoiesis in vivo. Blood 78:1954

49. Molineux G, Migdalska A, Szmitkowski M, Zsebo KM, Dexter TM (1991) Effects on hematopoiesis of recombinant stem cell factor (ligand for *c-kit*) administered in vivo to mice either alone or in combination with granulocyte colony-stimulating factor. Blood 78:961

0013-7227/93/1323-0946$03.00/0
Endocrinology

Vol. 132, No. 3
Printed in U.S.A.

Synergistic Roles of Interleukin-6, Interleukin-1, and Tumor Necrosis Factor in the Adrenocorticotropin Response to Bacterial Lipopolysaccharide *in Vivo**

ROBERT S. PERLSTEIN, MARK H. WHITNALL, JOHN S. ABRAMS, EDWARD H. MOUGEY, AND RUTH NETA

Department of Experimental Hematology (R.S.P., R.N.) and the Department of Physiology (M.H.W.), Armed Forces Radiobiology Research Institute, Bethesda, Maryland 20889-5145; Neuroendocrinology and Neurochemistry Branch, Department of Medical Neurosciences (E.H.M.), Walter Reed Army Institute of Research, Washington, D.C. 20307-5100; and the Department of Immunology, DNAX Research Institute (J.S.A.), Palo Alto, California 94304

ABSTRACT

Administration of lipopolysaccharide (LPS) results in activation of the hypothalamic-pituitary-adrenal axis. LPS induces the release of a number of proinflammatory cytokines, *i.e.* interleukin-1 (IL-1), IL-6, and tumor necrosis factor (TNF), which activate the hypothalamic-pituitary-adrenal axis as well and may mediate the effects of LPS. Variations in the kinetics of appearance of IL-1, TNF, and IL-6 after LPS challenge suggested that these cytokines may play different roles at different times. To elucidate the mutual dependence and contribution of individual cytokines in the course of LPS-induced ACTH release, we used blocking antibodies to IL-6, TNF, and the IL-1 receptor. Our results demonstrate that anti-IL-6 antibody abrogated ACTH induction throughout the course of the response both 2 and 4 h after LPS challenge. In contrast, anti-IL-1 receptor and anti-TNF antibody, given individually, blocked ACTH production at 4 h, but not at 2 h. Only combined administration of these two antibodies diminished, but did not eliminate, ACTH release at 2 h. This is the first demonstration that all three inflammatory cytokines are obligatory for LPS-induced elevation of plasma ACTH. In addition, these results suggest that IL-1, IL-6, and TNF play different roles in LPS-induced ACTH release. (*Endocrinology* **132:** 946–952, 1993)

INFLAMMATION and/or infection lead to activation of the hypothalamic-pituitary-adrenal (H-P-A) axis (1, 2). For many years, this phenomenon was studied in models employing lipopolysaccharide (LPS), a component of bacterial cell walls of gram-negative bacteria (3–6). More recently, a number of proinflammatory cytokines, *i.e.* interleukin-1 (IL-1), IL-6, and tumor necrosis factor (TNF), were shown to similarly activate the H-P-A axis both *in vivo* and *in vitro* (7–9). The finding that these biochemically distinct cytokines had similar effects suggested redundancy. Our previous work, however, indicated that interaction of these cytokines was required for ACTH induction (10, 11).

More specifically, we demonstrated in C3H/HeN mice that within 2 h of ip administration, IL-1 is a potent inducer of ACTH, whereas pharmacological amounts (up to 10 μg) of IL-6 induced only a negligible response (10). However, the combination of IL-1 and IL-6 produced a synergistic response within 30 min of injection (10), and IL-1 induces IL-6 within 2 h of injection (11–13). Together, these results suggested that IL-1 may need to interact with the IL-6 it induces endogenously in stimulating ACTH release. This hypothesis was further supported by our finding that pretreatment with murine monoclonal anti-IL-6 antibody blocked the IL-1-induced ACTH response (11).

LPS induces the release of IL-1, TNF, and IL-6 (14), which may mediate its stimulatory effect on the H-P-A axis. Therefore, the use of cytokine blocking antibodies to modulate the LPS-induced ACTH response should aid in elucidating the mutual dependence and contribution of endogenously produced individual cytokines. Indeed, Rivier *et al.* (5) reported that monoclonal anti-IL-1 receptor antibody partially blocks the H-P-A response to LPS in mice (5). In addition, depletion of cytokines, in particular IL-1, by destruction of macrophages using liposome-encapsulated dichloromethylene diphosphonate blocks the H-P-A response to subpyrogenic amounts of LPS in rats (6).

Moreover, variations in the kinetics of appearance of IL-1, TNF, and IL-6 after LPS challenge have been observed (13, 15–21), suggesting that these cytokines may play different roles at different times. TNF levels were consistently found to peak approximately 1 h after LPS administration and then rapidly declined (13, 15–20), in part probably because TNF release is especially sensitive to negative feedback by the glucocorticoid end product of H-P-A activation (18, 19). In contrast, IL-1 and IL-6 levels were found to peak somewhat later (within 2–4 h) and were sustained longer (15, 17–19, 21). It was, therefore, postulated that TNF initiates, while IL-1 and IL-6 sustain, H-P-A activation after LPS

Received July 28, 1992.

Address all correspondence and requests for reprints to: Dr. Robert S. Perlstein, USAF MC, EXH, AFRRI, Bethesda, Maryland 20889-5145

* This work was supported by the Armed Forces Radiobiology Research Institute, Defense Nuclear Agency, under work units 00129 and 00105. The views presented in this paper are those of the authors; no endorsement by the Defense Nuclear Agency or the Department of Defense has been given or should be inferred. Research was conducted according to the principles enunciated in the Guide for the Care and Use of Laboratory Animals prepared by the Institute of Laboratory Animal Resources, National Research Council.

exposure (8).

In this report, we present results which indicate that IL-1, IL-6, and TNF are required for LPS-induced ACTH induction, and their relative contributions depend on the time interval after LPS challenge.

Materials and Methods

Experimental animals

Female C3H/HeN mice were purchased from the Animal Genetics and Production Branch, NCI (Frederick, MD). Mice were handled as previously described (10).

In the first set of experiments, groups of four to six mice were injected ip with vehicle (0.5 ml pyrogen-free normal saline), control antibody, or antibodies directed against the IL-1 receptor, IL-6, or TNF at 1630 h on day 1. At 0800 h the next morning (day 2), LPS was administered ip to all of the pretreated groups as well as a group that had not received any pretreatment. Either 2 or 4 h later, unanesthetized mice were decapitated (model 130 Rodent Decapitator, Harvard Apparatus, South Natick, MA) with minimal stress to obtain plasma samples for ACTH.

In the second set of experiments, groups of four to six mice were injected ip with vehicle, recombinant human IL-1α (rhIL-1α), rhIL-6, recombinant human TNFα (rhTNFα), or combinations of these cytokines and decapitated 30–180 min later. In a final set of experiments, groups of four to six mice were pretreated with vehicle and antibodies on day 1, as described in the preceding paragraph, injected with a combination of rhIL-1α and rhTNFα at 0800 h on day 2, and decapitated 120 min later.

In addition, 5–10 noninjected control mice were killed on the day of each experiment.

Cytokines and LPS

rhIL-1α (117-271 Ro 24-5008, lot IL-1 2/88; SA, 3×10^8 U/mg) was generously provided by Dr. Peter Lomedico, Hoffman LaRoche, Inc. (Nutley, NJ). rhIL-6 (SDZ 280-969, batch PPG 9001; SA, 5.2×10^7 U/mg) was a gift from Dr. E. Liehl, Sandoz, Vienna, Austria). rhTNFα (lot CP4026P08; SA, 9.6×10^6 U/mg) was provided by Biogen (Cambridge, MA). LPS (protein free; prepared from *Escherichia coli* K235 by the phenol-water extraction method) was kindly provided by Dr. Stefanie Vogel, Uniformed Services University of the Health Sciences (Bethesda, MD). The recombinant cytokines were diluted in 0.5 ml pyrogen-free saline on the day of injection.

Antibodies

Rat monoclonal antibody to mouse rIL-6 (MP5 20F3) was prepared using semipurified Cos-7 mouse IL-6 as an immunogen, as previously described (22). Rat monoclonal antibody to β-galactosidase (GL 113) was used as an isotype control. Rat monoclonal immunoglobulin G1, antimurine IL-1 receptor (anti-IL-1R) antibody (35F5) (23) was generously provided by Dr. R. Chizzonite, Hoffman LaRoche. Hamster monoclonal antibody to murine TNFα (TN3.19.12) (24) was a kind gift from Dr. R. Schreiber, Washington University (St. Louis, MO). The antibodies were diluted in 0.5 ml pyrogen-free saline on the day of injection. The amount of antibody injected (anti-IL-6, anti-IL-1R, and anti-TNF) was approximately the same as the quantity we used in earlier work to block LPS-, IL-1-, and TNF-induced radioprotection (11, 25). Moreover, the amount of anti-IL-1R antibody used (250 μg) was similar to the quantity of the same antibody (200 μg) found to be effective by Rivier *et al.* (5) in partially blocking LPS-induced ACTH release and reducing by 90% IL-1-induced leucocytosis. None of the antibodies injected by themselves had an effect on ACTH release.

Measurement of ACTH in plasma

ACTH was assayed in plasma from decapitated mice using an ^{125}I RIA kit (INCSTAR Corp., Stillwater, MN), as previously described (10). The ACTH antibody used in this assay is derived from rabbits immunized against ACTH-(1–24), a region that is identical in human and murine ACTHs. The threshold sensitivity of this assay was 8 pg/ml.

Statistical analysis

In Figs. 1 and 3, evaluation of the results was carried out using analysis of variance, followed by the Scheffe F test. In Figs. 2 and 4, comparison of the response to each cytokine treatment at each time point with the response to simultaneously injected vehicle was made using Student's *t* test. Comparison of the response to combined cytokine treatment with the sum of the responses to each cytokine treatment given separately at each time point was made as a 1 degree of freedom contrast. For each time point, each *P* value stated reflects a Bonferroni correction for the number of tests run.

Results

LPS-induced ACTH release

The ACTH levels in the plasma of mice receiving various amounts of LPS at 2, 4, and 6 h are presented in Table 1. The administration of all doses of LPS resulted in a maximal ACTH response at 2 h, which progressively diminished at 4 and 6 h. All maximal ACTH responses at 2 h were similar. Therefore, we chose 1 μg LPS to study the modulation of the 2 h ACTH response to LPS. The 4 h ACTH response was similar after 5–50 μg LPS. Therefore, we chose 5 μg LPS to study the modulation of the 4 h ACTH response to LPS. The 6 h ACTH response after all doses of LPS injected was not substantial enough to allow further study. Thus, the magnitude of the ACTH response to LPS in C3H/HeN mice is less than that observed in BALB/c mice by Rivier *et al.* (5). This probably is related to genetic differences between these two strains.

Effect of antibody pretreatment on the plasma level of ACTH 2 h after challenge with LPS

Figure 1A demonstrates the effect of pretreatment with anti-IL-6 antibody, anti-IL1R antibody, anti-TNF antibody, the combination of anti-IL-1R antibody and anti-TNF antibody, or antigalactosidase antibody on the 2 h ACTH response to 1 μg LPS. Pretreatment with anti-IL-6 antibody completely blocked the response to LPS, while the combination of anti-TNF antibody and anti-IL-1R antibody only partially blocked the response. In contrast, pretreatment with

TABLE 1. Plasma ACTH levels after ip injection of LPS

LPS dose (μg)	2 h	4 h	6 h
Vehicle	69.2 ± 8.8	66.3 ± 8.51	68.6 ± 3.86
1	185.7 ± 6.0	109.8 ± 8.4	65.6 ± 6.3
2	211.0 ± 18.7	102.0 ± 5.8	65.0 ± 3.0
5	165.8 ± 15.8	142.9 ± 7.6	69.4 ± 5.3
10	170.8 ± 7.3	130.4 ± 4.3	61.0 ± 2.9
25	178.2 ± 12.2	135.6 ± 8.7	102.0 ± 17.9
50	170.0 ± 15.0	145.0 ± 11.1	105.0 ± 9.4

Values are expressed as picograms per ml. Female C3H/HeN mice received various amounts of LPS ip and then were decapitated to obtain plasma for ACTH measurements 2, 4, or 6 h later. Each value shown is the mean ± SEM for 5 animals, except for the vehicle values, which represent 10 animals each.

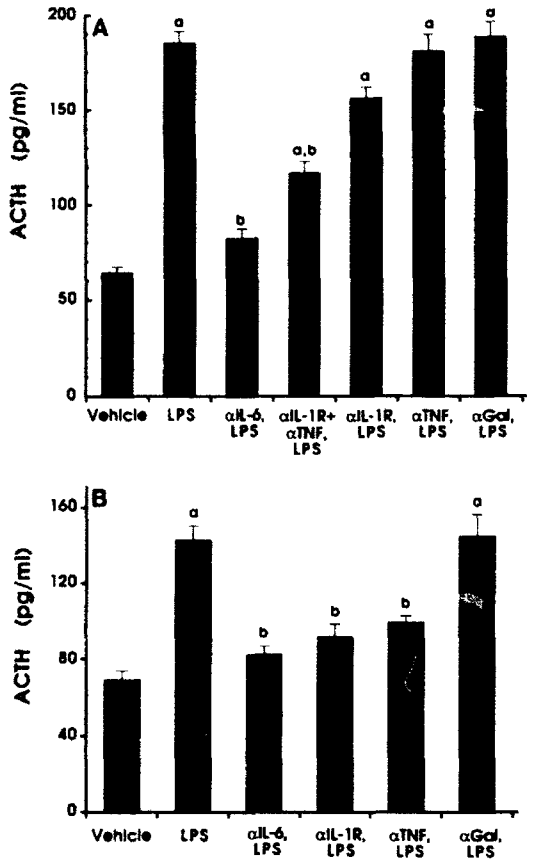

FIG. 1. C3H/HeN mice received ip injections of antibody [600 μg anti-IL-6 (αIL-6), 600 μg α-galactosidase (αGal), 250 μg αIL-1R, 100 μg αTNF, or 250 μg αIL-1R and 100 μg αTNF combined] 16 h before ip challenge with 1 μg LPS (A) or 5 μg LPS (B). Other mice were administered vehicle, 1 μg LPS (A), or 5 μg LPS (B) without antibody pretreatment. Blood samples were obtained 2 h (A) or 4 h (B) after LPS or vehicle alone. Each *bar* represents the mean ± SEM for 8–34 animals. a, $P < 0.05$ *vs.* vehicle alone; b, $P < 0.05$ *vs.* αGal plus LPS.

anti-TNF, anti-IL-1R, or control antibody did not attenuate the ACTH response.

Effect of antibody pretreatment on the plasma level of ACTH 4 h after challenge with LPS

Figure 1B demonstrates the effect of pretreatment with anti-IL-6 antibody, anti-IL-1R antibody, anti-TNF antibody, or antigalactosidase antibody on the 4 h ACTH response to 5 μg LPS. Pretreatment with any of the three anticytokine antibodies alone substantially blocked the ACTH response to LPS, while pretreatment with control antibody had no effect. All of the anticytokine antibodies were equally effective.

Release of ACTH after the injection of a combination of rhIL-1α and rhTNFα

Preliminary experiments indicated that rhTNFα administered ip to mice by itself induced a minimal ACTH response. Therefore, we examined the effect of the combined injection of suboptimal amounts of rhIL-1α and rhTNFα. Combined administration of 10 ng rhIL-1α and 1 μg rhTNFα resulted in a significant increase in circulating ACTH at 30, 60, 120, and 180 min compared with the response to simultaneously injected vehicle (Fig. 2). The responses to simultaneously injected vehicle were inconsequential (Fig. 2). When the responses to the rhIL-1/rhTNF combination were compared with those achieved with 10 ng rhIL-1α or 1 μg rhTNFα given separately, the responses to the combined injection were significantly greater than the sum of the responses to each cytokine injected alone at 120 and 180 min (Fig. 2).

Effect of antibody pretreatment on plasma ACTH 2 h after the combined injection of rhIL-1α and rhTNFα

Figure 3 demonstrates the effect of pretreatment with anti-IL-6 antibody, anti-IL-1R antibody, or antigalactosidase antibody on the 2 h ACTH response to the combined injection of 10 ng rhIL-1α and 1 μg rhTNFα. Pretreatment with anti-IL-6 antibody was as effective as anti-IL-1R antibody in blocking the ACTH response to the combined rhIL-1/rhTNF injection. Pretreatment with either of these antibodies produced a significant decline compared to pretreatment with control antibody.

Release of ACTH after the injection of a combination of rhTNFα and rhIL-6

We previously observed that suboptimal amounts of rhIL-1α and rhIL-6 synergistically stimulate the release of ACTH (12). To determine whether a similar interaction occurs between rhTNFα and rhIL-6, we evaluated the effect of the combined injection of rhTNFα and rhIL-6. After the combined administration of 1 μg rhTNFα and 1.25 μg rhIL-6, a significant increase in circulating ACTH was observed at 30, 60, 120, and 180 min compared with the response to simultaneously injected vehicle (Fig. 4). The responses to simultaneously injected vehicle were inconsequential (Fig. 4).

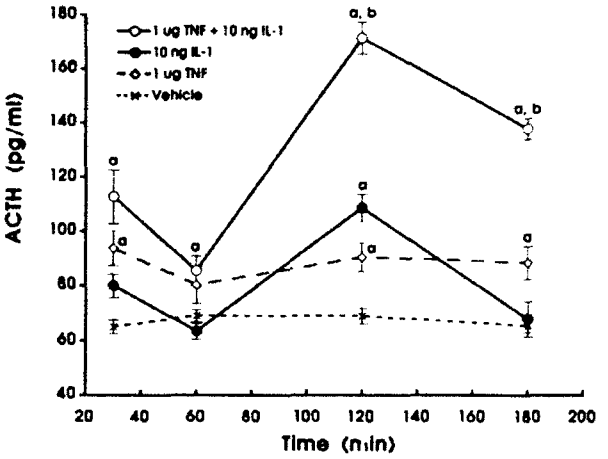

FIG. 2. Comparison of the time course of increase in plasma ACTH in C3H/HeN mice after ip injection of 10 ng rhIL-1α combined with 1 μg rhTNFα, 10 ng rhIL-1α, or 1 μg rhTNFα. The mean vehicle responses at each time point are also shown. Each time point represents the mean ± SEM of hormone determinations for 6–28 animals. a, $P < 0.05$ *vs.* the response to simultaneously injected vehicle; b, $P < 0.05$ *vs.* the sum of the responses to rhIL-1α and rhTNFα injected separately.

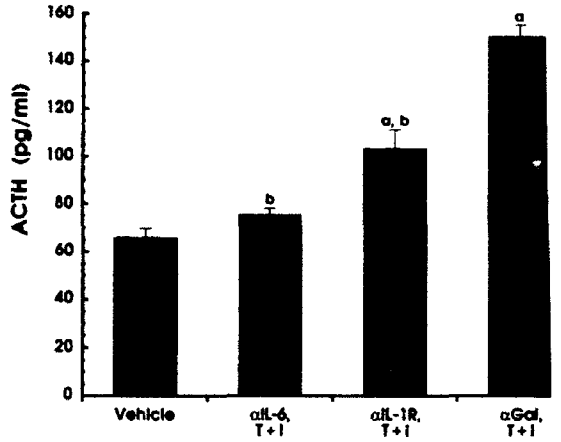

FIG. 3. C3H/HeN mice received ip injection of antibody [600 μg anti-IL-6 (αIL-6), 600 μg α-galactosidase (αGal), or 250 μg αIL-1R] 16 h before ip injection of 10 ng rhIL-1α combined with 1 μg rhTNFα (T+I). Other mice were administered vehicle without antibody pretreatment. Blood samples were obtained 2 h after T+I or vehicle alone. Each *bar* represents the mean ± SEM for 13–15 animals. a, $P < 0.05$ *vs.* vehicle alone; b, $P < 0.05$ *vs.* αGal plus T+I.

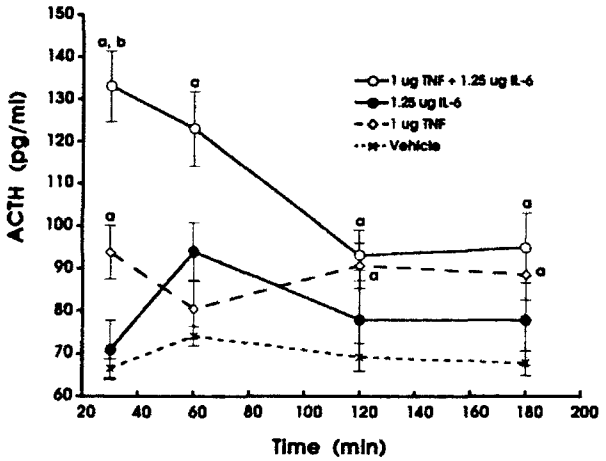

FIG. 4. Comparison of the time course of increase in plasma ACTH in C3H/HeN mice after ip injection of 1 μg rhTNFα combined with 1.25 μg rhIL-6, 1 μg rhTNFα, or 1.25 μg rhIL-6. The mean vehicle responses at each time point are also shown. Each time point represents the mean ± SEM of hormone determinations for 7–28 animals. a, $P < 0.05$ *vs.* the response to simultaneously injected vehicle; b, $P < 0.05$ *vs.* the responses to rhTNFα or rhIL-6 injected separately.

When the early responses to the rhTNF/rhIL-6 combination were compared with those to 1 μg rhTNFα or 1.25 μg rhIL-6 given separately, the responses to the combined injection were significantly greater than the responses to each cytokine injected alone (but not significantly greater than the sum of the responses to each cytokine injected alone; Fig. 4).

Discussion

Previous studies demonstrate that IL-1, IL-6, and TNF each stimulate the H-P-A axis *in vivo* via a CRH-dependent mechanism (7–9, 26–32) and *in vitro* at the level of the hypothalamus and pituitary (7–9, 27, 33, 34). On a molar basis, IL-1 is a more potent stimulator than TNF or IL-6 (31, 35). Our results demonstrate that IL-6 plays a fundamental role in LPS-induced ACTH release, but the participation and interaction of IL-1 and TNF are also required. In addition, the relative importance of these three cytokines varies at different times after LPS challenge.

Pretreatment with anti-IL-6 antibody completely abrogated the ACTH response to LPS 2 and 4 h after injection. Furthermore, the synergistic induction of ACTH after the combined injection of rhTNFα and rhIL-1α was blocked by anti-IL-6 antibody.

Inexplicably, although we were able to eliminate LPS-induced ACTH responses by pretreatment with anti-IL-6 antibody, ip administration of large doses (10 μg) of IL-6 to mice elicited only a minimal response (10). This suggests that IL-6 in the circulation may require an additional factor(s) to induce ACTH release. Alternatively, it is possible that systemic IL-6 does not reach the necessary local site(s) in the brain, whereas the anti-IL-6 antibody neutralizes LPS- or IL-1-stimulated IL-6 produced in the hypothalamus and/or pituitary gland (36–39). If a cofactor(s) is required for IL-6 to stimulate ACTH release, it is not clear at what level the interaction takes place, *e.g.* at the target cell level or due to facilitated transport across the blood-brain barrier.

Our results suggest that both IL-1 and TNF play important roles as IL-6 cofactors. The ACTH response 2 h after LPS challenge was not blocked by pretreatment with anti-IL-1R or anti-TNF antibody given separately, but was diminished by the combination of these antibodies; moreover, pretreatment with either anti-IL-1R or anti-TNF antibody alone totally blocked the 4 h ACTH response. Our previous observations that IL-1 and IL-6 synergize in inducing ACTH release (10) and that the 2 h ACTH response to IL-1 may be dependent upon an obligatory interaction between IL-1 and the IL-6 it induces endogenously (11) further suggest that IL-1 is an important cosecretagogue for IL-6 in stimulating the H-P-A axis. The coinjection of rhTNFα and rhIL-6 resulted in a greatly augmented (but not synergistic) ACTH response, suggesting a lesser role for TNF-IL-6 interaction in ACTH induction.

Since anti-IL-6 antibody totally abrogated ACTH release, while the combination of anti-IL-1R and anti-TNF antibodies only partially blocked the ACTH response 2 h after LPS administration, it is possible that in addition to IL-1 and TNF, other factors cooperate with IL-6. Among these, the arachidonic acid cascade metabolites, *i.e.* prostaglandins, leukotrienes, and epoxygenase products, which have been shown to modulate CRH release from the hypothalamus (40) and ACTH release from the pituitary (41) *in vitro*, seem likely candidates. Other possible factors are histamine (3) and IL-2 (8, 9, 42).

In addition to directly stimulating the hypothalamus and pituitary in conjunction with IL-6, LPS-induced IL-1 and TNF also contribute to stimulation of the H-P-A axis by inducing IL-6 production. In contrast to observations with anti-IL-6 antibody, pretreatment with either anti-IL-1R or anti-TNF antibody blocked the 4 h, but not the 2 h, ACTH response to LPS. The greater efficacy of these antibodies at 4 h may be due in part to their ability to interfere with TNF/

IL-1 induction of IL-6. There is ample evidence that LPS-induced elevation of IL-6 depends upon IL-1 and TNF induced by LPS. LPS stimulates the release of IL-1 and TNF *in vitro* (43, 44), including the production of IL-1 in the hypothalamus and pituitary (45, 46) and TNF in central nervous system microglial cells (47). *In vivo*, serum levels of TNF peak before IL-1 and IL-6 after LPS administration (13, 15–21). TNF and IL-1, in turn, both stimulate the release of IL-6 (11–13, 43, 44, 48–50). TNF is a much less potent inducer of IL-6 than IL-1 in mice (11). This may help to explain why ip injection of TNF stimulated only a minimal ACTH response in mice, in contrast to reports of more substantial ACTH responses after iv TNF administration to rats (32, 51). At the local level, subpopulations of nonneuronal cells in both the hypothalamus (36) and pituitary (37, 38) of rats spontaneously produce IL-6, and IL-1 enhances the release of IL-6 from cultures of rat anterior pituitary cells (39).

The synergistic induction of ACTH after coinjection of rhIL-1α and rhTNFα was completely blocked by pretreatment with anti-IL-6 antibody, suggesting that these cytokines synergistically induced IL-6 to produce the ACTH response. Indeed, recent *in vivo* (13) and *in vitro* (52) studies have demonstrated that IL-1 and TNF can synergistically stimulate IL-6 production.

Previous work employing blocking antibodies to TNF or IL-1 provides further support for the hypothesis that increased IL-6 levels during inflammation are dependent on TNF and IL-1. Results from our own laboratory (unpublished), as well as reports by a number of other investigators (13, 15, 17, 22) show that pretreatment with anti-TNF antibody substantially diminished IL-6 2–4 h after administration of LPS [as well as LPS-induced increases in IL-1 (15, 17)]. In addition, we observed that pretreatment with anti-IL-1R antibody markedly diminished the IL-6 response 4 h after LPS administration (unpublished). Similarly, pretreatment with anti-IL-1R antibody significantly attenuated the plasma IL-6 response to a turpentine-induced sterile abscess in mice (53).

It is also likely that LPS directly stimulates the release of IL-6, especially 2 h after injection. The ability of LPS to induce IL-6 in various cell cultures has been observed by a number of investigators (54, 55), including nonneuronal cells in the hypothalamus (36) and pituitary (37, 39), and Romero *et al.* (56) reported that IL-1 receptor antagonist blocks IL-1β-induced, but not LPS-induced, IL-6 release from cultures of rat anterior pituitary cells. In addition, in a recent *in vivo* study, IL-1 receptor antagonist did not block IL-6 induction after the administration of sublethal amounts of LPS (57).

In summary, in mice injected with sublethal amounts of LPS, IL-6, IL-1, and TNF play different roles in initiating and sustaining an ACTH response. The presence of IL-6, derived from the direct effects of LPS and/or its induction by TNF/IL-1, is obligatory at both time points studied. However, to elicit an ACTH response, an interaction with another factor may be required. IL-1 and TNF appear to be essential in sustaining the IL-6 levels required to maintain an ACTH response, especially 4 h after LPS administration and, in addition, may play an interactive role with IL-6 at both time points. The definitive explanation of how these cytokines mediate the activation of the H-P-A axis by LPS will have to take into account the contribution of cytokines produced in the hypothalamus and pituitary gland, and how and if they are induced by circulating cytokines originating in the periphery.

Acknowledgments

We thank Drs. T. J. MacVittie and G. D. Ledney for critically reviewing this manuscript; Drs. P. Lomedico, E. Liehl, S. Vogel, R. Chizzonite, and R. Schreiber and Biogen for generously providing cytokines and anticytokine antibodies; Dr. W. Jackson for assisting with the statistical analysis of the data; and Petty Officer Sam Tom, Miss Faith Selzer, and Mr. Clint Wormley for their technical assistance.

References

1. **Dinarello CA** 1984 Interleukin-1 and the pathogenesis of the acute-phase response. N Engl J Med 311:1413–1418
2. **Sibbald WJ, Short A, Cohen MP, Wilson RF** 1977 Variations in adrenocortical responsiveness during severe bacterial infections. Unrecognized adrenocortical insufficiency in severe bacterial infections. Ann Surg 186:29–33
3. **Nakano K, Suzuki S, Oh C** 1987 Significance of increased secretion of glucocorticoids in mice and rats injected with bacterial endotoxin. Brain Behav Immunol 1:159–172
4. **Yasuda N, Greer MA** 1978 Evidence that the hypothalamus mediates endotoxin stimulation of adrenocorticotropic hormone secretion. Endocrinology 102:947–953
5. **Rivier C, Chizzonite R, Vale W** 1989 In the mouse, the activation of the hypothalamic-pituitary-adrenal axis by a lipopolysaccharide (endotoxin) is mediated through interleukin-1. Endocrinology 125:2800–2805
6. **Derijk R, Van Rooijen N, Tilders FJH, Besedovsky HO, Del Rey A, Berkenbosch F** 1991 Selective depletion of macrophages prevents pituitary-adrenal activation in response to subpyrogenic, but not to pyrogenic, doses of bacterial endotoxin in rats. Endocrinology 129:330–338
7. **Whitnall MH**, Regulation of the hypothalamic corticotropin-releasing hormone neurosecretory system. Prog Neurobiol, in press
8. **Eskay RL, Grino M, Chen HT** 1990 Interleukins, signal transduction, and the immune system-mediated stress response. Adv Exp Med Biol 274:331–343
9. **Imura H, Fukata J, Mori T** 1991 Cytokines and endocrine function—an interaction between the immune and neuroendocrine systems—review. Clin Endocrinol (Oxf) 35:107–115
10. **Perlstein RS, Mougey EH, Jackson WE, Neta R** 1991 Interleukin-1 and interleukin-6 act synergistically to stimulate the release of adrenocorticotropic hormone *in vivo*. Lymphokine Cytokine Res 10:141–146
11. **Neta R, Perlstein R, Vogel SN, Ledney GD, Abrams J** 1992 Role of interleukin 6 (IL-6) in protection from lethal irradiation and in endocrine responses to IL-1 and tumor necrosis factor. J Exp Med 175:689–694
12. **Neta R, Vogel SN, Sipe JD, Wong GG, Nordan RP** 1988 Comparison of *in vivo* effects of human recombinant IL 1 and human recombinant IL 6 in mice. Lymphokine Res 7:403–412
13. **Shalaby MR, Waage A, Aarden L, Espevik T** 1989 Endotoxin, tumor necrosis factor-α and interleukin 1 induce interleukin 6 production *in vivo*. Clin Immunol Immunopathol 53:488–498
14. **Vogel SN, Hogan MM** 1990 Role of cytokines in endotoxin-mediated host responses. In: Oppenheim JJ, Shevach EN (eds) Immunophysiology, Role of Cells and Cytokines in Immunity and Inflammation. Oxford University Press, Oxford, pp 238–258
15. **Fong Y, Tracey KJ, Moldawer LL, Hesse DG, Manogue KB, Kenney JS, Lee AT, Kuo GC, Allison AC, Lowry SF, Cerami A**

1989 Antibodies to cachectin/tumor necrosis factor reduce interleukin 1β and interleukin 6 appearance during lethal bacteremia. J Exp Med 170:1627–1633

16. **Waage A, Halstensen A, Shalaby MR, Brandtzaeg P, Kierulf P, Espevik T** 1989 Local production of tumor necrosis factor alpha, interleukin 1, and interleukin 6 in meningococcal meningitis. Relation to the inflammatory response. J Exp Med 170:1859–1867
17. **Zanetti G, Heumann D, Gerain J, Kohler J, Abbet P, Barras C, Lucas R, Glauser M-P, Baumgartner J-D** 1992 Cytokine production after intravenous or peritoneal gram negative bacterial challenge in mice. J Immunol 148:1890–1897
18. **Chensue SW, Terebuh PD, Remick DG, Scales WE, Kunkel SL** 1991 *In vivo* biologic and immunohistochemical analysis of interleukin-1 alpha, beta and tumor necrosis factor during experimental endotoxemia. Am J Pathol 138:395–402
19. **Zuckerman SH, Shellhaas J, Butler LD** 1989 Differential regulation of lipopolysaccharide-induced interleukin 1 and tumor necrosis factor synthesis: effects of endogenous and exogenous glucocorticoids and the role of the pituitary-adrenal axis. Eur J Immunol 19:301–305
20. **Michie HR, Manogue KR, Spriggs DR, Revhaug A, O'Dwyer S, Dinarello CA, Cerami A, Wolff SM, Wilmore DW** 1988 Detection of circulating tumor necrosis factor after endotoxin administration. N Engl J Med 318:1481–1486
21. **Fong Y, Moldawer LL, Marano M, Wei H, Tatter SB, Clarick RH, Santhanam U, Sherris D, May LT, Sehgal PB, Lowry SF** 1989 Endotoxemia elicits increased circulating β2-IFN/IL-6 in man. J Immunol 142:2321–2324
22. **Starnes HF, Pearce MK, Tewari A, Yim JH, Zou J-C, Abrams JS** 1990 Anti-IL-6 monoclonal antibodies protect against lethal *Escherichia coli* infection and lethal tumor necrosis factor-α challenge in mice. J Immunol 145:4185–4191
23. **Chizzonite R, Truitt T, Kilian PL, Stern AS, Nunes P, Parker KP, Kaffka KL, Chua AO, Lugg DK, Gubler U** 1989 Two high-affinity interleukin-1 receptors represent separate gene products. Proc Natl Acad Sci USA 86:8029–8033
24. **Sheehan KCF, Ruddle NH, Schreiber RD** 1989 Generation of hamster monoclonal antibodies that neutralize tumor necrosis factors. J Immunol 142:3884–3893
25. **Neta R, Oppenheim JJ, Schreiber RD, Chizzonite R, Ledney GD, MacVittie TJ** 1991 Role of cytokines (interleukin 1, tumor necrosis factor, and transforming growth factor β) in natural and lipopolysaccharide-enhanced radioresistance. J Exp Med 173:1177–1182
26. **Spangelo BL, MacLeod RM** 1990 Regulation of the acute phase response and neuroendocrine function by interleukin 6. Progr Neuroendocrin Immunol 3:167–175
27. **Lyson K, McCann SM** 1991 The effect of interleukin-6 on pituitary hormone release *in vivo* and *in vitro*. Neuroendocrinology 54:262–266
28. **Naitoh Y, Fukata J, Tominaga T, Nakai Y, Tamai S, Mori K, Imura H** 1988 Interleukin-6 stimulates the secretion of adrenocorticotropic hormone in conscious, freely-moving rats. Biochem Biophys Res Commun 155:1459–1463
29. **Whitnall MH, Perlstein RS, Mougey EH, Neta R** 1992 Effects of interleukin-1 on the stress-responsive and -nonresponsive subtypes of corticotropin-releasing hormone neurosecretory axons. Endocrinology 131:37–44
30. **Dunn AJ** 1990 Interleukin-1 as a stimulator of hormone secretion. Prog Neuroendocrin Immunol 3:26–34
31. **Besedovsky HO, Del Rey A, Sorkin E, Dinarello CA** 1986 Immunoregulatory feedback between interleukin-1 and glucocorticoid hormones. Science 233:652–654
32. **Bernardini R, Kamilaris TC, Calogero AE, Johnson EO, Gomez ET, Gold PW, Chrousos GP** 1990 Interactions between tumor necrosis factor-alpha, hypothalamic corticotropin-releasing hormone, and adrenocorticotropin secretion in the rat. Endocrinology 126:2876–2881
33. **Lyson K, McCann SM** 1992 Involvement of arachidonic acid cascade pathways in interleukin-6-stimulated corticotropin-releasing factor release *in vitro*. Neuroendocrinology 55:708–713
34. **Navarra P, Pozzoli G, Brunetti L, Ragazzoni E, Besser M, Grossman A** 1992 Interleukin-1β and interleukin-6 specifically increase the release of prostaglandin E_2 from rat hypothalamic explants *in vitro*. Neuroendocrinology 56:61–68
35. **Warren RS, Fletcher H, Starnes J, Alcock N, Calvano S, Brennan MF** 1988 Humoral and metabolic response to recombinant human tumor necrosis factor in rat: *in vitro* and *in vivo*. Am J Physiol 255:E206–E212
36. **Spangelo BL, Judd AM, MacLeod RM, Goodman DW, Isakson PC** 1990 Endotoxin-induced release of interleukin-6 from rat medial basal hypothalami. Endocrinology 127:1779–1785
37. **Spangelo BL, MacLeod RM, Isakson PC** 1990 Production of interleukin-6 by anterior pituitary cells *in vitro*. Endocrinology 126:582–586
38. **Vankelecom H, Carmeliet P, Van Damme J, Billiau A, Denef C** 1989 Production of interleukin-6 by folliculo-stellate cells of the anterior pituitary gland in a histiotypic cell aggregate culture system. Neuroendocrinology 49:102–106
39. **Spangelo BL, Judd AM, Isakson PC, MacLeod RM** 1991 Interleukin-1 stimulates interleukin-6 release from rat anterior pituitary cells *in vitro*. Endocrinology 128:2685–2692
40. **Bernardini R, Chiarenza A, Calogero AE, Gold PW, Chrousos GP** 1989 Arachidonic acid metabolites modulate rat hypothalamic corticotropin-releasing hormone secretion *in vitro*. Neuroendocrinology 50:708–715
41. **Cowell AM, Flower RJ, Buckingham JC** 1991 Studies on the roles of phospholipase A2 and eicosanoids in the regulation of corticotrophin secretion by rat pituitary cells *in vitro*. J Endocrinol 130:21–32
42. **Cambronero JC, Rivas FJ, Borrell J, Guaza C** 1992 Interleukin-2 induces corticotropin-releasing hormone release from superfused rat hypothalami: influence of glucocorticoids. Endocrinology 131:677–683
43. **Dinarello CA** 1991 Interleukin-1 and interleukin-1 antagonism. Blood 77:1627–1652
44. **Neta R, Sayers TJ, Oppenheim JJ** 1992 Relationship of TNF to interleukins. In: Aggarwal BB, Vilcek J (eds) Tumor Necrosis Factors: Structure, Function, and Mechanism of Action. Marcel Dekker, New York, pp 499–566
45. **Rettori V, Dees WL, Hiney JK, Milenkovic L, McCann SM,** Interleukin-1 alpha (IL-1α)-immunoreactive neurons in the hypothalamus of the rat are increased after lipopolysaccharide (LPS) injection. 74th Annual Meeting of The Endocrine Society, San Antonio TX, 1992, p 185 (Abstract 534)
46. **Koenig JI, Snow K, Clark BD, Toni R, Cannon JG, Shaw AR, Dinarello CA, Reichlin S, Lee SL, Lechan RM** 1990 Intrinsic pituitary interleukin-1 beta is induced by bacterial lipopolysaccharide. Endocrinology 126:3053–3058
47. **Ricciardi-Castagnoli P, Pirami L, Righi M, Sacerdote P, Locatelli V, Bianchi M, Sassano M, Valsasnini P, Shammah S, Panerai AE** 1990 Cellular sources and effects of tumor necrosis factor-α on pituitary cells and in the central nervous system. Ann NY Acad Sci 594:156–168
48. **Libert C, Brouckaert P, Shaw A, Fiers W** 1990 Induction of interleukin 6 by human and murine recombinant interleukin 1 in mice. Eur J Immunol 20:691–694
49. **McIntyre KW, Stepan GJ, Kolinsky KD, Benjamin WR, Plocinski JM, Kaffka KL, Campen CA, Chizzonite RA, Kilian PL** 1991 Inhibition of interleukin 1 (IL-1) binding and bioactivity *in vitro* and modulation of acute inflammation *in vivo* by IL-1 receptor antagonist and anti-IL-1 receptor monoclonal antibody. J Exp Med 173:931–939
50. **Mengozzi M, Bertini R, Sironi M, Ghezzi P** 1991 Inhibition by interleukin 1 receptor antagonist of *in vivo* activities of interleukin 1 in mice. Lymphokine Cytokine Res 10:405–407
51. **Sharp BM, Matta SG, Peterson PK, Newton R, Chao C, McAllen K** 1989 Tumor necrosis factor-alpha is a potent ACTH secretagogue: comparison to interleukin-1 beta. Endocrinology 124:3131–3133
52. **Benveniste EN, Sparacio SM, Norris JG, Grenett HE, Fuller GM** 1990 Induction and regulation of interleukin-6 gene expression in rat astrocytes. J Neuroimmunol 30:201–212
53. **Gershenwald JE, Fong YM, Fahey TJ, Calvano SE, Chizzonite R, Kilian PL, Lowry SF, Moldawer LL** 1990 Interleukin 1 receptor blockade attenuates the host inflammatory response. Proc Natl Acad Sci USA 87:4966–4970

54. **Kotloff RM, Little J, Elias JA** 1990 Human alveolar macrophage and blood monocyte interleukin-6 production. Am J Respir Cell Mol Biol 3:497–505
55. **Jirik FR, Podor TJ, Hirano T, Kishimoto T, Loskutoff DJ, Carson DA, Lotz M** 1989 Bacterial lipopolysaccharide and inflammatory mediators augment IL-6 secretion by human endothelial cells. J Immunol 142:144–147
56. **Romero LI, Lechan RM, Clark BD, Dinarello CA, Reichlin S,** IL-1 receptor antagonist inhibits hIL-1 beta but not bacterial lipopolysaccharide (LPS) stimulated IL-6 secretion by rat anterior pituitary cells. 73rd Annual Meeting of The Endocrine Society, Washington DC, 1991, p 150 (Abstract 479)
57. **Fischer E, Marano MA, Van Zee KJ, Rock CS, Hawes AS, Thompson WA, DeForge L, Kenney JS, Remick DG, Bloedow DC, Thompson RC, Lowry SF, Moldawer LL** 1992 Interleukin-1 receptor blockade improves survival and hemodynamic performance in *Escherichia coli* septic shock, but fails to alter host responses to sublethal endotoxemia. J Clin Invest 89:1551–1557

In: *The Biology of Nitric Oxide.*
S. Moncada, M.A. Marletta, J.B. Hibbs, Jr., and E.A. Higgs, eds.
Portland Press, London, 1992.

Electron paramagnetic resonance detection of nitric oxide-dependent spin adducts in mouse jejunum

L. Steel-Goodwin[1], C. M. Arroyo[1], B. Gray[2] and A. J. Carmichael[1]
[1] Radiation Biophysics and [2] Radiation Biochemistry Departments, Armed Forces Radiobiology Research Institute, Bethesda, Maryland 20889-5145, U.S.A.

Abstract

The electron paramagnetic resonance (EPR) spectra of aqueous solutions containing nitric oxide (NO) and the spin trap 3,5-dibromo-4-nitrosobenzene-sulphonate (DBNBS) have previously been described [1]. Similar NO-derived DBNBS adducts plus the DBNBS oxidation product were observed in 50 mM phosphate-buffered incubation media (pH 7.0) upon addition of NO. Moreover, the above adducts plus additional DBNBS radicals were observed in incubation media following suspension of mouse jejunal slices (~ 1 cm length) for 20 min at 37 °C when NO was added. Less intense DBNBS spin adduct spectra were observed in analogously treated jejunum slices that had no NO added. This result suggests a continuous production of NO by jejunum which may play a role in peristalsis. Moreover, the basal level of NO production was stimulated in the presence of the radioprotectant, *N*-(2-mercaptoethyl)-1,3-diaminopropane [WR-1065].

Introduction

Endothelium-derived relaxing factor (EDRF) has been identified as NO or compounds derived from this labile gas [2]. There have been numerous attempts to isolate this ephemeral gas from a variety of cells and tissues. One approach employs spin traps which form free radical adducts with half-lives sufficiently long to permit EPR detection [1]. Papers reporting the presence of NO-derived radical adducts produced by cell systems have appeared recently [3, 4]. Therefore, it is reasonable to expect that NO-derived radical adducts may be trapped and detected by EPR in tissue slices using spin traps. The gut is an appropriate source of tissue slices which may be expected to elaborate NO. EDRF has been demonstrated in the ileocolonic junction of dogs [5] and the guinea pig stomach [6]. Also, the NO synthase enzyme has been immunologically detected in myenteric plexi throughout the gut of the rat [7]. Finally, the peristaltic, rhythmic contractions and relaxations occurring in the gut could reasonably be expected to result in part from the effect of NO on gut smooth muscle. This paper reports results of spin trapping experiments carried out with gut tissue slices which elaborate NO or free radicals derived from NO.

Materials and methods

Mice were euthanized by cervical dislocation, the small intestine was removed and flushed with 50 mM sodium phosphate-buffered (pH 7.0) 0.9% sodium chloride solution (PBS) and a slice of jejunum (~ 1 cm) was placed in incubation medium. The incubation medium (pH 7.0±0.1) was PBS supplemented with 11 mM-glucose, 2 mM-KCl, 26 mM-$NaHCO_3$, 1.18 mM-KH_2PO_4 and 2 mM-$CaCl_2.2H_2O$ [8]. *N*-(2-mercaptoethyl)-1,3-diaminopropane [WR-1065, H_2N-$(CH_2)_3$-NH-$(CH_2)_2$-SH] was hydrated in incubation medium immediately before addition to solutions. The spin trap DBNBS and bovine copper/zinc superoxide dismutase (SOD) were weighed and added to test tubes. These materials were hydrated with incubation medium within one hour of their experimental use. NO was delivered from a compressed gas cylinder. Incubations having 10 mM-DBNBS and 300 units ml^{-1} SOD were carried out in polyethylene test tubes. Spectra were made with fluids preincubated for 20 min at 37 °C before transfer to a quartz flat cell which was then installed on a Varian E-109 X-band spectrometer. The EPR instrument was operated at a magnetic field set at 338.8 mT, microwave frequency about 9.500 GHz, microwave power 20 mW, receiver gain 2×10^5, modulation frequency 100 KHz, modulation amplitude 2 mT, time constant 4 s, scan time 16 min, scan range 0.1 T and temperature 25 °C. Hyperfine values were determined by direct measurement from the spectra.

Results and discussion

Figure 1 shows EPR spectra of DBNBS radical adducts observed following exposure of materials to NO gas. Figure 1*a*, the incubation medium, has DBNBS adducts (open arrows) with a hyperfine coupling constant, $a_N = 0.959$ mT, which corresponds to the previously reported value for aqueous solutions exposed to NO gas [1]. In addition, the oxidation product DBNBS also appears to be present with a coupling constant, $a_N = 1.25$ mT [9]. Figure 1*b* is a spectrum made with incubation medium after 20 min at 37 °C without NO bubbling. This spectrum is representative of random noise. Figure 1*c* is the spectrum resulting from a jejunum tissue slice incubated for 20 min at 37 °C and then gently bubbled for 5–10 s with NO. This spectrum has both NO-derived adducts (open arrows) and the oxidation product DBNBS (solid arrows) seen in Figure 1*a*. In addition, there appear to be less intense EPR shoulders in the spectrum that are not seen in the incubation medium alone.

Figure 2 shows EPR spectra resulting when incubation medium containing jejunum slices was treated with various compounds. Figure 2*a* was made after 0.1 ml of NO-saturated, anaerobic water was added to a jejunum slice following a 20 min incubation at 37 °C. In addition to DBNBS oxidation product (solid arrows) plus NO-derived adducts (open arrows) there are two maxima which correspond to shoulders seen in Figure 1*c*. The quantity of NO introduced and the method of its delivery may have subtle influences on the spectral results. Figure 2*b* shows the spectrum resulting from incubation of a jejunum slice for 20 min at 37 °C. The analogous control lacking tissue (Figure 1*b*) indicates that unstimulated mouse jejunum slices do elaborate NO. Figure 2*c* is a spectrum made with jejunum incubated with 5 mM-WR-1065 for 20 min at 37 °C. The DBNBS oxidation product plus the NO-derived maxima are present. WR-1065 appears to stimulate NO production in jejunum slices because these maxima are more intense than those observed with unstimulated slices (Figure 2*b*). It is important to note that the

Figure 1

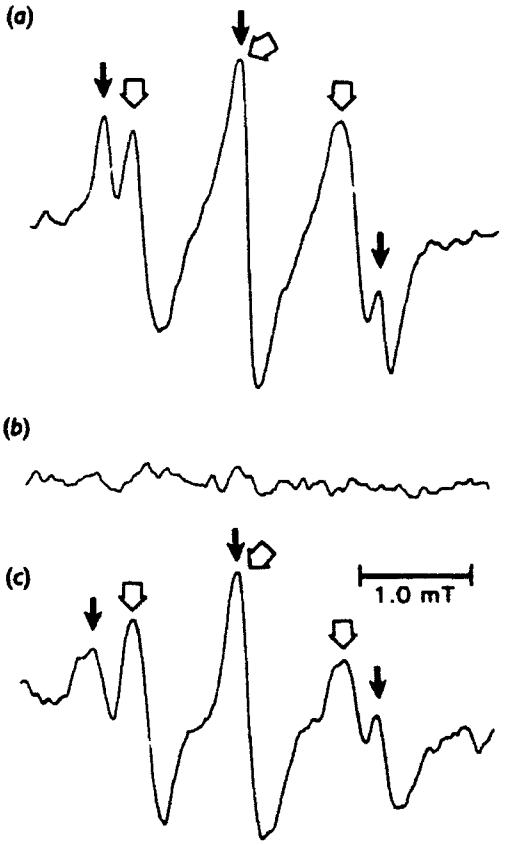

EPR spectra of DBNBS radical adducts following exposure of materials to NO gas

(a) Incubation medium suspended for 20 min at 37 °C and bubbled with NO gas. (b) Incubation medium suspended for 20 min at 37 °C without NO bubbling. (c) Jejunum slice incubated for 20 min at 37 °C and bubbled with NO gas. Filled arrows indicate the DBNBS oxidation product and open arrows indicate the NO-derived DBNBS spin adduct.

control spectrum (Figure 2*d*) made with incubation medium and WR-1065 does have EPR-detectable radicals present. The spectrum is not random noise (Figure 1*b*). However, the pattern does not correspond to any of the other spectra containing gut tissue slices. Minor spectral details seen in Figure 2*c* could result from the contribution of WR-1065 as well as the jejunal slices. It is possible that WR-1065 reacts with DBNBS to produce the spectrum observed in Figure 2*d*.

These results support the conclusions that mouse jejunum slices continuously produce a low level of NO. Additionally, WR-1065 stimulates the basal level of NO production by jejunal slices. It is possible that this production of NO plays an important role in the rhythmic relaxations of peristalsis.

Supported by the Armed Forces Radiobiology Research Institute, Defense Nuclear Agency. Views presented in this paper are those of the authors; no endorsement by the Defense Nuclear Agency has been given or should be inferred. Research was conducted according to the principles

Figure 2

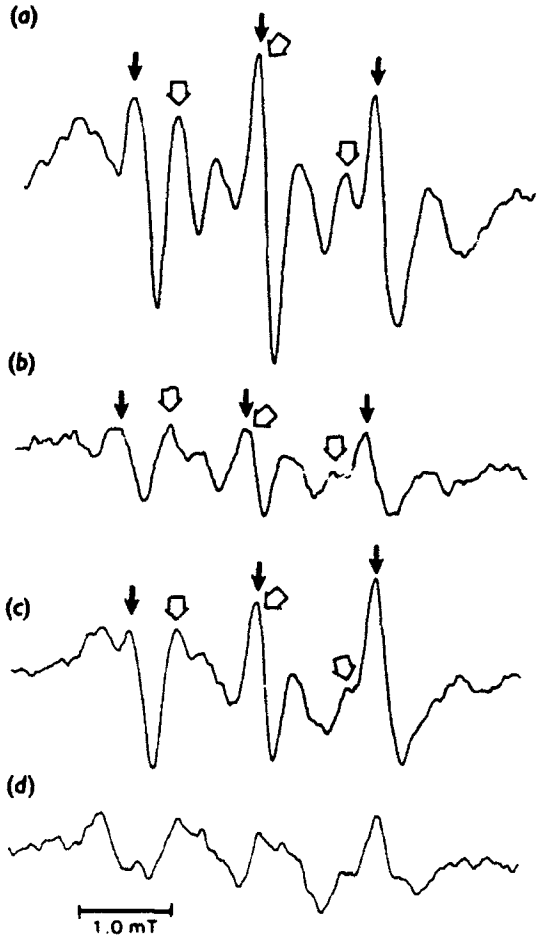

EPR spectra following treatment of incubation medium containing jejunum slices with various compounds

(a) Jejunum slice incubated for 20 min at 37 °C to which 0.1 ml of NO-saturated anaerobic water was added. (b) Jejunum slice incubated for 20 min at 37 °C. (c) Jejunum slice incubated for 20 min at 37 °C with 5 mM-WR-1065. (d) Control incubation medium plus 5 mM-WR-1065 incubated for 20 min at 37 °C. The arrows indicate the some products as in Figure 1.

enunciated in the 'Guide for the Care and Use of Laboratory Animals' prepared by the Institute of Laboratory Animal Resources, National Research Council.

References

1 Arroyo, C. M. & Kohno, M. (1990) Free Radical Res. Commun. **14**, 145–155
2 Moncada, S., Palmer, R. M. J. & Higgs, E. A. (1991) Pharmacol. Rev. **43**, 109–142
3 Arroyo, C. M. & Ferraz, C. (1991) Eur. J. Pharmacol. **208**, 157–161
4 Pronai, L., Ichimori, K., Nozaki, H., Nakazawa, H., Okino, H., Carmichael, A. J. & Arroyo, C. M. (1991) Eur. J. Biochem. **202**, 923–930
5 Bult, H., Boeckxstaens, G. E., Pelckmans, P. A., Jordaens, F. H., van Maercke, Y. M. & Herman, A. G. (1990) Nature (London) **345**, 346–347
6 Desai, K. M., Sessa, W. C. & Vane, J. R. (1991) Nature (London) **351**, 477–479

7. Bredt, D. S., Hwang, P. M. & Snyder, S. H. (1990) Nature (London) 347, 768–770
8. Garthwaite, J., Garthwaite, G., Palmer, R. M. J. & Moncada, S. (1989) Eur. J. Pharmacol. 172, 413–416
9. Nazhat, N. B., Yang, G., Allen, R. E., Blake, D. R. & Jones, P. (1990) Biochem. Biophys. Res. Commun. 166, 807–812

RADIATION RESEARCH 133, 12–19 (1993)

Radiolysis in Aqueous Solution of Dinucleoside Monophosphates by High-Energy Electrons and Fission Neutrons

Y. N. VAISHNAV AND C. E. SWENBERG

Radiation Biochemistry Department, Armed Forces Radiobiology Research Institute, Bethesda, Maryland 20889-5145

VAISHNAV, Y. N., AND SWENBERG, C. E. Radiolysis in Aqueous Solution of Dinucleoside Monophosphates by High-Energy Electrons and Fission Neutrons. *Radiat. Res.* 133, 12–19 (1993).

The radiation chemistry in aqueous solution of the dinucleoside monophosphate d-[CpT] and its sequence isomer d-[TpC] in air or nitrogen was examined using different qualities and quantities of radiations. High-performance liquid chromatography and gas chromatography–mass spectrometry were used to analyze the high-energy electron (13.2 MeV) exposure products or fission-neutron exposure products of d-[CpT] and d-[TpC]. A comparison of product profiles obtained from irradiated d-[CpT] and d-[TpC] suggests that, at relatively low radiation doses (50–250 Gy), products are formed by N-glycosidic or phosphodiester bond-cleavage, while at higher doses (500–1000 Gy) additional products were detected as a consequence of ring-modification mechanisms. The plots of radiation dose-yield and corresponding calculated *G* values of the released undamaged bases and nucleosides from d-[CpT] and d-[TpC] suggest a base-sequence dependence and a quality- and quantity-dependent response to ionizing radiation. Although the product quantities formed from sequence isomers were slightly different, we found no qualitative differences in the product formed at the lowest doses examined

INTRODUCTION

Cytotoxic, carcinogenic, and mutagenic effects in cells exposed to ionizing radiation are thought to be primarily the result of damage to DNA (*1–3*). Recent interest in radiotherapy with heavy particles and radioprotection against such particles encourages the search for the molecular basis of their action (*4*). Understanding the fundamental biochemical pathways involved in radiation sensitivity in relation to radiation damage to the primary target molecule, presumably DNA, in cells requires identification of the sensitive and reactive sites of DNA. The identification of such sensitive and reactive sites in cells is exceedingly difficult, as cellular systems are highly complicated (*5*). One approach is to study model systems. Dinucleotides are suitable, small, two-base models for investigating the effects of ionizing radiation on single-strand DNA. Products of gamma radiolysis of d-[TpT] and X-irradiated "purine–pyrimidine" dinucleotide sequence isomers were reported in the pioneering research of Cadet, Box, and co-workers (*6–11*).

Our present study examines effects of different qualities and quantities of radiation on dinucleoside monophosphates of "pyrimidine-pyrimidine" systems,[1] which hopefully will improve our perspective on the radiation chemistry of native DNA. To compare and correlate the effects of different radiations with different values of linear energy transfer (LET), aqueous solutions of 2′-deoxycytidylyl-(3′-5′)-thymidine (d-[CpT]) and its sequence isomer thymidylyl-(3′-5′)-2′-deoxycytidine (d-[TpC]) (see Fig. 1 for chemical structures) were exposed to different doses of high-energy electrons (13.2 MeV, low LET) or fission-neutrons (high LET), and the product profiles were analyzed by high-performance liquid chromatography (HPLC). Individual products were isolated and characterized by gas chromatography/mass spectrometry (GC/MS) and their *G* values were determined.

MATERIALS AND METHODS

The dinucleoside monophosphates d-[CpT] and d-[TpC] and samples of cytosine, thymine, 2′-deoxycytidine, thymidine, thymidine-3′-phosphate, thymidine-5′-phosphate, 2′-deoxycytidine-3′-phosphate, and 2′-deoxycytidine-5′-phosphate were purchased from Sigma Chemical Co. (St. Louis, MO); HPLC-grade acetonitrile was obtained from Aldrich Chemical Co. (Milwaukee, WI). *N,O*-bis(Trimethylsilyl)trifluoroacetamide (BSTFA) was purchased from Supelco, Inc. (Bellefonte, PA). All the HPLC analyses were performed using a Kratos Analytical Spectroflow 400 solvent delivery system (Ramsey, NJ) on-line with a Nelson 4100 computing integrator and an Applied Biosystems (Ramsey, NJ) Model 783 absorbance detector gradient controller. Mass spectral analysis was performed using the Kratos Analytical 25RFA mass spectrometer systems (Manchester, UK). Samples were analyzed by a direct insertion probe at 70 eV in an electron impact mode or were converted into their corresponding trimethylsilyl (TMS) ethers and injected into the gas chromatography column and analyzed by mass spectrometry (*14*). The TMS derivatives were prepared by dissolving 50 μg of each HPLC-purified material in 25 μl of BSTFA. Samples were allowed to react and equilibrate at room temperature for 18 h before analysis. A Carlo Erba (Strada Rivoltana, Italy) high-resolution gas chromato-

[1] Y. N. Vaishnav and C. E. Swenberg, Radiolysis of dinucleoside monophosphate and its sequence isomer by high-energy electrons and fission neutrons. Abstract p32–18, 9th International Congress of Radiation Research, Toronto, Canada, 1991.

0033-7587/93 $5.00

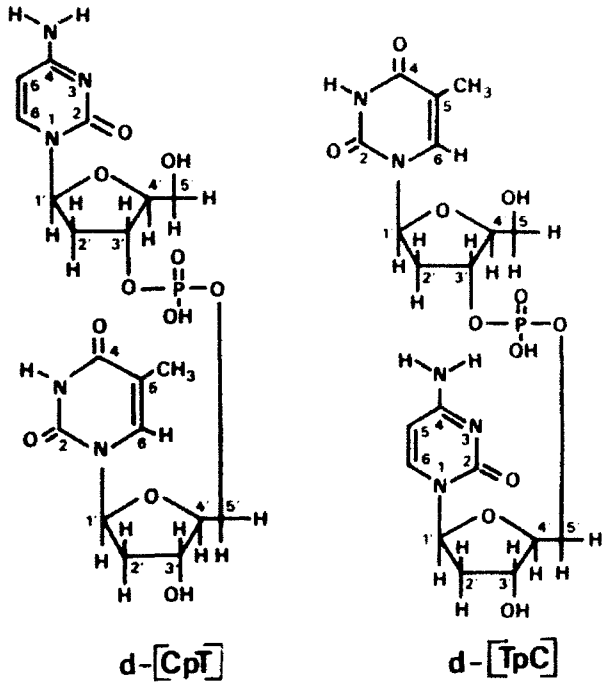

FIG. 1. Chemical structures of dinucleoside monophosphates.

graph was interfaced with the mass spectrometer. GC/MS analyses were performed using a fused silica capillary column (50 × 0.32 mm i.d.). The injection port and the ion source were monitored at 270°C with the GC/MS interfaced at 290°C. Helium was used as carrier gas at an inlet pressure of 10 kPa and the split mode was used for GC/MS analysis. The mass spectrometer was calibrated using perfluorokerosines for a mass range of 18–800 AMU.

Sample preparation and irradiation. In a closed polypropylene container, solution (1 mmol dm^{-3}) of either d-[CpT] or d-[TpC] was prepared in deionized water in the presence of either air or nitrogen. Samples (200 μl) were exposed to 0, 50, 250, 500, or 1000 Gy of 13.2-MeV electron irradiation (3.2 Gy/pulse) or fission neutrons at 4°C. Irradiated samples were subsequently frozen in liquid nitrogen until HPLC analysis. A reverse-phase analytical column (Spheris, 250 mm × 4.6 mm) was used in solvent gradient mode of 0.1 mol dm^{-3} ammonium acetate versus acetonitrile. The HPLC product profiles of the irradiated samples and unirradiated controls were recorded by optical detection at 254 nm (or in some cases 220 nm), and the individual components were isolated from the mixture product. Aliquots from individual components were reinjected into the HPLC column, using identical HPLC elution conditions, and the observed retention times were compared with available standards. For further characterization of the HPLC-purified individual components, individual components were freeze-dried and treated with BSTFA, and resulting silyl ethers were characterized by GC/MS.

Dosimetry. Samples were exposed to either 13.2-MeV electrons or fission neutrons. For experiments with high-energy electron irradiation, a linear accelerator (LINAC) was used with the average dose rate 3.2 Gy/pulse (4-μs pulse). Dosimetry measurements were performed by measuring the dose to individual pulses using lithium fluoride thermoluminesent dosimeters (TLD). The total dose was determined by the product of the number of pulses and the dose per pulse. The AFRRI TRIGA Mark-F reactor was used to obtain a mixed neutron to γ-ray field with a total dose rate of about 80 Gy min^{-1} and a ratio of neutron to γ-ray kerma in free air of about 15–18. Dosimetry measurements were done using 0.5 cm^{-3} ionization chambers constructed of A-150 tissue-equivalent (TE) plastic filled with TE gas and magnesium filled with argon to separate the neutron and γ-ray components (13).

RESULTS

The HPLC product profiles in aqueous solution (pH 7.0) generated from the high-energy electron and fission-neutron irradiation of d-[CpT] and d-[TpC] in air were recorded. Figure 2 is an example of an HPLC product profile obtained after 13.2-MeV electron irradiation of d-[CpT]. The individual components of the irradiation products from the product profiles labeled a to p are listed in Table I. Equimolar concentrations of d-[CpT] and d-[TpC] were exposed to total radiation doses of 0, 50, 250, 500, or 1000 Gy. Equal volumes (10-μl aliquot) for irradiated and unirradiated samples were injected into the HPLC column under elution conditions identical to those described under Materials and Methods. Major components were isolated and identified by comparing HPLC retention times with available standards and also by isolating the individual components, freeze-drying, and subsequently treating with BSTFA. Silyl derivatives so formed were further analyzed by GC/MS and/or a direct insertion probe/mass spectrometry (DIP/MS) as described under Materials and Methods. The observed HPLC retention times and prominent mass spectral fragmentation patterns are listed in Table I.

To quantify radiation-induced release of the free bases and nucleosides cytosine (C), 2-deoxycytidine (dC), thymine (T), and thymidine (dT) (products labeled c, f, h, and m, respectively), equimolar mixtures of varying concentra-

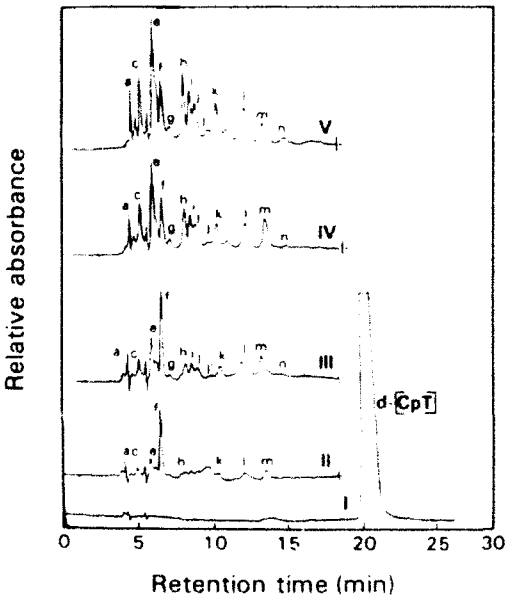

FIG. 2. HPLC product profiles of high-energy electron (13.2 MeV) irradiated d-[CpT] in aqueous solution and in air. I to V refer to radiation doses: control, 50, 250, 500, and 1000 Gy, respectively. The major irradiation product components, labeled a through p, were isolated, quantified, and characterized by HPLC and GC/MS and are listed in Table I.

TABLE I

Isolation and Characterization of the Products from Irradiation of d-[CpT] and d-[TpC]

HPLC peak	Retention time (min)	Compound	Prominent MS peaks (m/z, percentage intensity[a])
a	4.5	2'-Deoxycytidine-3'-phosphate	595 (0.1), 505 (0.3), 449 (0.3), 447 (0.3), 331 (10), 313 (15), 299 (60), 285 (30.0)
b	4.7	2'-Deoxycytidine-5'-phosphate	667 (0), 652 (0.1), 595 (0.1), 429 (0.2), 341 (0.4), 313 (0.3), 299 (0.2), 255 (0.4), 241 (0.6)
c	5.1	Cytosine	255 (55), 254 (90), 240 (100), 183 (20), 168 (45), 147 (60), 125 (10), 98 (28)
d	5.5	Thymidine-3'-phosphate	538 (0.1), 523 (0.2), 429 (0.1), 369 (0.1), 341 (30), 299 (25), 147 (100), 120 (20)
e	6.0	Thymidine-5'-phosphate	538 (0.4), 523 (0.4), 241 (50), 211 (10), 81 (30)
f	6.3	2'-Deoxycytidine	433 (3.0), 428 (2.0), 240 (5.0), 183 (10), 184 (10), 170 (50), 103 (20), 59 (15)
g	7.0	5,6-Dihydro-5,6-dihydroxythymidine	448 (25), 433 (30), 318 (5.0), 301 (10), 259 (100), 203 (5.0), 174 (5) 133 [illegible]
h	8.1	Thymine	270 (100), 255 [illegible], 170 (10), 147 (30), 131 (5), 113 (30), 81 (5), 59 (13)
i	8.4	5,6-Dihydro-5,6-dihydroxyuracil	434 (5.0), 419 (10), 362 (30), 347 (18), 331 (70), 245 (40), 130 (10), 73 (100)
j'	8.8	5,6-Dihydroxy-uracil	432 (15), 417 (30), 343 (5.0), 147 (60), 73 (100)
j	9.3	[b]	[b]
k	10.2	[b]	[b]
l	12.0	[b]	[b]
m	13.1	Thymidine	458 (1), 443 (2), 270 (5), 255 (3), 183 (10), 170 (35), 147 (30), 129 (10), 81 (25), 59 (10)
n	14.4	2'-Deoxycytidylyl-(3'-5')-5,6-dihydro-5,5-dihydroxythymidine	[c]
o	15.2	[b]	[b]
p	19.2	5,6-Dihydro-5,6-dihydroxythmidylyl-(3'–5')-2'-deoxycytidine	[c]

[a] HPLC-purified samples were transformed into their TMS derivatives; the TMS derivatives were subsequently analyzed by GC/MS and/or DIP/MS.
[b] Not identified.
[c] HPLC-purified samples were hydrolyzed by acid, and hydrolysates were treated with BSTFA. Subsequently the TMS preparations were analyzed by GC/MS, and corresponding base moieties were characterized.

tions of authentic samples of C, dC, T, and dT in water were eluted through a reverse-phase analytical HPLC column. No differences were observed in the retention times or peak areas whether the mixtures of C, dC, T, and dT or the individual bases or nucleosides were injected into the HPLC column. Calibration curves were determined by integration of peak areas as a function of concentration. These calibration curves were used for quantification of radiation-induced release of undamaged base and nucleoside moieties from irradiated d-[CpT] and d-[TpC] in aqueous solution as a function of dose.

Figure 3 is a representative comparison of products generated in aqueous solution from high-energy electron or fission-neutron irradiation (500 Gy) of d-[CpT] or d-[TpC] under aerobic conditions. The majority of the products formed are qualitatively similar for the two LETs investigated, although the quantities of the products formed differ slightly; there are, however, several significant differences. Specifically, the products labeled i and k are not detectable in neutron-irradiated d-[CpT] (Fig. 3A-I) or in neutron-irradiated d-[TpC] (Fig. 3B-I). Product p from neutron-irradiated d-[TpC] (Fig. 3B-I) is not detectable in high-energy electron-irradiated d-[TpC] (Fig. 3B-II). Product o from high-energy electron-irradiated d-[TpC] (Fig. 3B-II) was completely absent in neutron-irradiated d-[TpC] (Fig. 3B-I).

Figure 4 provides an example illustrating the effects of different gaseous environments on product yields. When d-[CpT] and/or d-[TpC] is irradiated using fission neutrons (500 Gy) in the presence of either air or nitrogen in deionized water (pH 7.0), no significant qualitative differences are observed in the product profiles. However, several quantitative differences are evident; for example, the product labeled m resulting from fission-neutron-irradiated d-[CpT] in air (Fig. 4A-I) versus nitrogen (Fig. 4A-II) and product label[illegible] p from fission-neutron-irradiated d-[TpC] in air (Fig. 4B-I) versus nitrogen (Fig. 4B-II) are attributed to oxygen-dependent reactions.

To compare and correlate quantitatively the efficiencies of the postirradiation release of free bases and free nucleo-

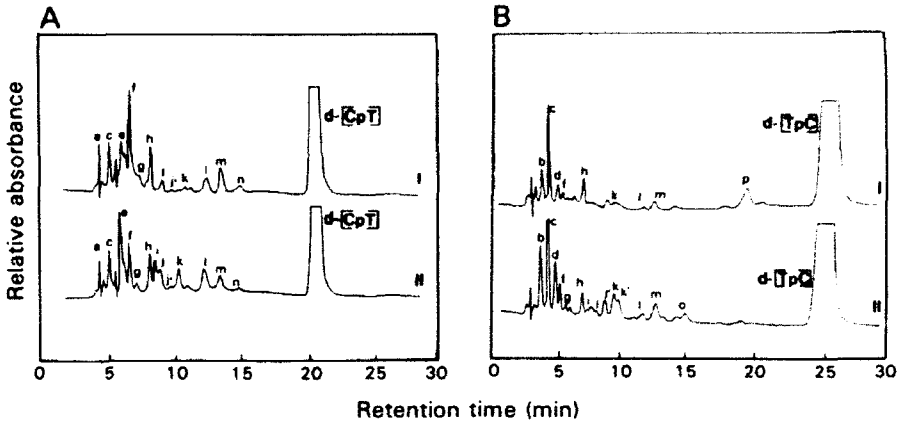

FIG. 3. HPLC profiles. Fission-neutron versus high-energy electron (500 Gy each) irradiation of d-[CpT] and d-[TpC] in air: (A) I, neutron-irradiated d-[CpT]; (A) II, high-energy electron-irradiated d-[CpT]; (B) I, neutron-irradiated d-[TpC]; and (B) II, high-energy electron-irradiated d-[TpC]. Representative examples of HPLC product profiles were obtained after irradiation of d-[CpT] or d-[TpC] in aqueous solution.

sides, aqueous solutions (1 mmol dm^{-3}, pH 7.0) were exposed to either fission-neutron or high-energy electron radiation in the presence of air or nitrogen, and the yields in μmol dm^{-3} were calculated at radiation doses of 50, 100, and 250 Gy according to the procedures of Roots and coworkers (*14*). The average G values (the number of molecules of product formed per 100 eV energy absorbed) and corresponding SEMs are listed in Table II.

Structural elucidation of the irradiation products from d-[CpT] and d-[TpC], labeled a to p in Fig. 5, was performed using data obtained from GC/MS and/or DIP/MS after treating purified individual components with BSTFA. Prominent mass spectral peaks (m/z) and corresponding relative intensities are listed in Table II. The TMS derivatives of the radiation-induced intact free bases C and T and nucleosides dC and dT (c, h, f, and m, respectively, in Table I) and the modified bases thymine glycol and uracil glycol (g and i, respectively, in Table I) exhibited excellent capillary column GC/MS and DIP/MS properties under our experimental protocol. However, several of the TMS preparations of nucleotides underwent thermal degradation at least to some extent; hence DIP/MS was used to characterize the TMS derivatives of nucleotides. Electron impact mass spectra and fragmentation patterns of TMS derivatives of nucleic acid components have been extensively studied and reported by McCloskey and co-workers (*15, 16*), and mass spectral data of both modified bases (g and i) have been discussed by Dizdaroglu (*17, 18*). Our structural assignments for the TMS derivatives of products labeled a to p are consistent with those already reported (*15–18*). In characterizing modified intact d-[CpT] and d-[TpC], HPLC-purified products peak-labeled n and p were hydrolyzed using 6 N HCOOH and hydrolysates were subsequently dried and treated with BSTFA according to procedures described by Dizdaroglu (*17*). The presence of thymine glycol and intact cytosine was revealed by GC/MS assay of the TMS deriva-

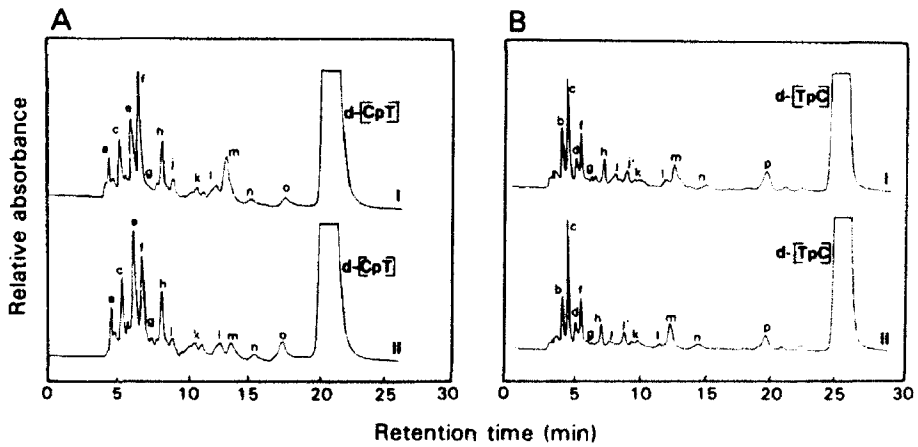

FIG. 4. HPLC profiles. Fission-neutron irradiation of d-[CpT] and d-[TpC] in air versus nitrogen (radiation dose: 500 Gy each): (A) I, irradiated d-[CpT] in air; (A) II, irradiated d-[CpT] in nitrogen; (B) I, irradiated d-[TpC] in air; and (B) II, irradiated d-[TpC] in nitrogen. Representative examples of HPLC product profiles were obtained after irradiation of d-[CpT] or d-[TpC] in aqueous solution.

TABLE II

***G* Values for Postirradiation Release of Undamaged Nucleobases and Nucleosides from d-[CpT] and d-[TpC]**

Dinucleotide	Released product	*G* values ± SEM[a] H-E (e^-) in air	Neutrons in air	Neutrons in nitrogen
d-[CpT]	Cytosine	0.008 ± 0.001	0.019 ± 0.002	0.009 ± 0.001
	Thymine	0.008 ± 0.001	0.024 ± 0.005	0.014 ± 0.001
	2-d-Cytidine	0.025 ± 0.002	0.028 ± 0.003	0.008 ± 0.001
	Thymidine	0.008 ± 0.001	0.015 ± 0.002	0.005 ± 0.001
d-[TpC]	Cytosine	0.013 ± 0.001	0.010 ± 0.002	0.007 ± 0.001
	Thymine	0.014 ± 0.002	0.009 ± 0.001	0.007 ± 0.001
	2-d-Cytidine	0.015 ± 0.004	0.019 ± 0.001	0.004 ± 0.001
	Thymidine	0.005 ± 0.002	0.007 ± 0.001	0.010 ± 0.001

[a] The release of intact nucleobases and nucleosides is measured after irradiation of 0, 50, 100, 250, 500, and 1000 Gy; the *G* values for the free bases and nucleosides were calculated after irradiation with 50, 100, and 250 Gy and are means of at least three independent experiments. The *G* values are defined as the number of molecules of product formed per 100 eV energy absorbed.

tives in both samples, confirming the chemical structures of n and p as modified d-[CpT] and d-[TpC], respectively, and that the modification had taken place at 5,6-positions of the thymine moieties of d-[CpT] and d-[TpC].

DISCUSSION

To obtain an improved perspective of the radiation chemistry of native DNA and to determine whether nucleoside sequence is important in determining the types and amount of damage caused by radiations of different LET, we selected a "pyrimidine–pyrimidine" system consisting of the dinucleoside monophosphate d-[CpT] and its sequence isomer d-[TpC]. Aqueous solutions of d-[CpT] or d-[TpC] were exposed to either fission neutrons or high-energy electrons, and products were analyzed. The chemical nature of the postirradiation release of free and modified bases, free nucleosides, and free and modified nucleotides were identified and quantified by standard HPLC and by GC/MS or DIP/MS. The HPLC and GC/MS methodologies for the isolation, purification, and structural elucidation of the radiation-induced products were selected since both the methodologies are quite specific and sensitive, having detection capability of approximately 1–5 pmol. In most instances these procedures allow assaying radiation damage in small DNA oligomers without the necessity of further degradation by acidic conditions. Acid hydrolysis is known to lead to artifactual lesions (*19*). For the structural characterizations, we first isolated individual components from the radiation product mixtures by HPLC, freeze-dried the isolated individual components, and subsequently treated them with BSTFA. The resulting silyl ether derivatives were analyzed by GC/MS. To minimize the possibilities of thermal degradation, several TMS ethers of nucleotides isolated from the product profiles were further characterized by DIP/MS. The nucleotide dimers were exposed to varying doses of radiation, and the detectable products were characterized. Comparisons of the product profiles generated from the fission-neutron or high-energy electron irradiation of d-[CpT] and d-[TpC] suggest that independent of the quality of the radiation, at relatively low radiation doses (50–250 Gy), most of the detectable products originated from N-glycosidic or phosphodiester bond-cleavage, whereas at higher doses (500–1000 Gy) additional products appear to be formed by ring modification. For example, product n in Fig. 2 and product p in Fig. 3B-I are ring-modified products detectable at doses 500 Gy or greater; products m and f (Figs. 2, 3, and 4) are present at all radiation doses examined independent of the sequence isomer. At the lower doses, we found no qualitative differences in product formation although the quantities of the product formed were different; however, product p, intact modified d-[TpC], in Fig. 3B-I was not apparent in Fig. 3B-II, thereby signifying a radiation quality-dependent response to ionizing radiation. Teoule and Cadet (*7*) had previously investigated radiation damage to DNA monomer. Based on the studies of Teoule and Cadet and Box and co-workers (*6–11*) of dinucleoside monophosphates, certain expected products were not observed in our studies. For example, in the case of dinucleotides containing thymidine, the principal known modification is that in which the base moiety degrades to formamide. It is possible that the yields are small and that these expected products are among the several minor products not identified in our investigation. Mechanistic rationales for product formation have been described and discussed elsewhere (*5, 20*).

High-performance liquid chromatography in conjunction with proton magnetic resonance (PMR) spectrometry is an excellent analytical technology for the direct determination of absolute stereochemistry including anantiomeric forms (*11, 12*) of organic compounds, for example, glycols of thymine and uracil as well as 5,6-dihydro-5,6-dihydroxy modification of d-[CpT] or d-[TpC] obtained in this investigation. However, at least 100 μg of purified glycol is re-

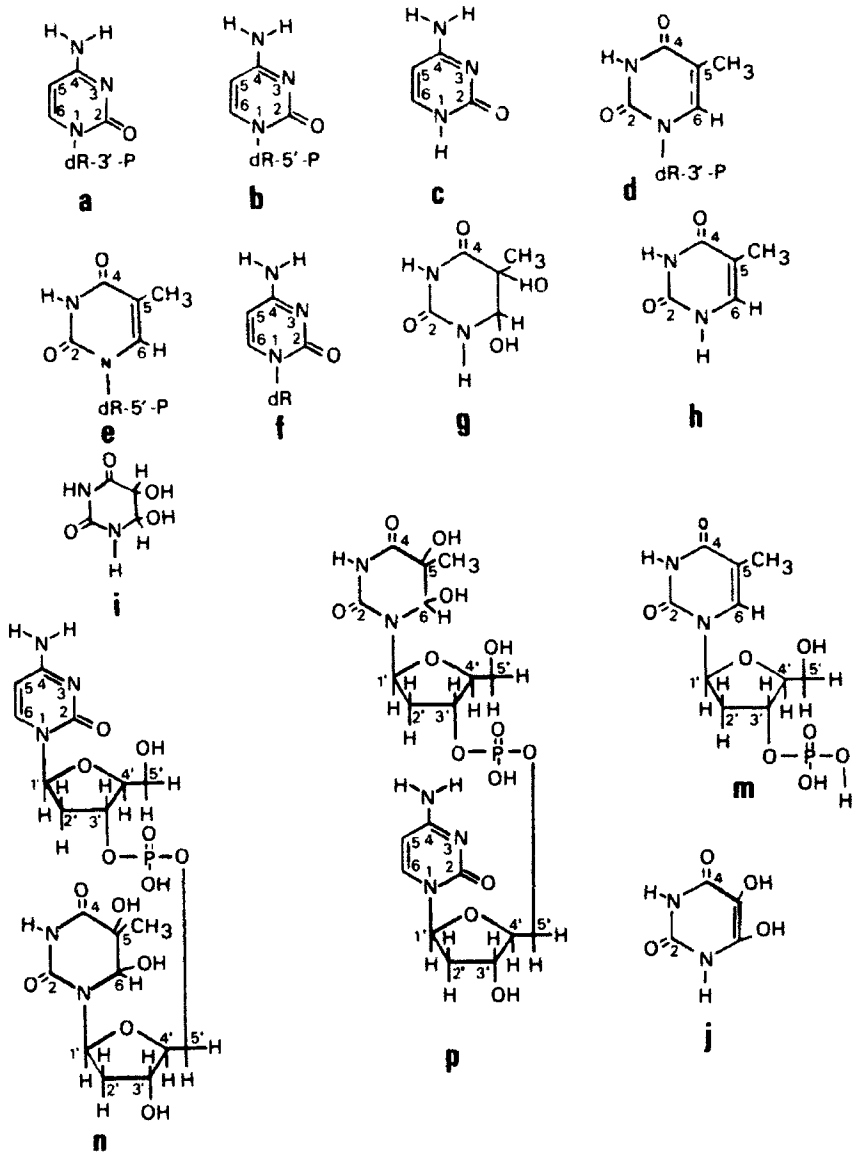

FIG. 5. Chemical structures of the identified irradiation products from d-[CpT] and d-[TpC]. Labels a to p correspond to those in Table I.

quired for the acceptable PMR spectra for full characterization. Our experimental procedure yielded only nanomolar quantities of purified materials which was sufficient for GC/MS analysis but not for detailed direct configurational assignments by PMR. The stereochemistry of glycols of thymine and cytosine (uracil glycol-deamination product of cytosine) observed in the present studies, both had *cis* configurations with respect to 5,6-hydroxy groups. These configurations were verified indirectly by comparison of mass spectral peak intensity ratios, with the corresponding reference *cis*-oriented TMS derivative of glycol mass spectra. The reference mass spectra for *cis*- and *trans*-TMS derivatives of thymine glycol were generously provided by Dr. Swartz of Wake Forest University (Winston-Salem, NC) and mass spectra of *cis*-uracil glycol have been reported by Dizdaroglu and co-workers (*21*).

The TMS derivatives of hydrolysates of products n and p, modified dinucleoside monophosphates, also revealed the presence of thymine glycol in *cis* configuration in both of the glycol moeities upon GC/MS analysis and comparison with the reference mass spectra. The *trans* isomer was not detected in either of the cases. It is possible that the yields of *trans* isomer of thymine and cytosine were low and that they were also among the several minor products not identified in our investigation.

A recent report by Fox and McNally (*22*) suggest that fission neutrons produce fewer single-strand breaks but approximately the same number of double-strand breaks in Chinese hamsterV79 cells after exposure to equal doses of X or γ rays. This suggests there is a difference in the details of the molecular types of damage produced by different qualities of radiations (*23*). For an end point such as cell

killing, neutrons are approximately 1.5 to 6 times more effective than either X or γ rays (*24*). In the cells, radiation damage is generally considered to be brought about by a combination of indirect and direct effects as described by Roots and co-workers (*25*). The indirect effect consists of the interactions of target molecule (DNA) with the products of water radiolysis, hydroxyl radical ($OH^{\bullet}$), hydrogen atom ($H^{\bullet}$) and solvated electrons (e^{-}_{aq}). The direct effect consists of excitation and ionization of target molecules by the particle and its secondaries. In low-LET radiation, DNA damage occurs primarily via indirect effect. In the case of high-LET radiation, for example, fission-neutron damage occurs primarily via high-energy recoil protons (*26*). Direct and indirect action are not completely distinct because radiolysis produts produced by indirect action can react with radicals formed in the target molecules by either indirect or direct action. In the present studies, several quantitative differences were observed in the product profiles obtained from high- and low-LET irradiated (equal doses) d-[CpT] and d-[TpC] may have arisen due to some combinations of direct and indirect effects. As expected, these differences were not so large since irradiation were performed on relatively small sized target molecules, and in dilute aqueous solution.

During the course of our studies, we observed generation of free bases, nucleosides and mononucleotides along with free glycols of bases, and intact 5,6-dihydro-5,6-dihydroxythymine modification of d-[CpT] and d-[TpC] prior to acid hydrolysis. The chemical nature of the products detected from irradiated d-[CpT] and d-[TpC] are consistent with those observed by Ward and Cuo (*27*) and Teoule and co-workers (*28*). On the other hand, we did not observe intact glycol derivatives or any other base-modified thymidine, 2-deoxycytidine or uridine (modified intact nucleoside), or corresponding intact modified nucleoside monophosphates prior to acid hydrolysis, which is consistent with the observations made by Belfi and co-workers (*8*). This rules out the possibility of two chemical effects, namely, base modification and strand scission, having occurred simultaneously on the same target molecule. Teoule and co-workers (*28*) have also reported that, even at relatively low radiation doses, bases such as thymine and cytosine are released from DNA. Detection of free thymine and uracil glycols could also be a result of secondary radiation products, at least in part.

A recent report by Roots *et al.* (*14*) suggest a possible correlation of strand break yields with release of intact bases in SV40 DNA. Several other authors have also reported release of intact bases after irradiation under nitrogen (*29*), in air (oxygenated solution) (*27*), and in cultured mammalian cells (*30*); the release of intact nucleosides from dinucleotides has been verified by Box and co-workers (*11*). To compare and quantify the radiation-produced damage in model compounds exposed to fission neutrons or high-energy electrons and to test the assumption that the amount of intact bases released might correlate with the extent of DNA strand breaks, we compared the yields of release of intact nucleobases (C and T) and nucleosides (dC and dT) from d-[CpT] and d-[TpC] after radiation exposure. The G values calculated according to the equation of Roots and co-workers (*14*) are given in Table II. The G values for released intact C, dC, T, and dT after fission-neutron irradiation in air from d-[CpT] are significantly greater than the G values of high-energy electron-irradiated d-[CpT] in air. On the other hand, fission-neutron-irradiated d-[TpC] in air showed a somewhat different trend: only G values for the release of C and T were slightly higher when d-[TpC] was exposed to high-energy electron irradiation (in air). Our G values do not include the effect of radiation-induced labile bonds formed since we did not determine the G values after incubating irradiated samples at 37°C for a specific time (t = 3–6 h) (*14, 27*). The initial G values obtained in this study clearly suggest a dependence on base sequence and radiation quality for the amount of radiation damage.

The yields of primary radicals in aqueous solutions exposed to ionizing radiation can be altered by saturating the solution with different gases prior to irradiation (*31*). Several radiobiological end points (for example, enhancement of radiosensitivity of cells in saturated air compared to nitrogen-saturated conditions) can be altered by such modifications (*32*). At the molecular level, these yield differences in DNA base products are known to be a function of oxygen concentration (*33*). We examined the effects of fission-neutron irradiation for air-saturated versus nitrogen-saturated solutions of d-[CpT] and d-[TpC]. Our observed product G values were significantly lower when dinucleotides were irradiated in nitrogen-saturated solution as opposed to oxygenated solution, an effect attributed to the presence of oxygen.

Although the dinucleoside monophosphates studied here are crude DNA models, they are nevertheless useful since the fundamental reaction pathways are presumably similar to those occurring in longer DNA segments. In the absence of repair processes, our data demonstrate that the "pyrimidine–pyrimidine" system, composed of only two nucleobases, responds differently to ionizing radiation of different qualities. Future objectives will be to extend these investigations to the radiation chemistry of larger oligomers having specific lengths and base sequence, to quantify the amount and type of products generated, and to determine whether multicenter damage sites exist.

ACKNOWLEDGMENT

This research was supported by the Armed Forces Radiobiology Research Institute, Defense Nuclear Agency, under work unit 00145.

RECEIVED: April 8, 1992; ACCEPTED: August 31, 1992

REFERENCES

1. R. Teoule, Radiation-induced DNA damage and its repair. *Int. J. Radiat. Biol.* **51**, 573–589 (1987).

2. M. Raha and F. Hutchinson, Deletions induced by γ rays in the genome of *Escherichia coli*. *J. Mol. Biol.* **220**, 193–198 (1991).
3. M. Erreraa, Les effects des radiations nucleaires a faibles doses. *La Recherche* **16**, 959–968 (1985).
4. M. Sotheim-Maurizot, M. Charlier, and R. Sabattier, DNA radiolysis by fast neutrons. *Int. J. Radiat. Biol.* **57**, 301–313 (1990).
5. D. Schulte-Frohlinde, Studies of radiation effects on DNA in aqueous solution. *ICRU NEWS* 4–15, December (1989).
6. J. Cadet and L. Voituriez, Seperation par chromatographie sur couche minceet par chromatographie liquide a haute performance de dinucleoside-monophosphates modified par action du rayonnment gamma. *J. Chromatogr.* **178**, 337–343 (1979).
7. R. Teoule and J. Cadet, Radiation-induced degradation of the base component in DNA and related substances-final product. *Mol. Biol. Biochem. Biophys.* **27**, 171–203 (1978).
8. C. A. Belfi, A. V. Arakali, C. R. Paul, and H. C. Box, Radiation chemistry of a dinucleoside monophosphate and its sequence isomer. *Radiat. Res.* **106**, 17–30 (1986).
9. C. R. Paul, A. V. Arakali, J. C. Wallace, J. McReynolds, and H. C. Box, Radiation chemistry of 2′-deoxycytidylyl-(3′-5′)-2′-deoxy-guanosine and its sequence isomer in nitrous oxide and oxygen saturated solutions. *Radiat. Res.* **112**, 464–478 (1987).
10. C. R. Paul, C. A. Belfi, A. V. Arakali, and H. C. Box, Radiation damage to dinucleoside monophosphates: Mediated versus direct damage. *Int. J. Radiat. Biol.* **51**, 103–114 (1987).
11. H. C. Box, C. R. Paul, and J. Przybyszewski, Studies on radiation damage using DNA oligomers. *Free Radical Res. Commun.* **6**, 123–126 (1989).
12. Y. N. Vaishnav, E. Holwitt, C. E. Swenberg, H.-C. Lee, and L.-S. Kan, Synthesis and characterization of stereoisomers of 5,6-dihydro-5,6-dihydroxy-thymidine. *J. Biomol. Struct. Dyn.* **8**, 935–951 (1991).
13. M. Dooley, L. J. Goodman, G. H. Zeman, R. B. Schwartz, C. M. Eisenhauer, and P. K. Blake, Ionization chamber intercomparison in mixed neutron and γ ray radiation fields by National Bureau of Standards and Armed Forces Radiobiology Research Institute. Technical Report TR 86–3, Armed Forces Radiobiology Research Institute, Bethesda, MD, 1986. [Available from National Technical Information Services, Springfield, VA, Accession number A 178336.]
14. R. Roots, E. Henle, W. R. Holley, and A. Chatterjee, Measurements of nucleic bases released after γ irradiation of DNA in solution in air. *Radiat. Res.* **125**, 288–292 (1991).
15. J. A. McCloskey, Mass spectrometry. In *Basic Principles in Nucleic Acid Chemistry* (P. O. P. Ts'o, Ed.), Vol. 1, pp. 209–309. Academic Press, New York, 1974.
16. J. A. McCloskey, A. M. Lowson, K. Tsuboyama, P. M. Krueger, and R. N. Stillwell, Mass spectrometry of nucleic acid components. Trimethylsilyl derivatives of nucleotides, nucleosides and bases. *J. Am. Chem. Soc.* **90**, 4182–4184 (1968).
17. M. Dizdaroglu, Application of capillary gas chromatography–mass spectrometry to chemical characterization of radiation-induced base damage of DNA: Implications for assessing DNA repair processes. *Anal. Biochem.* **144**, 593–603 (1985).
18. M. Dizdaroglu, Use of capillary gas chromatography for identification of radiation-induced DNA base damage and DNA base-amino acid cross-links. *J. Chromatogr.* **295**, 103–121 (1984).
19. N. E. Geacintov and C. E. Swenberg, Chemical, molecular biology, and genetic technique for correlating DNA damage induced by ionizing radiation with biological end-points. In *Physical and Chemical Mechanisms in Molecular Radiation Biology* (W. A. Glass and M. N. Varma, Eds.), pp. 453–474. Plenum, New York, 1991.
20. F. Hutchinson, Chemical changes induced in DNA by ionizing radiation *Prog. Nucleic Acid Res. Mol. Biol.* **32**, 115–154 (1985).
21. M. Dizdaroglu, E. Holwitt, M. P. Hagan, and W. F. Blakely, Formation of cytosine glycol and 5,6-dihydroxycytosine in deoxyribonucleic acid on treatment with osmium tetroxide. *Biochem. J.* **235**, 531–536 (1986).
22. J. C. Fox and N. J. McNally, Cell survival and DNA double-strand break following x-ray or neutron irradiation of V79 cells. *Int. J. Radiat. Biol.* **54**, 1021–1030 (1988).
23. K. M. Prise, S. Davies, and B. D. Michael, The relationship between radiation-induced DNA double strand breaks and cell kill in hamster V79 fibroblasts irradiated with 250 kVp x-rays, 2.3 MeV neutrons of 238-Pu alpha particles. *Int. J. Radiat. Biol.* **52**, 893–902 (1987).
24. G. W. Barendsen, Radiobiology of neutrons. *Int. J. Radiat. Oncol. Biol. Phys.* **8**, 2103–2107 (1982).
25. R. Roots, A. Chatterjee, P. Chang, L. Lommel, and E. A. Blakely, Characterization of hydroxyl radical-induced damage after sparsely and densely ionizing irradiation. *Int. J. Radiat. Biol.* **47**, 157–166 (1985).
26. D. E. Watt, Absolute biological effectiveness of neutrons and photons. *Radiat. Prot. Dosim.* **23**, 63–67 (1988).
27. J. F. Ward and I. Kuo, Strand-breaks, base release and postirradiation changes in DNA gamma-irradiated in dilute oxygen-saturated aqueous solution. *Radiat. Res.* **66**, 485–498 (1976).
28. R. Teoule, A. Bonicel, C. Bert, J. Cadet, and M. Polverelli, Identification of radioproducts resulting from the breakage of thymine moiety by gamma irradiation of *E. coli* DNA in an aerated aqueous solution. *Radiat. Res.* **57**, 46–58 (1974).
29. M. Ullrich and U. Hagen, Base liberation and concomitant reactions in irradiated DNA solution. *Int. J. Radiat. Biol.* **19**, 507–517 (1971).
30. M. R. Mattern, P. V. Hariharan, B. E. Dunlap, and P. A. Cerutti, DNA degradation and exicision repair in gamma-irradiated Chinese hamster ovary cells. *Nature* **245**, 230–232 (1973).
31. A. F. Fuciarelli, B. J. Wegher, W. F. Blakely, and M. Dizdaroglu, Yields of radiation-induced base products in DNA: Effects of DNA conformation and gassing conditions. *Int. J. Radiat. Biol.* **58**, 397–415 (1990).
32. C. J. Koch, A thin-film culturing technique allowing rapid gas–liquid equilibrium with no toxicity to mammalian cells. *Radiat. Res.* **97**, 434–442 (1980).
33. A. F. Fuciarelli, B. J. Wegher, W. Gajewski, M. Dizdaroglu, and W. F. Blakely, Quantitative measurement of radiation-induced base products in DNA using gas chromatography–mass spectrometry. *Radiat. Res.* **119**, 219–231 (1989).

Pharmacology Biochemistry and Behavior, Vol. 44, pp. 809-814, 1993

0091-3057/93 $6.00 + .00

Effects of Sublethal Doses of Ionizing Radiation on Repeated Acquisition in Rats

PETER J. WINSAUER[1] AND PAUL C. MELE

Behavioral Sciences Department, Armed Forces Radiobiology Research Institute, National Naval Medical Command, Bethesda, MD 20889-5145

Received 6 July 1992

WINSAUER, P. J. AND P. C. MELE. *Effects of sublethal doses of ionizing radiation on repeated acquisition in rats.* PHARMACOL BIOCHEM BEHAV 44(4) 809-814, 1993.– To extend previous research on the effects of ionizing radiation on learning, dose-effect data with ^{60}Co γ-rays were collected for individual rats responding under a repeated-acquisition procedure. Under this procedure, subjects acquired a different three-response chain each session by responding (nose push) on one of three transilluminated response keys in the presence of each of three sequentially ordered colors. The response chain was maintained under a second-order fixed ratio (FR) 2 schedule of food presentation. An error produced a 5-s timeout but did not reset the three-response chain. Acquisition of each response chain was defined by a decrease in errors as the session progressed (i.e., within-session error reduction). Each session ended after 200 reinforcements or 90 min, whichever occurred first. When day-to-day acquisition for all four subjects reached a steady state, the effects of three or four doses of γ-rays were assessed. In general, radiation doses of 1, 3, 4.5, and 8 Gy of gamma radiation delivered at a dose rate of 2.5 Gy/min produced a dose-dependent decrease in the overall response rate for 24–72 h after exposure in all four subjects. Radiation exposure also produced an increase in percent errors but only at doses that substantially decreased overall rate of responding. Unlike the effects on response rate, which were relatively consistent over a 72-h period, the effects on accuracy were greater at 72 h than at 24 h in three of four subjects. The results indicate that the repeated-acquisition procedure may be particularly useful for quantifying the effects of ionizing radiation on acquisition behavior or learning and that γ-rays can differentially affect behavioral measures of rate and accuracy over a 72-h period following exposure.

Repeated acquisition Operant behavior γ-rays Rats

FEW studies have examined the effects of ionizing radiation on learning, or the acquisition of behavior. Moreover, these studies, which involved both monkeys and rats, have produced widely differing results ranging from improved to disrupted learning [see (15) for review]. In the studies involving monkeys, for example, the reported inconsistencies can often be attributed to different tasks or doses and types of radiation or simply to the lack of data in general. However, in the rat studies where the effects of radiation have in general been tested on only one type of learning (i.e., maze learning), the inconsistencies in the data are still marked. Two reports (3,9), for example, found that rats exposed to either 4.8 Gy of whole-body X-rays or 24.2 Gy of cranial X-rays actually performed better on a maze task than nonirradiated control rats. Although the effects in these studies have been explained in various ways (e.g., irradiated subjects may be less distractible), the failure to find convincing evidence that ionizing radiation affects the acquisition of behavior in a consistent manner is somewhat surprising.

One possible explanation may be related to the fact that there are large individual differences in rates of acquiring behaviors. This aspect of learning, along with the well-established finding (11) that subjects reacquire specific tasks at a faster rate (i.e., subjects "learn to learn"), have consistently posed problems for the study of learning and those variables affecting it. For these reasons, as Anger and Setzer (1) state in their article examining the effects of a pesticide on learning, certain types of learning such as maze learning may not be the most appropriate baseline for the evaluation of toxic agents because it can be a one-time learning phenomenon and is not repeatable in the same subject [cf. (17)]. The important distinction between testing the effects of a toxic agent on learning and testing the effects of a toxic agent on retention of learning was demonstrated in a radiation study by Urmer and Brown (24). They found that sublethal doses of ionizing radiation in rats produced no disruptive effects on the retention of response patterns acquired preirradiation but did produce a decrement in the capacity of subjects to reorganize the

[1]To whom requests for reprints should be addressed.

For ease of comparison with previous research, all the radiation doses cited (either roengten or rad) have been converted to Gray (Gy). The conversion factor for roengten to rad is 0.966 to account for the difference between air and muscle. Rad can be converted to Gray by multiplying the dose by 1/100.

preirradiation response pattern into a new response pattern postirradiation.

To deal with some of the problems involved in studying learning and the effects of drugs on learning, for example, Thompson (21,22) adapted a repeated-acquisition technique and used each subject as its own control. The repeated acquisition of behavioral chains provided a baseline under which the effects of various drugs on learning could be examined repeatedly, and the use of each subject as its own control helped deal with the problem of intersubject variability. The results indicated that repeated-acquisition procedures provide a sensitive baseline for assessing the effects of drugs on learning in individual subjects and that learning was more sensitive to drug effects than a performance condition where learning was not required. Shrot et al. (18), for example, developed this procedure in rats to examine the effects of microwave radiation on learning. Although there were methodological differences (e.g., only a single condition and auditory cues vs. visual cues), they found that microwave radiation was highly disruptive to learning at certain power densities. Since then, other investigators have effectively used this procedure with a variety of species to examine the effects of many toxic agents [e.g., carbon monoxide (19), carbaryl (1), and lead (7)] on acquisition behavior.

To examine the effects of ionizing radiation on learning in individual rats, the present research used a repeated-acquisition task similar to that used by Thompson (21,22). More specifically, the subject's task was to acquire a different three-response chain each session by responding sequentially on three keys in the presence of three colors. Acquisition of each response chain was defined by a decrease in errors as the session progressed. Following baseline stabilization where acquisition for each subject reached a steady state, dose-effect data were obtained for three or four doses of ^{60}Co γ-rays.

METHOD

Subjects

Four adult male Sprague-Dawley rats (R-9, R-13, R-14, and R-16) maintained at approximately 80% of their free-feeding weights (373, 404, 373, and 393 g, respectively) served as subjects. Food was earned during the experimental session and, if necessary, was provided in the home cage after the session to maintain subjects at their 80% weight. All subjects were housed individually in plastic Microisolator cages containing sterilized hardwood-chip bedding. The housing room was maintained at 21 ± 1°C with 50 ± 10% relative humidity on a 12 L : 12 D cycle, which began at 6:00 a.m. each day. Acidified water (pH 2.5-3) was available in the home cage throughout the experiment to minimize the possibility of opportunistic bacterial infection. Each subject had an extensive history of repeated acquisition of three-response chains under fixed-ratio (FR) schedules.

Apparatus

Four identical modular test chambers (Coulbourn Instruments, Inc., Model E10-10TC) configured specifically for rodents were used. The front wall of each chamber contained a houselight, speaker, auditory feedback relay, pellet trough (10 cm above the floor and centered), and three response keys aligned horizontally (8 cm apart, center to center, and 4.5 cm above the floor). Each response key could be transilluminated by three Sylvannia 28ESB indicator lamps, one with a red plastic cap, one with a green, and one with a yellow. Response keys required a minimum force of 0.15 N for activation and produced an audible click of the feedback relay. Each chamber was enclosed within a sound-attenuating cubicle equipped with a fan for ventilation. White noise was continuously present in each chamber to mask extraneous sounds. The chambers were connected to a PDP11/73 computer (Digital Equipment Corp., Bedford, MA) programmed in SKED-11 software (State Systems, Inc., Kalamazoo, MI) and to cumulative recorders (Gerbrands Corp., Arlington, MA) located in a nearby room.

Procedure

Baseline. During each session, all three response keys were illuminated at the same time with one of three colors, either green, red, or yellow. The rodent's task was to respond (nose push) on the correct key in the presence of each sequentially illuminated set of colors (e.g., keys green, center correct; keys red, left correct; keys yellow, right correct; reinforcement). The same chain [in this case, center-left-right (CLR)] was repeated throughout a given session. The three-response chain was maintained by food presentation under an FR 2 schedule, that is, every second completion of the chain illuminated the pellet trough and produced a 45-mg pellet. A completion of the response chain that did not produce food was followed by a 0.4-s presentation of the pellet trough light. When the subject pressed an incorrect key (in the example, the left or right key when the green light was presented), the error was followed by a 5-s timeout. During the timeout, the key lights were turned off and responses had no programmed consequence. An error did not reset the three-response chain, that is, the stimuli were the same before and after the timeout.

To establish a steady state of repeated acquisition, the three-response chain was changed from session to session. A typical set of five chains was CLR, RCL, LRC, CRL, and RLC, with the order of the color presentations always green, red, yellow (reinforcement). The chains were carefully selected in several ways and there were restrictions on their ordering across sessions. More specifically, each sequence was scheduled with equal frequency and adjacent positions within a sequence for a given session were different. Occasionally, a correct sequence position for a given color was the same two sessions in a row.

Sessions were conducted Monday through Friday between 9:00 a.m. and 2:00 p.m. Each session was terminated after 200 reinforcements or 90 min, whichever occurred first. The data for each session were analyzed in terms of a) the overall response rate (total responses/min, excluding timeouts) and b) the overall accuracy, expressed as percent errors [(errors/total responses) × 100]. In addition to these measures based upon session totals, within-session changes in responding were monitored by a cumulative recorder and the computer. For example, acquisition of a response chain was indicated by within-session error reduction, that is, a decrease in the number of errors between food presentations as the session progressed.

Radiation testing. Following baseline stabilization, dose-effect data were obtained for multiple doses of gamma radiation. Subjects received bilateral, whole-body, midline tissue doses of 1, 3, 4.5, and 8 Gy of γ-rays administered at a fixed rate of 2.5 Gy/min from a ^{60}Cobalt source. These doses were selected from a range of doses previously found to have an effect on other schedule-controlled operant behaviors [e.g., fixed-interval (FI) and FR schedules (13)]. In general, doses of radiation were given in a mixed order except for the 8-Gy dose, which was administered last in three of four subjects. Subject R-16 received the 8-Gy dose as a third exposure and

was allowed 13 weeks of baseline recovery before being given a final 4.5-Gy exposure. The minimum time between exposures for doses less than 8 Gy was 4 weeks. This interval was chosen to allow for a) complete baseline recovery [cf. (13)] and b) the collection of sufficient control data prior to the next exposure.

For irradiation, subjects were placed in well-ventilated, clear plastic restraining tubes. A clear plastic stand, which held the tubes in a stacked position, allowed all four subjects to be exposed at one time, if desired. Dosimetry for bilateral irradiations was completed prior to the actual animal irradiations. Standard Task Group 21, Radiation Therapy Committee of the American Association of Physicists in Medicine (AAPM), protocol procedures (20) were used. A 50-cm^3 ionization chamber was used to obtain the free-in-air (FIA) tissue dose rate at the appropriate exposure position. A 0.5-cm^3 tissue-equivalent ion chamber was also used to obtain the tissue dose rate in the same position in a tissue-equivalent rat phantom. The tissue-to-air ratio (TAR) was calculated by dividing the nominal 0.5-cm^3 chamber reading by the 50-cm^3 chamber reading. The administered dose (midline tissue at the abdomen) to each animal was determined by the TAR value, the FIA value, duration of the irradiation, and other factors such as temperature and pressure. Each irradiation was conducted on a Monday and required approximately 20 min. This time included the actual exposure and the time necessary for transporting rats to and from the exposure area. Sham irradiations, which also included transport, consisted of subjects' being placed in the restraining tubes for a comparable amount of time.

RESULTS

Under baseline conditions, stable responding in the repeated-acquisition task was obtained in each of the four subjects. Stability was reflected in the consistent levels of overall response rate and accuracy for each subject from session to session. Acquisition of response chains was characterized by a steady state in terms of stable within-session error reduction, that is, the number of errors decreased as each session progressed.

Figure 1 shows the overall response rate and percent errors for each subject during control sessions and sessions at 24 and 72 h following γ-ray irradiation. Although all subjects were tested daily after radiation exposure, the data from these two sessions most clearly illustrate the effects obtained. In general, the effects at 48 h after exposure were comparable to those at 24 h; and in three of four cases, those at 96 h were comparable to those at 72 h. For the sessions presented, a dose of radiation was considered to have an effect to the extent that the postirradiation data fell outside the control range. As shown in the upper panel, despite relatively large individual differences in the control ranges, radiation exposure dose dependently decreased the overall response rate in each of the four subjects during both the 24- and 72-h sessions. Although there was an instance in which the effect of radiation at 72 h was larger than that at 24 h (i.e., the rate-decreasing effect obtained at the 8-Gy dose in RP-16), the effects on response rate during the 24-h session were in general larger than or consistent with those that occurred 72 h after exposure. This was in particular evident in RP-16 and RP-9 at the 4.5-Gy dose, where the rate-decreasing effects obtained 24 h after exposure were notably larger than those obtained 72 h after exposure.

As can be seen in the lower panel of Fig. 1, the differences in control ranges for percent errors across subjects were not as large as those for overall response rate (i.e., accuracy was comparable for all four subjects). In general, exposure to radiation produced dose-dependent increases in percent errors in each subject. These effects were most evident at the 8-Gy dose for both the 24- and 72-h sessions. In this regard, the effects on accuracy were unlike those on overall response rate, where an intermediate dose (4.5 Gy) of radiation produced an effect in three of four subjects. Note that exposure to 4.5 Gy only increased percent errors in RP-16 and RP-9 at 72 h. In other words, decreases in response rate tended to occur at lower doses than those required to increase percent errors and increases in percent error occurred only at doses that substantially decreased overall response rate.

Interestingly, the effects of the 8-Gy dose of radiation on percent errors were different from the effects on response rate in that percent errors were affected more at 72 h than at 24 h in three of four rats. In these three rats, the increase in percent errors at 72 h occurred at a time when the overall response rates were comparable to those at 24 h. Moreover, in RP-9 this noticeably larger effect at 72 h occurred at the 4.5-Gy dose of radiation when the decrease in overall response rate was less than that which occurred at 24 h (i.e., at a time when response rate appeared to be returning to control levels).

Figure 2 illustrates some of the within-session effects of an 8-Gy dose of radiation in subject RP-9. Each cumulative record represents a complete session from a different day. As can be seen in the control record, errors decreased in frequency while the number of correct completions of the chain increased in frequency as the session progressed. This within-session error reduction, which occurred shortly after the start of the session, reflects acquisition of the response chain. Following acquisition, the pattern and rate of correct responding remained relatively constant throughout the session. Although some pausing did occur toward the end the session, the rat did obtain the total number of available reinforcers. At 24 h after an 8-Gy dose of radiation (middle record), there was a substantial decrease in the overall rate of responding, a decrease in the number of correct sequence completions, and an increase in pausing. Note that periods of no responding occurred earlier in the session and were longer in duration than under control conditions. In addition, there was little evidence of any within-session error reduction, as indicated by the relatively constant error rate that occurred on the event pen when the subject was responding. At 72 h after the 8-Gy exposure (bottom record), similar within-session effects on overall response rate occurred. As can be seen, long pauses occurred throughout the session and the total number of reinforcers obtained during the session was substantially reduced. In this session, however, the total number of errors was greater than that in the 24-h session even though the overall response rate was comparable. This difference in accuracy is evident in the pattern and frequency of errors indicated by the event pen in both records. In general, the within-session effects of this dose of radiation were replicated in two of the remaining three rats. Although RP-16 did show an increase in percent errors and a decrease in overall response rate at this dose, there was little or no difference in the within-session effects at 24 and 72 h.

Three of four rats (RP-9, RP-13, and RP-16) received a total γ-ray dose of 16.5 Gy. The other rat, RP-14, received a total dose of 13.5 Gy. This total dose was lethal in RP-9, RP-13, and RP-14. RP-9 and RP-13 died within 2 weeks of their final 8-Gy exposure, whereas RP-14 (the subject that received the smallest total dose) died more than 2 months later after completely recovering baseline levels of responding. The

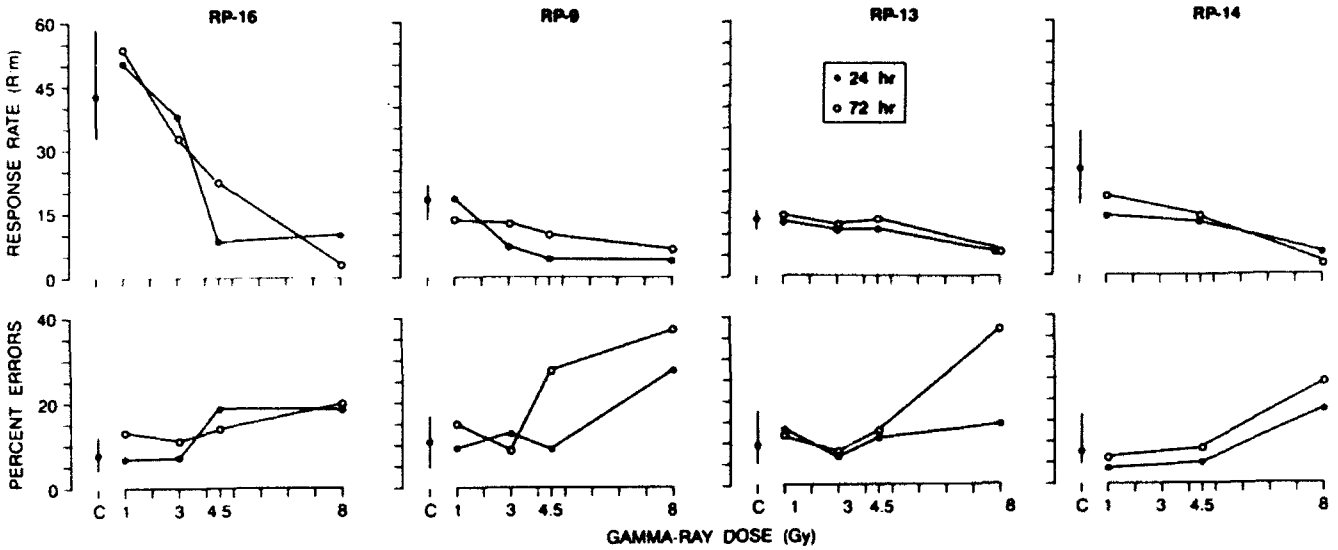

FIG. 1. Effects of varying doses of ^{60}Co γ-rays on the overall response rate (upper panel) and percent errors (lower panel) for each subject. The unconnected filled point and vertical line at C indicate the mean and range of the control data (i.e., data from the 10 baseline sessions immediately preceding the first exposure and 2–5 sessions between irradiations where sham exposures were conducted). The filled points indicate the data obtained 24 h after each exposure; the open points indicate the data obtained 72 h after each exposure.

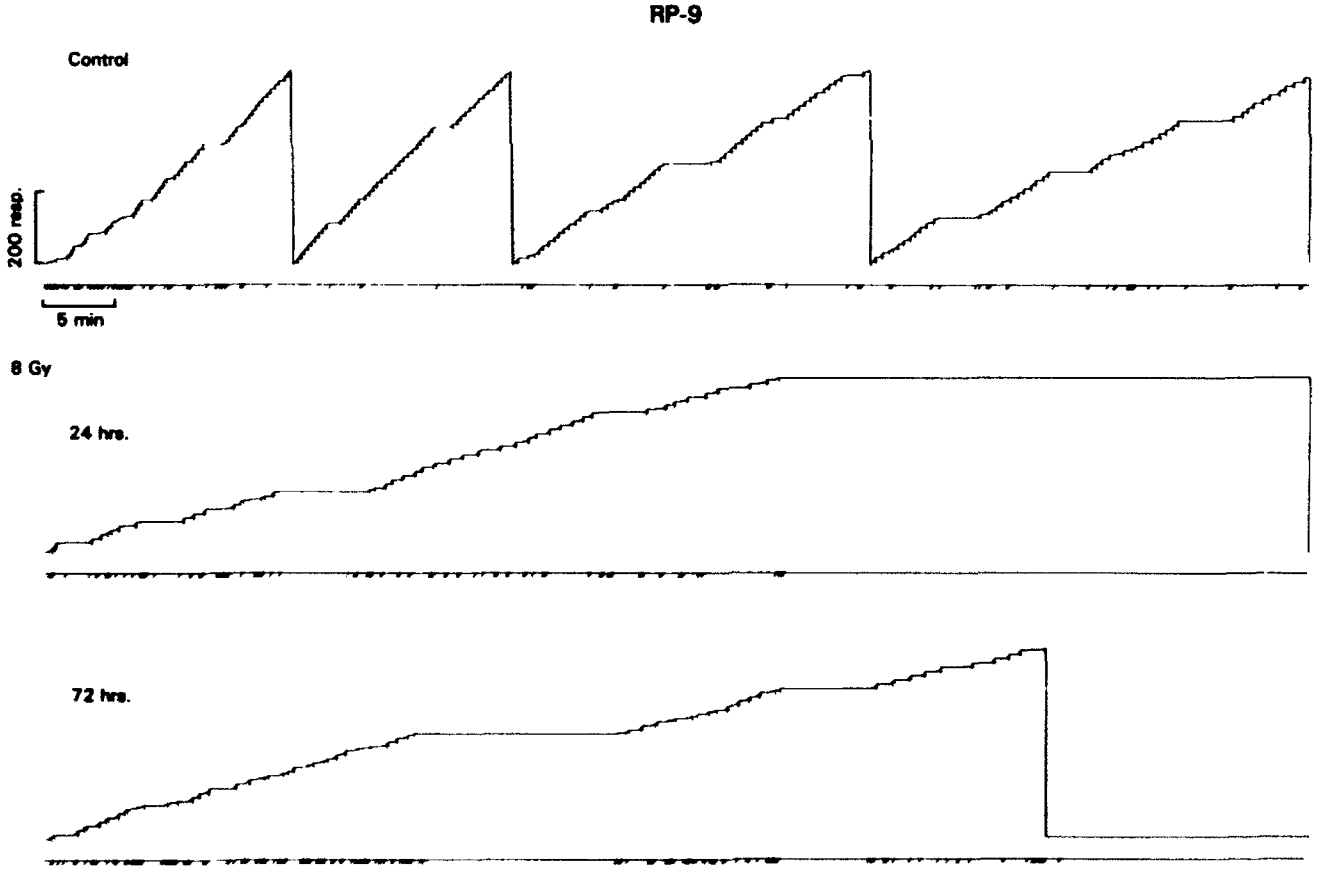

FIG. 2. Within-session effects of ^{60}Co γ-rays during a control session (top record) and two sessions following exposure to an 8-Gy dose (middle and bottom records) in subject RP-9. Each of the three cumulative records is from a different day and shows a complete 90-min session. In each record, the response pen stepped upward with each correct response and was deflected downward each time the three-response chain was completed. Errors are indicated by the event pen (below each record), which was held down for 5 s during each timeout.

surviving subject, RP-16, received the 8-Gy dose and a 4.5-Gy dose 13 weeks afterward. Except for small decreases in food intake for several days following exposure, this subject remained in good health with baseline recovery after each exposure.

DISCUSSION

Unlike many of the previous studies examining the effects of ionizing radiation on acquisition behavior in rats, the present experiment found substantial effects on both rate and accuracy of responding after administration of 1-8 Gy of γ-rays. The large dose-dependent effects on overall response rate were similar to effects found in other studies using either X-rays or γ-rays and schedule-controlled operant behavior (4,5,12, 13,25). In these studies, whole-body irradiation with comparable doses produced dose-dependent decreases in responding regardless of the schedule (fixed ratio or variable interval) or positive reinforcer (food or water) used. Wicker and Brown (25), for example, found that repeated exposures with 1.9, 3.9, and 7.7 Gy of gamma radiation decreased responding under an FR 1 schedule of water presentation. More recently, Mele et al. (13) reported that 4.5 and 6.5 Gy of whole-body γ-ray exposure produced marked decreases in overall responding under an FR 50 schedule of milk presentation. As in the present study, the effects on response rate in that study tended to peak 24 h after exposure and remained evident for extended periods of time (e.g., 5 days) depending upon the dose administered. Also of note was the fact that repeated exposures at 6- to 9-week intervals showed no evidence of cumulative behavioral effects. More specifically, repeated exposures in the same subjects with the same doses produced reliable redeterminations whereas a subsequent exposure after these redeterminations with a different dose produced dose-dependent effects.

The effects of gamma radiation on accuracy in the present study were in general different from those found in previous studies involving other complex acquisition tasks (i.e., maze acquisition tasks). Only a few studies have reported error-increasing effects (6,8,24), and only two found effects of whole-body irradiation at comparably low sublethal doses and post-exposure days. Fields (8), for example, reported that maze errors in an elevated T-maze were greatest 72 h after exposure to 3.5 or 5.8 Gy of X-rays. Other maze studies, however, have found acquisition behavior relatively unaffected (2,9) or enhanced (3) after radiation exposure. Although the disruption of acquisition behavior under the repeated-acquisition task in this study occurred only at doses that substantially decreased overall response rate, the effects on percent errors were clearly evident in all four subjects. In one of the few other rodent studies using a repeated-acquisition procedure and a within-subject design, error-increasing effects were reported with microwave radiation. Schrot et al. (18) found that microwave exposure at varying power densities dose dependently increased errors four to six times over control levels while decreasing sequence-completion rates. In addition, higher power densities of microwave radiation completely disrupted the pattern of acquisition in each of the subjects tested.

The effects on accuracy in the present study may have been more extensive than those found in other studies involving ionizing radiation for a variety of reasons. First, use of a within-subject design may have helped eliminate some of the variability that can often obscure effects on learning in group studies [cf. (21)]. Another possibility is that the repeated-acquisition task used in the present study may be more sensitive than other tasks for examining the effects of radiation on acquisition behavior. Studies investigating the effects of both ionizing radiation (8,24) and microwave radiation (10,18) on accuracy have noted that complex behavioral tasks are more sensitive to radiation than simple behavioral tasks. This view has already been demonstrated to be true for a variety of drug effects (22,26). In regard to radiation effects, for example, Urmer and Brown (24) reported that the effects of 4 Gy of gamma radiation on learning were most notable when the subject was rechallenged or asked to "reorganize" a preirradiation response pattern into a new response pattern. If procedural manipulations of this type are critical to showing radiation-induced deficits in learning, as the authors suggest, a repeated-acquisition task may be particularly sensitive because subjects are rechallenged (i.e., required to learn a different sequence) daily.

A simple explanation could be that many prior studies (2,3,6,9) failed to examine the effects of radiation at the critical times postexposure. In the present study, the effects on percent errors were greater at 72 h than at 24 h in three of four subjects. These effects on accuracy were unusual in that peak effects on percent errors were obtained long after the onset of effects on overall response rate. Different time courses for radiation-induced decreases in response rate (and for recovery from such decreases) have already been shown to be partially dependent upon the schedule of reinforcement, type of reinforcer (positive or negative), and even the particular behavior being tested (12-15). However, these factors have not yet been shown to influence radiation-induced effects on accuracy. One factor that has been shown to play a role in the effects on response rate, but been restrictive to establishing effects on accuracy, is radiation sickness (i.e., a syndrome generally characterized in a variety of species by weakness, fatigue, lethargy, and a decrease in food intake). The influence of radiation sickness has previously been so problematic in many maze studies (3,6,9) that investigators have tested for effects on learning after long postirradiation intervals (e.g., 20-60 days). Unfortunately, all of these studies failed to find any significant disruptions of learning following radiation exposure.

The present study does seem to indicate that decreased motivation resulting from radiation sickness cannot solely account for the disruptive effects on accuracy and that motivational deficits associated with radiation sickness may have a time course independent of that for radiation-induced decreases in accuracy. At the doses tested (1-8 Gy), onset of radiation sickness in rats would in general be expected within the first 24 h after radiation exposure. Jarrard (12), for example, has shown that decreases in food consumption were clearly evident 24 h after exposure and beginning to return to baseline 72 h after exposure depending upon the dose. In their study on the effects of radiation on schedule-controlled performance, Mele et al. (13) also stress that there are severe limitations on attempts to relate radiation-induced changes in performance to specific food intake changes that occur during radiation sickness. They found little correlation between the magnitude and time course of disruption in performance and whether or not postsession chow was consumed. Moreover, repeated-acquisition studies with both monkeys (23) and pigeons (21) have specifically shown that prefeeding manipulations (which decrease deprivation level and, thereby, the effectiveness of food reinforcement) generally produce rate-decreasing effects but little or no effects on accuracy.

As was the case with another ^{60}Co gamma radiation study involving operant schedules of reinforcement and food pre-

sentation (13), lethality in this study did not appear to be strictly the result of the total cumulative dose received. Rather, lethality seemed to depend upon the order of doses administered and the interirradiation interval. Given the small number of animals used, it is impossible to say with any certainty to what degree lethality was influenced by radiation history. However, it should be noted that the lethal effects of radiation on individual subjects in this study were in accordance with previously established effects of γ-rays or X-rays on groups of rodents. Specifically, dose fractionation increased the total cumulative dose that could be tolerated without producing lethality (13,16), and recovery from behavioral disruptions did not necessarily reflect recovery from the long-term physiological effects that produce lethality (13,15). This last point was reflected in the present study, and in the Mele et al. study (13), by the fact that there was often a temporal separation between the more acute behavioral disruptions and the lethal effects. In the present study, for example, two of the three rats that died did so many days after showing more immediate behavioral disruptions. The third rat, RP-13, died over 2 months after completely recovering baseline levels of responding. Moreover, the data from the surviving subject (RP-16) seems to indicate that future studies that incorporate longer interirradiation intervals after high doses could potentially provide the same information about the acute effects of γ-rays on learning without obtaining a lethal effect.

In summary, the present research found that acute sublethal exposure to ionizing radiation readily disrupts learning in individual rats responding under a repeated-acquisition procedure. Although overall response rate was more sensitive to disruption than percent errors (i.e., decreases in response rate tended to occur at doses lower than those required to increase percent errors), presentation of three or four graded doses of ^{60}Co γ-rays did produce dose-dependent disruptive effects on both overall response rate and accuracy in all subjects tested. Of further importance was the finding that percent errors at a given dose were differentially affected during a 72-h period postexposure. Unlike the effects on response rate, which were relatively consistent (or in some cases lessened) over the 24- and 72-h periods after exposure, the effects on percent errors were notably larger at 72 h than at 24 h. Together, these findings emphasize the need for extending the evaluation of the effects of ionizing radiation in both rats and other species using complex operant procedures such as repeated acquisition.

ACKNOWLEDGEMENTS

The authors thank Dr. Donald M. Thompson for helpful comments on the manuscript and Ens. James F. Verrees for expert technical assistance in conducting this experiment. This work was supported by the Armed Forces Radiobiology Research Institute (AFRRI), Defense Nuclear Agency. Research was conducted according to the principles enunciated in the Guide for the Care and Use of Laboratory Animals prepared by the Institute of Laboratory Animal Resources, National Research Council, DHEW Pub. No. (NIH) 85-23, 1985. AFRRI is fully accredited by the American Association for Accreditation of Laboratory Animal Care.

REFERENCES

1. Anger, W. K.; Setzer, J. V. Effects of oral and intramuscular carbaryl administrations on repeated chain acquisition in monkeys. J. Toxicol. Environ. Health 5:793–808; 1979.
2. Arnold, W. J. Maze learning and retention after X-radiation of the head. J. Comp. Physiol. Psychol. 45:358–361; 1952.
3. Blair, W. C. The effects of cranial radiation on maze acquisition in rats. J. Comp. Physiol. Psychol. 51:175–177; 1958.
4. Brown, W. L. Response rate during X-irradiation and recovery following irradiation. J. Genet. Psychol. 108:117–120; 1966.
5. Brown, W. L.; Overall, J. E.; Logie, L. C.; Wicker, J. E. Lever-pressing behavior of albino rats during prolonged exposures to X-radiation. Radiat. Res. 13:617–631; 1960.
6. Burt, D. H.; Ingersoll, E. H. Behavioral and neuropathological changes in the rat following X-radiation of the frontal brain. J. Comp. Physiol. Psychol. 59:90–93; 1965.
7. Dietz, D. D.; McMillan, D. E.; Mushak, P. Effects of chronic lead administration on acquisition and performance of serial position sequences by pigeons. Toxicol. Appl. Pharmacol. 47:377–384; 1979.
8. Fields, P. E. The effect of whole-body X radiation upon activity drum, straightaway, and maze performance of white rats. J. Comp. Physiol. Psychol. 50:386–391; 1957.
9. Furchtgott, E. Effects of total body X-radiation on learning: An exploratory study. J. Comp. Physiol. Psychol. 44:197–203; 1951.
10. Galloway, W. D. Microwave dose-response relationships on two behavioral tasks. Ann. NY Acad. Sci. 247:410–416; 1975.
11. Harlow, H. F. The formation of learning sets. Psychol. Rev. 56: 51–65; 1949.
12. Jarrard, L. E. Effects of X-irradiation on operant behavior in the rat. J. Comp. Physiol. Psychol. 56:608–611; 1963.
13. Mele, P. C.; Franz, C. G.; Harrison, J. R. Effects of sublethal doses of ionizing radiation on schedule-controlled performance in rats. Pharmacol. Biochem. Behav. 30:1007–1014; 1988.
14. Mele, P. C.; Franz, C. G.; Harrison, J. R. Effects of ionizing radiation on fixed-ratio escape performance in rats. Neurotoxicol. Teratol. 12:367–373; 1990.
15. Mickley, G. A.; Bogo, V.; West, B. R. Behavioral and neurophysiological changes with exposure to ionizing radiation. In: Zajtchuk, R.; Bellamy, R. F.; Ingram, V. M., eds. Textbook of military medicine. *Medical consequences of nuclear warfare. Falls* Church, VA: TMM Publications; 1989:105–151.
16. Paterson, E.; Gilbert, C. W.; Matthews J. Time intensity factors and whole body irradiation. Br. J. Radiol. 25:427–433; 1952.
17. Peele, D. B.; Baron, S. P. Effects of scopolamine on repeated-acquisition of radial-arm maze performance by rats. J. Exp. Anal. Behav. 49:275–290; 1988.
18. Shrot, J.; Thomas, J. R.; Banvard, R. A. Modification of the repeated acquisition of response sequences in rats by low-level microwave exposure. Bioelectromagnetics 1:89–99; 1980.
19. Shrot, J.; Thomas, J. R.; Robertson, R. F. Temporal changes in repeated acquisition behavior after carbon monoxide exposure. Neurobehav. Toxicol. Teratol. 6:23–28; 1984.
20. Task Group 21, Radiation Therapy Committee AAPM. A protocol for the determination of absorbed dose from high energy photon and electron beams. Med. Phys. 10:741; 1983.
21. Thompson, D. M. Repeated acquisition as a behavioral base line for studying drug effects. J. Pharmacol. Exp. Ther. 184:506–514; 1973.
22. Thompson, D. M. Repeated acquisition of response sequences: Stimulus control and drugs. J. Exp. Anal. Behav. 23:429–436; 1975.
23. Thompson, D. M.; Moerschbaecher, J. M. An experimental analysis of the effects of d-amphetamine and cocaine on the acquisition and performance of response chains in monkeys. J. Exp. Anal. Behav. 32:433–444; 1979.
24. Urmer, A. H.; Brown, W. L. The effect of gamma radiation on the reorganization of a complex maze habit. J. Genet. Psychol 97:67–76; 1960.
25. Wicker, J. E.; Brown, W. L. The effect of gamma radiation upon operant water-reinforcement behavior. J. Genet. Psychol. 106: 295–299; 1965.
26. Winsauer, P. J.; Thompson, D. M.; Moerschbaecher, J. M. Comparison of drug effects on fixed-ratio performance and chain performance maintained under a second-order fixed-ratio schedule. J. Exp. Anal. Behav. 44:367–376; 1985.

Nucleic Acids Research, 1992, Vol. 20, No. 23 6167–6176

Differences in unwinding of supercoiled DNA induced by the two enantiomers of *anti*-benzo[a]pyrene diol epoxide

Rong Xu, Sheryl Birke, Susan E.Carberry+, Nicholas E.Geacintov*, Charles E.Swenberg[1] and Ronald G.Harvey[2]

Chemistry Department, New York University, New York, NY 10003, [1]Radiation Biochemistry Department, Armed Forces Radiobiology Research Institute, Bethesda, MD 20814 and [2]Ben May Institute, University of Chicago, Chicago, IL 60637, USA

Received October 27, 1992; Accepted October 30, 1992

ABSTRACT

The unwinding of supercoiled φX174 RFI DNA induced by the tumorigenic (+) and non-tumorigenic (−) enantiomers of *trans*-7,8-dihydroxy-*anti*-9,10-epoxy-7,8,9,10-tetrahydrobenzo[a]pyrene (BPDE) has been investigated by agarose slab-gel and ethidium titration tube gel electrophoresis. The differences in adduct conformations were verified by flow linear dichroism techniques. Both enantiomers cause a reversible unwinding by the formation of noncovalent intercalative complexes. The effects of covalently bound BPDE residues on the electrophoretic mobilities of the RF I DNA form in agarose gels were investigated in detail in the range of binding ratios $r_b \approx 0.0-0.06$ (covalently bound BPDE residues/nucleotide). In this range of r_b values, there is a striking difference in the mobilities of (+)-BPDE- and (−)-BPDE-adducted φX174 DNA in agarose slab-gels, the covalently bound (+)-BPDE residues causing a significantly greater retardation than (−)-BPDE residues. Increasing the level of covalent adducts beyond $r_b \approx 0.06$ in the case of the (+)-BPDE enantiomer, leads to further unwinding and a minimum in the mobilities (corresponding to co-migration of the nicked form and the covalently closed relaxed modified form) at r_b 0.10 ± 0.01; at still higher r_b values, rewinding of the modified DNA in the opposite sense is observed. From the minimum in the mobility, a mean unwinding angle (per BPDE residue) of $\theta = 12 \pm 1.5°$ is determined, which is in good agreement the value of $\theta = 11 \pm 1.8°$ obtained by the tube gel titration method. Using this latter method, values of $\theta = 6.8 \pm 1.7°$ for (−)-BPDE-φX174 adducts are observed. It is concluded that agarose slab gel techniques are not suitable for determining unwinding angles for (−)-BPDE-modified φX174 DNA because the alterations in the tertiary structures for $r_b < 0.06$ are too small to cause sufficiently large changes in the electrophoretic mobilities. The major *trans* (+)-BPDE-N²-guanosine covalent adduct is situated at external binding sites and the mechanisms of unwinding are therefore different from those relevant to noncovalent intercalative BPDE-DNA complexes or to classical intercalating drug molecules; a flexible hinge joint and a widening of the minor groove at the site of the lesion may account for the observed unwinding effects. The more heterogeneous (−)-BPDE-nucleoside adducts (involving *cis* and *trans* N²-guanosine, and adenosine adducts) are less effective in causing unwinding of supercoiled DNA for reasons which remain to be elucidated.

INTRODUCTION

Benzo[a]pyrene and related polycyclic aromatic hydrocarbons (PAH) are metabolized *in vivo* to potent mutagenic and tumorigenic diol epoxide derivatives [1]. These hydrophobic, electrophilic, and highly reactive compounds can bind both noncovalently and covalently to DNA in aqueous solutions. The formation of non-covalent complexes is important in determining the chemical reaction kinetics of these diol epoxide derivatives with nucleic acids [2], while the covalent binding to DNA is a critical step in the expression of their mutagenic and tumorigenic potentials [3]. The ultimate biologically active metabolite of benzo[a]pyrene, is the bay region 7,8-dihydroxy-9,10-epoxy-derivative. Among the four different stereoisomers of 7,8-dihydroxy-9,10-epoxy-7,8,9,10-tetrahydrobenzo[a]pyrene, the (+)-enantiomer of the diastereomer *trans*-7,8-dihydroxy-*anti*-9,10-epoxy-7,8,9,10- tetrahydrobenzo[a]pyrene ((+)-BPDE, known also as (+)-*anti*-BPDE, or (+)-BPDE 2) is the most active tumorigen and displays the highest mutagenic activity in mammalian cells [4–8]. In contrast, the (−)-enantiomer, (−)-BPDE (or (−)-*anti*-BPDE, or (−)-BPDE 2) is nontumorigenic [6,7], and its mutagenicity is quite different from that of the (+)-enantiomer [4,5,8]. Differences in covalent adduct conformations and extent of alteration of the local DNA structure,

* To whom correspondence should be addressed

+ Present address: Department of Chemistry, Hunter College of the City of New York, New York, NY 10021, USA

are believed to be two of the critical factors which distinguish the biological activities of (+)-BPDE and (−)-BPDE [2,4,9,10]. The two enantiomers of BPDE are characterized by differences in their chemical binding patterns with DNA [4, 11–13], and the conformations of the chemical DNA adducts which are formed [reviewed in 2,9,10]. Most recently, the solution conformations of the most abundant, stereochemically defined *trans*-adducts derived from the binding of (+)- and (−)-BPDE to the exocyclic amino group of guanosyl moieties in oligonucleotides has been determined by high resolution NMR methods: the bulky pyrenyl residues derived from these two stereoisomers are positioned in the minor groove of DNA, and are oriented in nearly opposite directions with respect to the 5′ → 3′ strand polarity; all hydrogen bonds are intact at 5°C and the B-DNA structure is maintained near and at the lesion site [14,15].

Differences in changes in the tertiary structures of DNA induced by the two enantiomers of BPDE, for example bends or flexible hinge joints at the site of the lesion, and unwinding of supercoils in closed circular DNA, could also play a role in defining the differences in the biological effects induced by these two isomers. The unwinding of supercoiled DNA by racemic BPDE ((±)-BPDE) via noncovalent complex [16,17] and covalent adduct [18–21] formation, has been investigated previously. In this work, the effects of the resolved enantiomers (+)-BPDE and (−)-BPDE are described for the first time, and unwinding angles θ are estimated by different methods.

MATERIALS AND METHODS

Preparation of BPDE-DNA adducts

The (+)-BPDE and (−)-BPDE enantiomers were obtained from the National Cancer Institute Chemical Carcinogen Reference Standard Repository. Supercoiled φX174 RFI DNA was purchased from Bethesda Research Laboratories (Gaithersburg, MD). The covalent binding reactions of the BPDE enantiomers with DNA were carried out in 5 mM Tris (Tris(hydroxymethyl)aminomethane) buffer containing 1 mM sodium ethylenediaminetetraacetate (EDTA) at pH 7.9 (TE buffer). Varying amounts of a concentrated BPDE-tetrahydrofuran solution (2–4 mM BPDE) were added to 500 μl aliquots of buffer solutions containing 12 μg of supercoiled DNA (7.5×10^{-5} M in concentration of nucleotides) to initiate the chemical binding reaction; the concentration of tetrahydrofuran did not exceed 3% by volume in any of the experiments. The samples were placed on a shaker for four hours at room temperature. Subsequently, the reaction mixtures were exhaustively dialyzed against TE buffer to remove the 7,8,9,10-tetrahydroxytetrahydro-benzo[a]pyrene (EPT) hydrolysis products.

Determination of extent of modification and product distribution by HPLC analysis

Spectroscopic methods based on the UV absorbance of the adducts in the 346–354 nm region were employed in most cases to estimate the level of covalent binding [22,23]; the accuracy of this rapid and convenient method was verified by enzymatically degrading the covalent BPDE-DNA adducts to nucleosides and quantitatively determining the fraction of unmodified and BPDE-modified nucleosides by reverse phase high performance liquid chromatography (HPLC) by established methods [13] and used routinely in our laboratory [24,25]. Briefly, the BPDE-supercoiled DNA adducts were first digested with DNase I in 40 mM Tris–HCl, 10 mM $MgCl_2$, and 12 mM $CaCl_2$ (pH = 7.8) buffer solution at 37°C. The adducts were further digested with snake venom phosphodiesterase I and alkaline phosphatase (Pharmacia LKB Biotechnology, Inc., Piscataway, NJ) in 100 mM Tris–HCl, 100 mM NaCl and 15 mM $MgCl_2$ solution for 24 hours at 37°C. The HPLC elution times of the different BPDE-DNA digests were compared with those of BPDE-N^2-dG and BPDE-N^6-dA standards using reverse phase HPLC methods as described elsewhere [24,25]. Using molar extinction coefficients of 29,000 $M^{-1}cm^{-1}$ at the 346 maximum [22] for (+)-BPDE-DNA adducts, and 15,000 M^{-1} at 352–354 nm for (−)-BPDE-DNA adducts (the absorption maxima are broader and less well defined [23,26]), agreement between the HPLC and spectrophotometric methods was within ±20%. The lower extinction coefficients for adducts with absorption maxima at 352–354 nm is in agreement with recent results obtained with site-specific and stereospecific BPDE-oligonucleotide adducts [25,27].

Gel electrophoresis

The electrophoretic mobilities of unmodified and BPDE-modified supercoiled DNA were compared using 1% agarose wedge-shaped slab-gels in 89 mM Tris base, 89 mM sodium borate, and 2 mM EDTA solution (TBE buffer). The final dimensions of the gels were 15×20 cm with the thick and thin ends about 11–15 and 3–5 mm thick, respectively. Before the samples were added to the gels, a loading buffer (1 mM EDTA, 2.5% Ficoll, and 0.005% bromophenol blue) was added. Electrophoresis was performed (thick → thin direction) using an LKB 2012 Maxiphor Submarine electrophoresis unit (Pharmacia/LKB, Piscataway, NJ) connected to a Buchler Model No. 3-1500 power supply (Haakebuchler, Saddle River, NJ) at 40–45 V and 24 mA for 22 hours. The gels were then stained with ethidium bromide (0.75 μg/ml) for 30 min, and destained for 30 min with water, photographed under UV illumination, and the film negatives were then subjected to densitometry analysis. The densitometer was a Fisher Scientific (Springfield, NJ) Model EC910, manufactured by E-C Apparatus Corporation (St. Petersburg, FL.), and was coupled to a computer system. In the range of DNA concentrations utilized, it was verified that the areas under the densitometer peaks were proportional to the amount of DNA added to the gels (40 ng DNA in 10 μl, per well).

In order to relate the decreases in mobilities of the partially relaxed supercoiled DNA bands to the number of superhelical turns removed by the covalently bound BPDE residues, different topoisomer distributions of φX174 DNA were prepared. Reaction mixtures were prepared containing 3.2 μg of φX174 DNA and 30 units of topoisomerase I ((Bethesda Research Laboratories) in 50 mM Tris–HCl, 50 mM KCl, 10 mM $MgCl_2$, 0.1 mM EDTA, 0.5 mM dithiothreitol, and 30 μg bovine serum albumin. The reactions were allowed to proceed at 37°C for time intervals of 1, 2, 4, 6, 10 and 18. The reactions were stopped by adding a 25:24:1 solution of phenol: chloroform: isoamyl alcohol, mixing and subsequent extraction with this solution (twice), and one extraction with chloroform.

Tube gel method: titration of superhelical turns with ethidium bromide

This approach [28,29] is particularly useful for determining the titratable superhelical density in carcinogen-modified DNA [30]. Briefly, agarose tube gels were prepared by pouring hot (60°C) 1% agarose solutions in 0.018 M NaCl TBE buffer containing

different amounts of ethidium bromide (0.001 – 0.10 μg/L) into 20 cm-long glass tubes with one of their ends closed with parafilm. After 45 min, the solidified tubular gels were cut to a length of 18 cm and inserted into a vertical tube gel apparatus with the upper and lower chambers filled with 0.018 M NaCl TBE buffer solution. About 200 ng of modified or unmodified supercoiled DNA in 10 μL of solution containing 4.5% ficoll and 2.4 μM ethidium bromide EB/(DNA nucleotide) ratio ≈ 0.2) were added to the tops of the tubes. Electrophoresis was performed at 95 – 100 V (2.5 mA/tube, up to 16 tubes at a time) for 3 hours at 20°C. After electrophoresis, the gels were extruded into separate large test tubes and the DNA bands were developed by adding a 0.7 μg/L EB solution for 30 min with shaking, and were subsequently photographed under UV illumination.

Flow linear dichroism measurements of relative adduct conformations

Linear dichroism (LD) measurements provide information on the relative orientations of the long axis of the pyrenyl residue relative to the average orientations of the planes of the DNA bases [31]. Briefly, the aqueous DNA solutions are placed within the annular space of a Couette cell consisting of two concentric suprasil cylinders, with the outer cylinder (23 mm inner diameter) remaining stationary, while the inner one (22 mm outer diameter) is rotated at speeds of 400 RPM. The resulting hydrodynamic flow gradient (900 s^{-1}) causes a partial orientation of the DNA bases perpendicular to the flow direction. The linear dichroism signal is defined as $LD = A_{\parallel} - A_{\perp}$ where $A_{\parallel}$ and $A_{\perp}$ are absorbances measured with the linearly polarized light E-vector oriented parallel and perpendicular with respect to the flow direction, respectively. Additional details concerning the LD apparatus may be found elsewhere [32,33].

RESULTS

Superhelical density

The superhelical density of the φX174 DNA used in these experiments can be most conveniently evaluated from ethidium bromide (EB) titration-unwinding data [34]. Because the hydrodynamic volume of supercoiled DNA molecules increases as the degree of superhelicity is decreased, the flow linear dichroism method can be used to monitor the degree of unwinding as the concentration of EB is increased [17,35]. A typical EB titration curve obtained by the flow linear dichroism method is shown in Fig. 1. The minimum in the LD signal, corresponding to a superhelical density of zero [17,35], is observed at the critical ratio of r_C = (EB added)/(DNA nucleotide) = 0.048 ± 0.003. Assuming that ~95% of the EB molecules are bound to the DNA at this equivalence point [36], the critical binding ratio v_C (bound EB molecules/nucleotide) is equal to $\approx 0.95 r_C$ = 0.046 ± 0.003. Defining the superhelical density σ in terms of the unwinding angle $\theta = 26°$ (per bound EB molecule) according to the formula $\sigma = -(v_C/18)\theta$ [37], we obtain a value of σ = −0.066 ± 0.004 under our own conditions of ionic strength (0.071) and temperature (24°C) which, after correcting for the differences in temperature and ionic strength, is close to the standard published values of −0.057 ± 0.010 at 37°C and 0.2 M NaCl concentration [37]. Since the number of base pairs in φX174 DNA is 5386 [38], this value of σ corresponds to 35 ± 3 superhelical turns per molecule at 24°C.

Unwinding due to formation of noncovalent, unstable BPDE-DNA complexes

When (+)-BPDE (or (−)-BPDE) molecules are added to an aqueous solution of φX174 DNA, there is an immediate increase in the magnitude of the LD signal which returns approximately to its initial value after some 12 – 15 min with exponential decay kinetics (Fig. 2). The first-order decay constant under the experimental conditions used here is 0.0020 s^{-1}. Because of the tendency of the planar DNA bases to orient with their normals parallel to the flow lines, the linear dichroism signal of the supercoiled DNA solution is negative in sign below 300 nm [35].

Linear dichroism characteristics and conformations of covalent BPDE-DNA adducts

After removing the BPT molecules from the equilibrated reaction mixtures by exhaustive dialysis, the LD spectra of covalent adducts shown in Fig. 3 are obtained. These spectra are analogous to those obtained with linear DNA [22,23,26,39–41], thus indicating that the adduct conformations in supercoiled DNA are similar to those observed in linear DNA.

The (−)-BPDE-φX174 covalent adducts (Fig. 3B) display a red-shifted (relative to BPDE or BPT in DNA-free aqueous solution) negative LD spectrum resembling in shape the LD (and

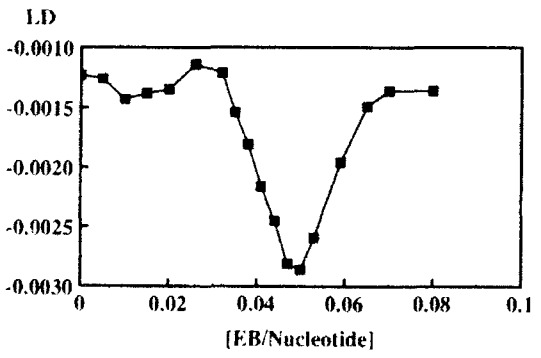

Figure 1. Linear dichroism signal measured within the DNA absorption band at 260 nm as a function of the ethidium bromide concentration expressed in terms of the molar ratio [EB added]/[DNA nucleotide]. The DNA concentration was 10^{-4} M, the buffer solution was identical to the one employed in the tube gel experiments (see Materials and Methods), the temperature was 24°C.

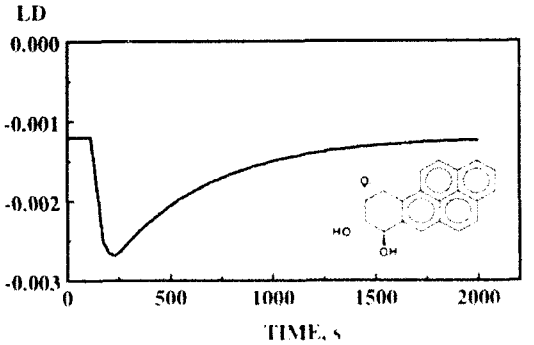

Figure 2. Kinetic trace of the linear dichroism signal measured at 260 nm (LD) reflecting the unwinding and rewinding of the supercoiled DNA (7.5×10^{-5} M) after the addition (at time $t \approx 100$ s) of (+)-BPDE (8.6 μM). Similar effects were observed in the case of the (−) enantiomer (data not shown). The structure of the (+)-BPDE enantiomer is also shown.

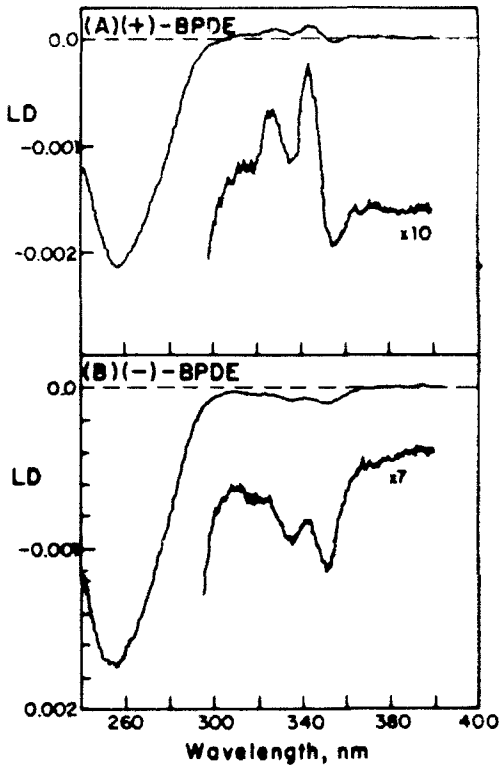

Figure 3. Linear dichroism spectra of covalent (+)-BPDE-φX174 and (−)-BPDE-φX174 adducts in solution (after exhaustive dialysis of the equilibrated reaction mixtures). In (A), the initially added BPDE concentration was as in the legend to Fig. 2, whereas in (B) all experimental conditions were as in (A), except that the initial reaction mixture contained 26×10^{-6} M (−)-BPDE.

absorption spectrum) of noncovalently bound intercalated DNA [23,32]. These types of quasi-intercalative binding sites have been designated as site I [2,9,10,39].

The LD spectrum of the (+)-BPDE-φX174 DNA adducts is mostly positive in sign above 300 nm and is characteristic of external site II adducts, although a negative LD signal due to the contribution of smaller fractions of site I adducts is also visible (Fig. 3A); in site II adducts, the pyrenyl residues are at least partially exposed to the aqueous environment [26,42,43] and are tilted ($> 50°$) away from the planes of the DNA bases [22,26,32,39,40].

Distribution of reaction products

Using initial reaction ratios r_i ([initial BPDE]/[DNA nucleotide]) in the range ≤ 0.5, it was found that 22 ± 4% of the initially added (+)-BPDE binds covalently to DNA. This fraction tends to decline with increasing values of $r_i \geq 0.5$. In the case of (−)-BPDE, 3.5−6.6% of the diol epoxide molecules were converted to covalent DNA adducts in the range of $r_i = 0.3-1.5$, the highest fraction being obtained at the lower r_i values. In the case of the (+)-BPDE-DNA adducts, only the *trans*-BPDE-N^2-dG adduct was detectable (> 90% of all adducts), consistent with previous findings using racemic BPDE and linear [4,11,13] and supercoiled [19,44] DNA. In the case of the (−)-BPDE-DNA adducts, the adduct distribution is more heterogeneous [4,11,13]. The (−)-*trans* N^2-dG, (−)-*cis* N^2-dG, (−)-*trans* N^6-dA, and other, unidentified adducts, accounted for 35 ± 5, 18 ± 2, 29 ± 6, and 18 ± 3% of all covalent BPDE products. However, only overall adduct levels are reported here since, in any event, the effects of different types of adducts on the unwinding of supercoiled DNA cannot be resolved in our experiments.

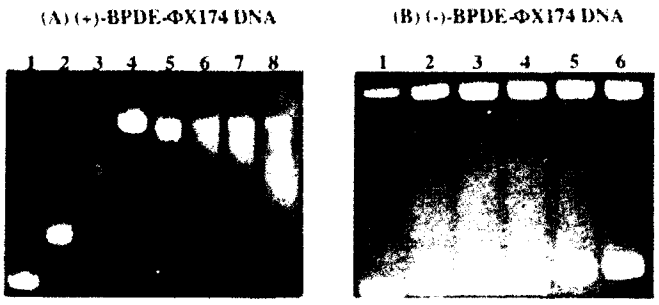

Figure 4. Photographs of ethidium-stained agarose slab gels comparing distances of migration of covalently modified BPDE-φX174 DNA samples at different levels of r_b (covalently bound BPDE residues/nucleotide). (A) (+)-BPDE-φX174 DNA adducts. (B) (−)-BPDE-φX174 DNA adducts. r_b values: (A) lanes (1) 0.0, (2) 0.036, (3) 0.054, (4) 0.10, (5) 0.12, (6) 0.12, (7) 0.14, (8) 0.16. (B) lanes (1) 0.0, (2) 0.020, (3) 0.030, (4) 0.038, (5) 0.045, (6) 0.053. All values of r_b are within ± 20%.

Gel electrophoresis

Photographs of ethidium bromide-stained agarose slab-gels showing some typical electrophoresis data obtained with covalent (+)-BPDE-φX174 and (−)-BPDE-φX174 DNA adducts are shown in Fig. 4. Typical densitometer tracings obtained from the negatives are displayed in Fig. 5. The relative proportions of the supercoiled RF I and relaxed (nicked) RF II DNA forms were somewhat variable from sample to sample.

The electrophoretic mobilities of the supercoiled DNA covalently modified with (+)-BPDE are markedly slowed relative to the unmodified DNA; approximate co-migration of the supercoiled DNA and the nicked form is observed for relatively high binding ratios $r_b = 0.09-0.11$ (10 ± 1% of the bases modified). This behavior is attributed to the removal of left-handed superhelical turns and the concomitant increase in the overall hydrodynamic size and lower electrophoretic mobilities of the BPDE-DNA molecules.

The mobilities of covalent adducts derived from the (−)-enantiomer are barely affected in the range of $r_b = 0.00-0.06$ (because of the low reactivities of the (−)-BPDE enantiomer with DNA, solubility problems at $r_i > 1.5$, as well as the relative scarcity and high cost of the BPDE enantiomers, no attempts were made to obtain adducts with higher levels of modification with this isomer.

Values of the relative mobilities as a function of the number of (+)-BPDE residues per genome are shown in Fig. 6; the data points represent the maxima in the distributions which are observed in the densitometer tracings (Fig. 5). At high (+)-BPDE adduct levels, these distributions are quite broad, especially beyond the value of $r_b = 0.10$; above this value of r_b, rewinding of the closed circular DNA gives rise to positive superhelicity, and is reminiscent of the effects observed with EB (Fig. 1).

In contrast to the behavior of the supercoiled band, the electrophoretic mobility of the slower, nicked band, increases somewhat upon modification with (+)-BPDE (Fig. 5). In the case of the (−)-BPDE-φX174 DNA adducts, the mobility of the nicked band does not seem to change visibly as a function of r_b.

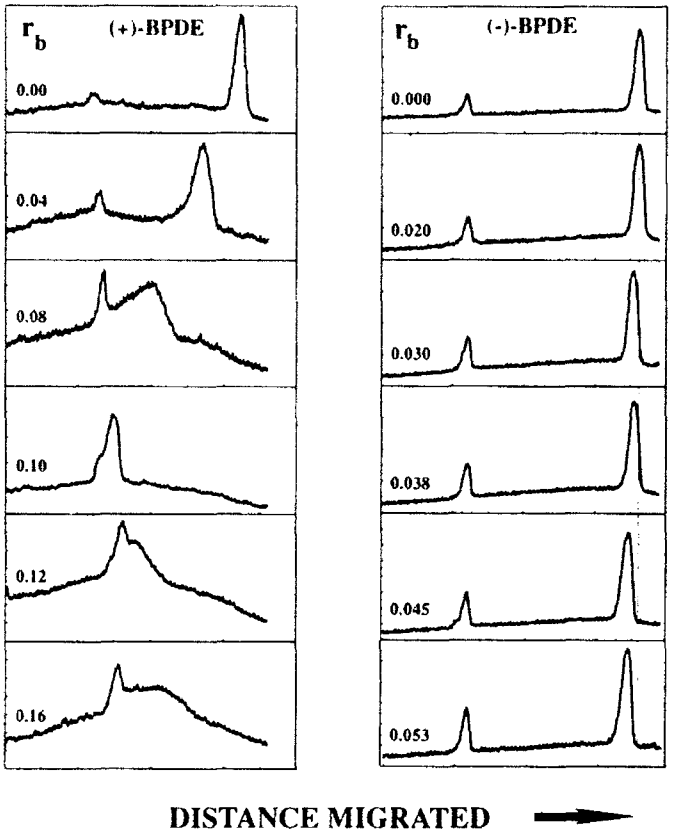

Figure 5. Densitometer tracings of photograph negatives (same data as in Fig. 4).

Comparisons of electrophoretic mobilities of (+)-BPDE-φX174 DNA adducts with mobilities of unmodified topoisomers

Samples of untreated supercoiled DNA were partially relaxed with topoisomerase I for varying amounts of time, and these solutions were then subjected to gel electrophoresis. Typical photographs of slab-gels are shown in Fig. 7A. In our φX174 RF I samples, we counted 19 bands, including the fully relaxed RF II and supercoiled RF I bands. This approach is not capable of revealing all of the bands corresponding to molecules with different number of superhelical turns, since some of the highest and lowest mobility bands cannot be resolved using agarose slab-gels; however, the resolved adjacent bands differ from one another by one superhelical turn [45]. The relationship between the band number (starting from the fastest bands) and relative electrophoretic mobilities (measured as a fraction of the distance on the slab-gels between the RF I and RF II bands in the unmodified samples) is plotted in Fig. 7B.

The relative mobilities of the (+)-BPDE-φX174 DNA adducts (Fig. 6) were then matched with those in Fig. 7B, and the corresponding band positions were plotted as a function of the number of covalently bound (+)-BPDE residues/φX174 DNA molecule (Fig. 8) as previously described for other bulky adducts [30,46]. A reasonably good straight line with a slope of $\Delta\tau/\Delta$[BPDE] = 0.017 ± 0.001 turns/adducts is obtained ([BPDE] = adducts/genome); the effective unwinding angle determined by this method is $360° \times \Delta\tau/\Delta$[BPDE] = 6.2 ± 0.5°.

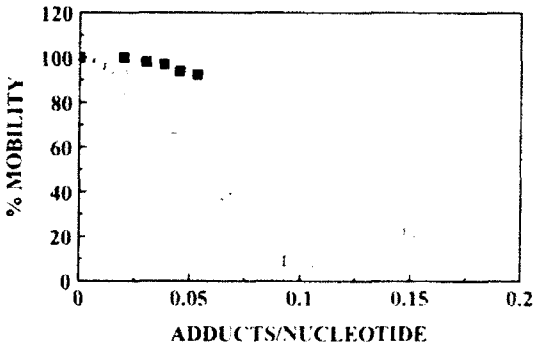

Figure 6. Relative mobilities of BPDE-supercoiled DNA adducts in electrophoretic agarose slab-gels as a function of the covalent modification level r_b. ..... (+)-BPDE-φX174 DNA adducts; ■ ..... (−)-BPDE-φX174 DNA adducts. The values provided correspond to maxima in the mobility distributions evaluated from densitometer tracings.

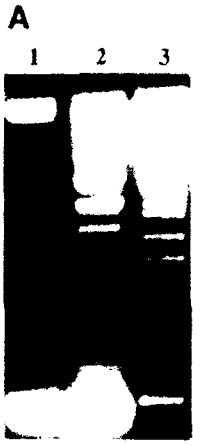

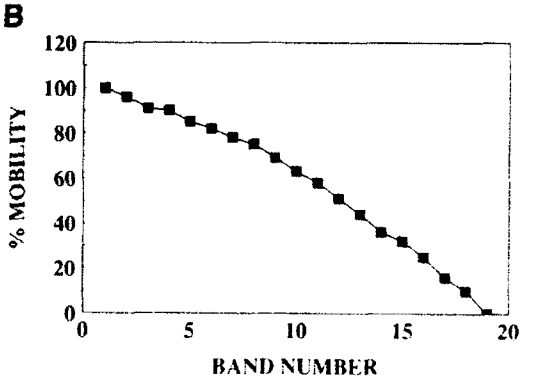

Figure 7. **(A)** Electrophoretic slab-gel separation of topoisomerase I-treated unmodified φX174 DNA. Lanes: (1) reference, untreated DNA, (2) treatment for 2 min, and (3) 4 min. **(B)** Positions of the different bands observed upon treating φX174 DNA with topoisomerase I. The distance of each band was measured relative to the distance between the fast RF I and slow RF II bands of untreated DNA measured on the same gels.

The experimental data points corresponding to 40 < [BPDE] < 200 adducts/genome lie well below the straight line in Fig. 8. Apparently, at low adduct levels, it is difficult to detect any changes in the mobilities due to removal of the first few superhelical turns.

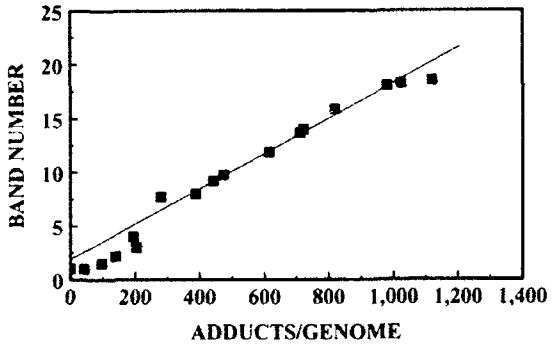

Figure 8. Comparisons of band positions of (+)-BPDE-φX174 DNA adducts with those of topoisomerase I-treated unmodified φX174 DNA as a function of covalently bound BPDE residues per DNA molecule (see text).

Unwinding measured by the tube gel method

Changes in electrophoretic mobilities of carcinogen-modified supercoiled DNA on agarose slab-gels may, in principle, also reflect alterations in the tertiary structures of the molecules other than those produced by changes in the number of superhelical turns. Other effects may include bends [47] or flexible hinge joints [2,23,31,41] at the site of binding. The adducts derived from the binding of (−)-BPDE appear to be predominantly stacked (or site I, quasi-intercalated [22,40]) with neighboring bases as judged from linear dichroism experiments with linear DNA [22,23,26,40,41] and with supercoiled DNA (Fig. 3) , while (+)-BPDE residues appear to be situated predominantly at external site II binding sites [22,23,26,32,40−43]; thus, we initially expected to find more unwinding in the case of (+)-BPDE- than in the case of (−)-BPDE-φX174 DNA adducts; however, the exact opposite conclusion can be derived from the agarose slab gel results (Figs. 4 & 5). Therefore, another method was sought to determine the losses of superhelical turns. The tube gel technique is convenient and suitable for this purpose. In this method [28,29], samples of the same DNA adduct solution are subjected to agarose gel electrophoresis in individual tubes, each containing EB molecules at different concentrations, thus producing different degrees of unwinding in each tube. The number of superhelical turns can be estimated from the EB concentration C′ in the tube in which the fully relaxed covalently closed circular DNA molecules co-migrate with the nicked form, using the equation [28,29]:

$$\upsilon_C = \upsilon_m \, KC'/(1 + KC') \qquad (1)$$

where K is the equilibrium binding constant of EB and υ_m is the maximum molar ratio of bound EB/nucleotide. Since the magnitude of K depends on the ionic strength and other factors, we determined its value under our own experimental conditions using standard equilibrium dialysis methods. A Scatchard plot was constructed (data not shown), which yielded values of $K = (3.0 \pm 0.1) \times 10^6\ M^{-1}$ and $\upsilon_m = 0.18$, similar to those reported by other workers [28,29]. The superhelical density is then calculated from the values of υ_C using the relationship $\sigma = -1.44\upsilon_C$. In these tube gel experiments, the levels of covalent BPDE adducts were held below $r_b = 0.06$, since the association constant for EB binding was not measurably affected in this range of BPDE binding levels (data not shown).

The tube gel experiments were run in two stages: (1) a coarse scale of incremental increases of the EB concentration C in each gel was employed in order to determine the approximate value of C′, (2) the experiments were then repeated with the same DNA sample using a narrower range of C near the value of C′ estimated from the first experiment. In this way, a more accurate value of C′ was obtained.

Examples of such experiments are shown in Fig. 9. Using a coarse range of C values, the value of C′ for unmodified φX174 RF I DNA is found to be in the range of 0.040−0.050 μg/ml (Fig. 9A); using a narrower range of C values, C′ is found to lie in the range of 0.042−0.046 μg/ml; the corresponding value of υ_C is 0.046 ± 0.002, yielding values of $\sigma = -0.066 \pm 0.003$ and 35 ± 2 superturns/DNA molecule, in excellent agreement with the data obtained from the linear dichroism EB-titration curve (Fig. 1).

Examples of similar experiments with (+)-BPDE-φX174 and (−)-BPDE-φX174 DNA adducts are shown in Figs. 9B and 9C, respectively. In both cases, rewinding of the DNA in the opposite sense is observed at ethidium concentrations C > C′. In the case of the (+)-BPDE adduct with a level of modification of r_b = 0.05, the value of C′ is 0.021 ± 0.003 μg/ml (Figs. 9B), which is considerably smaller than in the case of the unmodified DNA. In the case of the (−)-BPDE-φX174 DNA sample with a similar level of modification (r_b = 0.045), C′ = 0.030 ± 0.003 μg/ml. Thus, both enantiomers, upon binding covalently with DNA, give rise to measurable degrees of unwinding as measured by the tube gel method.

Particularly striking are the apparently small effects of the covalently bound (−)-BPDE residues on the mobilities of the modified DNA as measured by the agarose slab-gel method (Figs. 4 and 5), and the definite unwinding effect detected in the same range of binding by the gel method (Fig. 9C); the loss of superhelical turns increases with increasing levels of (−)-BPDE modification, and values of θ in the range of 6−8° are obtained (Table I).

DISCUSSION

Unwinding of supercoiled DNA by noncovalent binding of BPDE

Noncovalent BPDE-DNA complexes are formed on time scales of milliseconds after the addition of the PAH diol epoxides [2], and cause the rapid initial increase in the magnitude of the linear dichroism signal at 260 nm (LD_{260}) shown in Fig. 2. The decay kinetics of the LD_{260} signal are identical to the kinetics of disappearance of intercalated PAH diol epoxide molecules [17]. The LD_{260} signal decays because the BPT hydrolysis products are characterized by a ≈6 times smaller binding affinity (noncovalent complex formation) than BPDE [48]; the overall number of noncovalently bound intercalated molecules thus decreases with time.

Both enantiomers of BPDE cause the unwinding of supercoiled DNA by noncovalent complex formation. Most [16,23,48−50] though not all [49] non-covalent PAH diol epoxide—and other PAH metabolite—DNA [51] complexes appear to be intercalative in nature. Meehan et al. [16] have shown that the unwinding angle associated with (±)-BPDE intercalation is only 13°, about one half of the value observed with EB [37,52].

Slab-gel electrophoretic mobilities

Supercoiled form (RF I). There is a striking difference in the electrophoretic mobilities of adducts derived from the binding of (+)-BPDE and (−)-BPDE to φX174 DNA at similar values of r_b (≤ 0.06, Figs. 4−6). At the highest level of modification

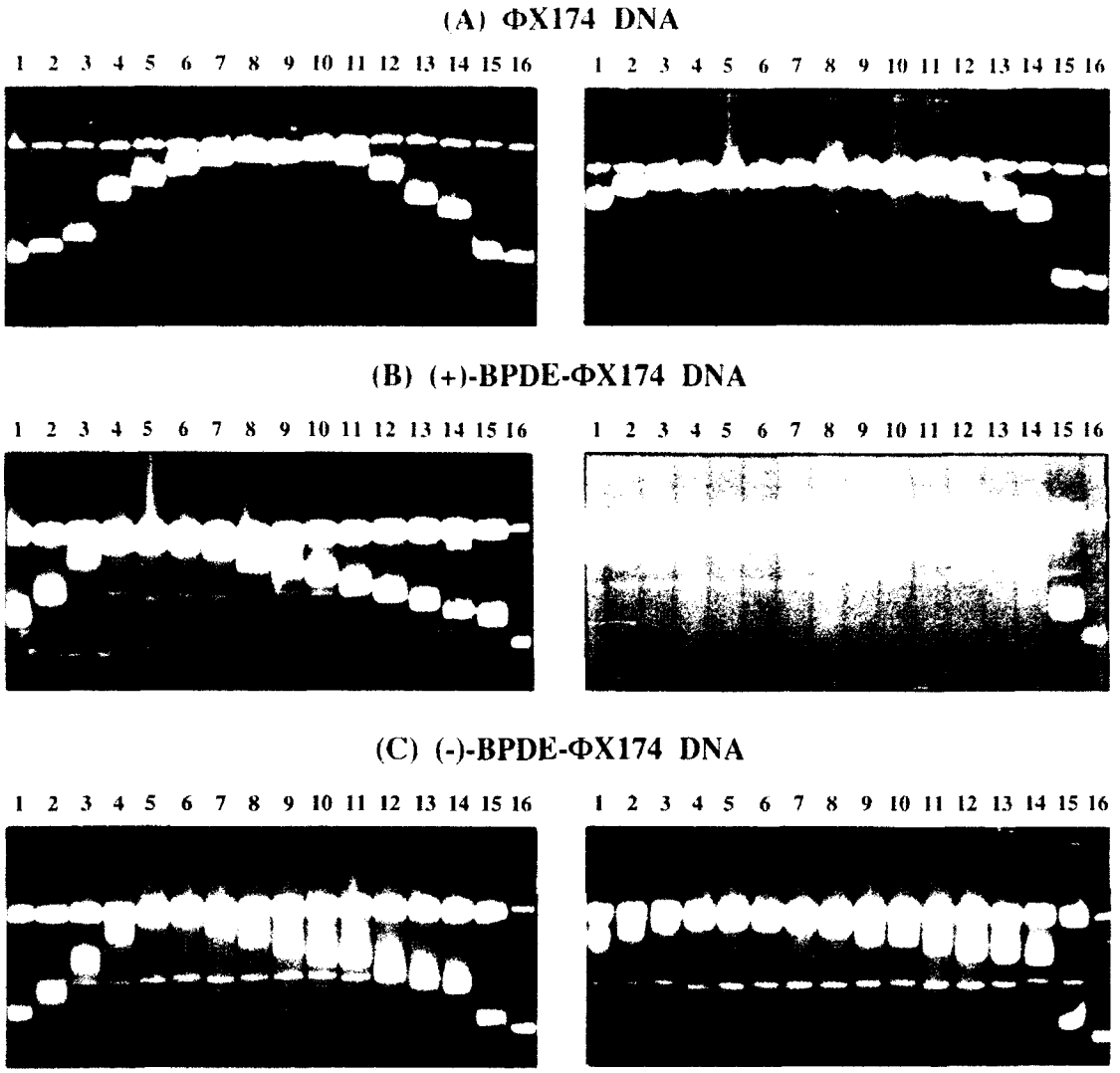

Figure 9. Photographs of tube gels of **(A)** untreated ϕX174 DNA, **(B)** (+)-BPDE-ϕX174 DNA adducts, r_b = 0.05, and **(C)** (−)-BPDE-ϕX174 DNA adducts, r_b = 0.045. Left: coarse Ethidium bromide concentration intervals; right: finer intervals. EB concentrations in μg/ml: **(A)** Left: (1) 0.001, (2) 0.005, (3) 0.010, (4) 0.020, (5) 0.025, (6) 0.030, (7)).035, (8) 0.040, (9) 0.050, (10) 0.060, (11) 0.070, (12) 0.090, (13) 0.090, (14) 0.110, (15) and (16) 0.00. **(A)** Right: (1) 0.022, (2) 0.026, (3) 0.030, (4) 0.034, (5) 0.038, (6) 0.042, (7))0.046, (8) 0.050, (9) 0.054, (10) 0.058, (11) 0.062, (12) 0.066, (13) 0.070, (14) 0.074, and (15) and (16) 0.000. **(B)** Left: (1) 0.001, (2) 0.005, (3) 0.010, (4) 0.015, (5) 0.020, (6) 0.025, (7)).030, (8) 0.035, (9) 0.040, (10) 0.045, (11) 0.050, (12) 0.060, (13) 0.070, (14) 0.080, and (15) 0.00, and (16) 0.00, unmodified DNA. **(B)** Right: (1) 0.010, (2) 0.012, (3) 0.014, (4) 0.016, (5) 0.018, (6) 0.020, (7))0.022, (8) 0.024, (9) 0.026, (10) 0.028, (11) 0.030, (12) 0.032, (13) 0.034, (14) 0.036, and (15) 0.00, and (16) 0.00, unmodified DNA. **(C)** Left: (1) 0.005, (2) 0.010, (3) 0.015, (4) 0.020, (5) 0.025, (6) 0.030, (7)).035, (8) 0.040, (9) 0.045, (10) 0.050, (11) 0.055, (12) 0.060, (13) 0.065, (14) 0.070, and (15) 0.00, and (16) 0.00, unmodified DNA. **(C)** Right: (1) 0.018, (2) 0.021, (3) 0.024, (4) 0.027, (5) 0.030, (6) 0.033, (7))0.036, (8) 0.039, (9) 0.042, (10) 0.045, (11) 0.048, (12) 0.051, (13) 0.054, (14) 0.057, and (15) 0.00, and (16) 0.00, unmodified DNA.

with (−)-BPDE, the average mobility of adducts is decreased by only ≈7%, while in the case of the adducts derived from (+)-BPDE the mobility is decreased by ≈45% (Fig. 6). The covalent adducts arising from the binding of (+)-BPDE are more effective than (−)-BPDE in decreasing the mobilities of covalent BPDE- supercoiled DNA adducts. Thus, decreases in the electrophoretic mobilities of racemic *anti*-BPDE-SV40 supercoiled DNA adducts previously observed in agarose gels [18−21], are predominantly associated with the (+) enantiomer.

Nicked form (RF II). The increase in the mobility of the nicked closed circular RF II band with increasing r_b for both BPDE isomers (Fig. 4) have also been observed with racemic *anti*-BPDE-DNA adducts [19,20]. The higher mobility of the modified form II DNA was attributed to a flexible hinge-like behavior at

Table I. Unwinding angles determined for covalent (−)-BPDE-ϕX174 DNA adducts at different values of r_b.

r_b[a] (1)	C'[b] (μg/ml) (2)	θ_C[c] (3)	Unwinding angle (4)
0	0.044	0.046 ± 0.0015	26 ± 2°
0.019 ± 0.002	0.038	0.041 ± 0.0017	6.8 ± 0.9°
0.030 ± 0.002	0.035	0.039 ± 0.0018	6.1 ± 0.7°
0.038 ± 0.003	0.033	0.037 ± 0.0019	6.2 ± 0.7°
0.046 ± 0.003	0.030	0.034 ± 0.0020	6.8 ± 0.7°
0.053 ± 0.004	0.026	0.030 ± 0.0021	7.8 ± 0.9°

[a]Covalently bound BPDE residues/nucleotide.
[b]Ethidium bromide concentration at which the covalently closed and nicked DNA co-migrate. Central value taken from the higher resolution tube gel experiments, the maximum uncertainties in these values is ±0.002 μg/ml (see text)
[c]Critical EB concentration ratio which leads to the complete relaxation of supercoiled modified DNA; the uncertainties reflect the extreme ranges of C'

the alkylation sites [19]. The observed reductions in the mobilities of short linear DNA fragments [47], and decreases in the degrees of alignment of high molecular weight linear DNA molecules modified with racemic BPDE and (+)-BPDE in hydrodynamic flow gradients [23,31,41], are consistent with this hypothesis.

Estimates of unwinding angle

Slab- gels. The unwinding angle θ can be estimated using the relationship [37]:

$$\theta = (\Delta\tau \times 360°)/(r_b \times 10{,}772) \qquad (2)$$

where $\Delta\tau$ is the number of superhelical turns removed at a given value of r_b, while 10,772 is the number of bases per genome of ϕX174. In principle, unwinding angles in carcinogen-modified superhelical DNA can be determined by comparing the changes in electrophoretic mobilities (Fig. 6) with those observed with the unmodified topoisomers (Fig. 7). However, only a lower limit of the unwinding angle θ can be obtained in this way, as is shown here. From Fig. 4, using r_b values of 0.05, the relative mobility of (+)-BPDE-DNA adducts is estimated to be $\approx$55%, while for the (−)-BPDE-DNA adducts it is $\approx$93%, corresponding to a loss of $\approx$ 10 and $\approx$ 1.5 superhelical turns respectively. The fastest mobility RF I band is known to consist of several highly wound topoisomers [45]. The loss of the first few N superturns is not expected to exhibit any noticeable changes in the observed average electrophoretic mobilities. Thus, at binding levels of r_b = 0.05, $\Delta\tau$ = N + 10, or = N + 1.5, for (+)-BPDE- and (−)-BPDE-ϕX174 DNA adducts, respectively. Since the values of $\Delta\tau$ = 10 and 1.5 represent lowest limits for the numbers of superhelical turns removed when r_b = 0.05, unwinding angles of $\theta > 7°$ and $\theta > 1°$ for (+)-BPDE-ϕX174 DNA and (−)-BPDE-ϕX174 DNA adducts, respectively, are estimated by this method and Eq. 2.

The observance of a minimum in the relative mobilities as a function of r_b in the case of adducts derived from (+)-BPDE (Fig. 6) provides yet another method for estimating the average unwinding angle per bound BPDE residue. With v_c = 0.10 ± 0.01, and using Eq. 2 with τ = 35 ± 3 (complete unwinding), yields a value of θ = 12 ± 1.5°.

Comparisons of unwinding angles θ determined by different techniques. The results are summarized in Table II. The average value of θ for (−)-BPDE-ϕX174 DNA adducts obtained by the tube gel method is 6.8 ± 1.7° . Good agreement is obtained in the case of (+)-BPDE-ϕX174 DNA adducts by the complete unwinding-agarose slab gel method (column 4) and the tube gel method (column 5); the average value of θ is 11.5 ± 2.4°. This value is, however, about twice as large as the value of θ estimated by the band counting method (column 2). This latter value (6.2 ± 0.5°) was obtained by comparing the slab-gel mobilities of (+)-BPDE-ϕX174 DNA adducts with those of unmodified isomers with the number of superturns/molecule between N and N+18 (Fig. 7). The value of N can be estimated from Eq. 2 using θ((+)-BPDE) = 11.5 ± 2.4°, and θ ((−)-BPDE) = 6.8 ± 1.7° and $\Delta\tau$ = N+10 and $\Delta\tau$ = N + 1.5 for (+)-BPDE-DNA and (−)-BPDE-DNA adducts, respectively. Values of N = 7.2 ± 2.7 and N = 8.7 ± 2.5 are obtained which are in reasonable agreement with one another, and also with the expected number of unresolvable fast electrophoretic bands [45].

In the case of (−)-BPDE-ϕX174 DNA adducts, the changes in the relative electrophoretic mobilities observed on agarose slab gels are too small to reflect the value of θ measured by the ethidium bromide titration tube gel method. This suggests that the slab gel electrophoresis method is not suitable for estimating unwinding angles in those cases in which the unwinding angle/ligand is small, and the degree of modification is also relatively low. In these cases, the removal of the first few superhelical turns does not appear to be sufficient to cause any significant changes in the electrophoretic mobilities in agarose slab gels.

Table II. Summary of unwinding angles obtained by different methods

ADDUCT FROM:	Slab Gel, $\Delta\tau/\Delta N$[a]	Slab Gel, Relative Mobilities[b]	Slab Gel, Complete unwinding [c]	Tube Gels
(1)	(2)	(3)	(4)	(5)
(+)-BPDE	6.2 ± 0.5°	> 7°	12 ± 1.5°	11 ± 1.8°
(−)-BPDE	–	> 1°	–	6.8 ± 1.7

[a]From topoisomer experiments, Fig. 8.
[b]Estimated from data in Fig. 6, see text.
[c]Estimated from the minimum in Fig. 6 at r_b = 0.010 ± 0.001.

The value of θ estimated from the data in Fig. 7 in the range of superhelicities between N and N+18 (Table II, column 2) is smaller than the overall, mean value of θ obtained by other methods (Table II, columns 4 & 5). This suggests that the unwinding angle/[BPDE] residue must be higher than the average value θ = 11.5 ± 2.4° for highly supercoiled ϕX174 isomers. Such a phenomenon was observed by Gamper et al. [19] for racemic BPDE-SV40 DNA adducts, who reported decreasing unwinding angles with increasing levels of modification in the range of 330°−30° , the highest values being obtained for highly supercoiled topoisomers. These values (or the inferred mean value) are substantially higher than those obtained by us with (+)-BPDE using a different kind of supercoiled DNA (Table II). Gamper et al. [19] worked with a 10% dimethyl sulfoxide (DMSO)-90% buffer mixture, while the organic solvent concentration (THF) in our reaction mixtures was less than 3%. However, we found that the levels of binding of (+)-BPDE to ϕX174 DNA (and the relative electrophoretic mobilities) were the same in the absence or presence of 10% dimethylsulfoxide during the preparation of the adducts (data not shown). Therefore, differences in reaction conditions do not appear to be the source of this discrepancy.

There is a difference in the adduct level (r_b) thresholds at which unwinding is first observed in our experiments on agarose slab gels and those of Gamper et al. [19]. These latter authors, based on the retardation of individual topoisomer bands induced by (±)-BPDE in a different gel system, observed significant decreases in mobilities of SV40 DNA at levels of modification of only 2−40 BPDE residues per genome. Drinkwater et al. [18] stated that the binding ratio r_b in agarose slab gelshad to be at least 0.015 (> 160 adducts/genome) in order to observe changes in electrophoretic mobilities on agarose slab gels. In our experiments, changes in electrophoretic mobilities of modified ϕX174 DNA are not observed unambiguously on slab-gels unless there are at least $\approx$200 (+)-BPDE adduct residues/genome ($r_b \geq 0.02$, Fig. 6), which is more consistent with the threshold established by Drinkwater et al. than the one found by Gamper et al. In these latter two investigations, racemic BPDE (rather than the resolved enantiomers) were used, and the sources of the supercoiled DNA were different from ours. It seems unlikely, though not certain, that these factors are the sources of the differences.

Our value of the mean unwinding angle for (+)-BPDE-DNA adducts ($11.5 \pm 2.4°$) is smaller than the value of $22 \pm 3°$ published by Drinkwater et al. [18]. Because the (+)-isomer of BPDE is about 3–4 times more reactive with respect to supercoiled DNA than the (−) enantiomer, the unwinding angle should be, all other things being equal, somewhat higher in the case of (+)-BPDE than in the case of racemic BPDE. This discrepancy is traceable to the differences in the values of r_b at which minima in the electrophoretic mobilities are observed (r_b (min) = 0.05 ± 0.008 in the case of Drinkwater et al., and r_b (min) = 0.10 ± 0.01, this work). Given the ± 20% uncertainty in our values of r_b, the discrepancy is not large. Inaccuracies in adduct level determinations could account for this difference. Another possible source of error is the absolute superhelical density which is used to calculate θ based on the experimentally determined values of r_b (min). In this work, we have made efforts to reduce the errors associated with these problems by (1) determining the superhelical density of the ϕX174 DNA samples under our own experimental conditions, and (2) basing adduct level determinations on two different methods.

Adduct conformations and mechanisms of unwinding

Classical intercalation involves the insertion of planar aromatic molecules between adjacent DNA base pairs, which leads to an extension of the phosphodiester backbone, an untwisting of base pairs, and thus to unwinding [53]. Flow linear dichroism studies indicate that the noncovalent binding of (+)-BPDE and (−)-BPDE to DNA leads to adduct conformations consistent with those of intercalative complexes [23]; however, noncovalent racemic BPDE-SV40 supercoiled DNA complexes are characterized by unwinding angles of 13° [16], which is much smaller than the value of 26° [37,52] obtained for the classical intercalator ethidium bromide. While the unwinding of supercoiled DNA by covalently bound (+)-BPDE is also close to 13° (Table II), the mechanisms of unwinding must be different in the noncovalent complex and covalent adducts since their conformations are quite different from one another [23,32]. While the unwinding of supercoiled DNA by drug molecules is often taken as evidence for an intercalative binding mechanism, Bauer has emphasized that the demonstration of duplex unwinding should not be considered as incontrovertible evidence for intercalation [37]. Other causes of duplex unwinding not involving intercalative binding have been documented, including the effects of covalently bound *cis*- and *trans*-dichlorodiammineplatinum (II) [54,55], dehydration [56], the binding of histones [57] and metal ions [58], and photochemical thymine dimer formation [59].

In the case of (+)-BPDE, over 90% of the adducts formed involve *trans*-addition (at the C10 position) to the exocyclic amino group of guanine in native [11–13] and in supercoiled [44] DNA. Recent high-resolution NMR experiments with stereospecific and site-specific (+)-BPDE-deoxyoligonucleotide adducts have shown that the pyrenyl residue is situated in a widened minor groove of B-DNA as gauged from the larger than normal distances between adjacent negatively charged phosphate moieties [14,15]. Possible mechanisms of unwinding based on this effect can be discussed in terms of a model recently proposed by Wilson et al. [53] for classical intercalators: because of the lowered repulsive interactions between neighboring phosphate groups due to the minor groove widening, an untwisting of the base pairs may occur which increases the favorable van der Waals contacts due to better overlap between adjacent base pairs. This mechanism of unwinding could be further complemented by a flexible hinge joint at the site of binding. Flow linear dichroism experiments [23,31,41] and molecular dynamic simulation studies [60] suggest that such effects are predominantly associated with (+)-BPDE, rather than with (−)-BPDE. Furthermore, using ligation and gel electrophoresis techniques [61] with covalent oligonucleotide adducts derived from the *trans* and *cis* addition of both (+)- and (−)-BPDE, we have shown that only the (+)-*trans*-BPDE-N^2-dG adduct gives rise to a flexible hinge joint at the site of binding (B.Mao, B.Li and N.E.Geacintov, in preparation).

Adducts derived from the binding of (−)-BPDE are chemically more heterogeneous. Little is known about the conformations of BPDE-dA adducts at this writing. The (−)-*trans*-BPDE-N^2-dG adducts are also situated in the minor groove, but their orientation are different from those of the analogous (+)-adducts [15]; unwinding due to the mechanism discussed above is therefore also expected. However, the absence of a prominent hinge joint in (−)-*trans*-BPDE-N^2-dG-oligonucleotides suggests that the overall unwinding may be lower than in the case of the structurally related (+)-*trans* adducts. The (−)-*cis* adducts appear to be situated inside the helix and are at least partially base-stacked with neighboring bases [25,27]. However, their conformation may be different from those of classical intercalative structures: the modified guanosyl residues may be displaced by the pyrenyl moieties in a quasi-intercalative carcinogen-base-stacked conformation, as proposed recently by Singh et al. based on potential energy minimization studies of analogous, higher energy *trans*-adducts [60]. The degree of unwinding associated with such conformations may be lower than for classical intercalation complexes.

Collectively, the heterogeneous (−)-BPDE adduct species give rise to a smaller unwinding angle than (+)-BPDE-N^2-dG lesions (Table II). The reasons for these differences are presently not well understood and must await further developments in the structural determinations of site-specific and stereospecific BPDE-oligonucleotides adducts [14,15], and the analysis of the associated structural effects involving unwinding of superhelical turns and other alterations in the tertiary structure of DNA.

ACKNOWLEDGEMENTS

This work was supported by the Department of Energy (Grants DEFGO2-86ER60405, and in part by Grant CA 20851 from the US Public Health Service, Department of Health and Human Resources, awarded by the National Cancer Institute. The assistance of Dr. Y.Mnyukh with the linear dichroism measurements is gratefully acknowledged.

REFERENCES

1. Conney, A.H. (1982) *Cancer Res.* **42**, 4875–4917.
2. Geacintov, N.E. (1988) *Polycyclic Aromatic Hydrocarbon Carcinogenesis, Structure-Activity Relationships* (S.K. Yang and B.D. Silverman, Eds.), CRC Press, Boca Raton, FL, Vol. II, pp. 181–206.
3. Singer, B. and Grunberger, D. (1983) *Molecular Biology of Mutagens and Carcinogens*, Plenum Press, New York.
4. Brookes, P. and Osborne, M.R. (1982) *Carcinogenesis* **3**, 1223–1226.
5. Wood, A.W., Chang, R.L., Levin, W., Yagi, H., Thakker, D.R., Jerina, D.M. and Conney, A.H. (1977) *Biochem. Biophys. Res. Commun.* **77**, 1389–1396.
6. Buening, M.K., Wislocki, P.G., Levin, W., Yagi, H., Thakker, D.R., Akagi, H., Koreeda, M., Jerina, D.M. and Conney, A.H. (1978) *Proc. Natl. Acad. Sci. (USA)* **75**, 5358–5361.
7. Slaga, T.J., Bracken, W.J., Gleason, G., Levin, W., Yagi, H., Jerina, D.M. and Conney, A.H. (1979) *Cancer Res.* **39**, 67–71.

8. Stevens, C.W., Bouck, N., Burgess, J.A. and Fahl, W.E. (1985) *Mutat. Res.* **152**, 5–14.
9. Harvey, R.G. and Geacintov, N.E. (1988) *Accs. Chem. Res.* **21**, 66–73.
10. Gräslund, A. and Jernström, B. (1989) *Quart. Rev. Biophys.* **22**, 1–37.
11. Meehan, T. and Straub, K. (1979) *Nature* **277**, 410–412.
12. Jeffrey, A.M. (1985) in: *Polycyclic Aromatic Hydrocarbons and Carcinogenesis*, ACS Symposium Series No. 283 (R.G. Harvey, Ed.), The American Chemical Society, Washington, DC, pp. 187–208.
13. Cheng, S.C., Hilton, B.D., Roman, J.M. and Dipple, A. (1988) *Chem. Res. Toxicol.* **2**, 334–340.
14. Cosman, M., de los Santos, C., Fiala, R., Hingerty, B.E., Ibanez, V., Margulis, L.A., Live, D., Geacintov, N.E., Broyde, S. and Patel, D.J. (1992) *Proc. Natl. Acad. Sci. (USA)* **89**, 1914–1918.
15. de los Santos, C., Cosman, M., Hingerty, B.E., Ibanez, V., Margulis, L.A., Geacintov, N.E., Broyde, S. and Patel, D.J. (1992) *Biochemistry* **31**, 5245–5252.
16. Meehan, T., Gamper, H. and Becker, J.F. (1982) *J. Biol. Chem.* **257**, 10479–10485.
17. Yoshida, H., Swenberg, C.E. and Geacintov, N.E. (1987) *Biochemistry (USA)* **26**, 1351–1358.
18. Drinkwater, N.R., Miller, J.A., Miller, E.C. and Yang, N.C. (1978)*Cancer Res.* **38**, 3247–3255.
19. Gamper, H.B., Straub, K., Calvin , M. and Bartholomew, J.C. (1980) *Proc. Natl. Acad. Sci. (USA)* **77**, 2000–2004.
20. Agarwal, K.L., Hrynio, T.P. and Yang, N.C. (1983) *Biochem. Biophys. Res. Commun.* **114**, 14–19.
21. Kakefuda, T. and Yamamoto, H.-Y. (1978) *Proc. Natl. Acad. Sci. (USA)* **75**, 415–419.
22. Geacintov, N.E., Ibanez, V., Gagliano, A.G., Jacobs, S.A. and Harvey, R.G. (1984) *J. Biomol. Structure & Dynamics* **1**, 1473–1484.
23. Roche, C.J., Geacintov, N.E., Ibanez, V. and Harvey, R.G. (1989) *Biophys. Chem.* **33**, 277–288.
24. Cosman, M., Ibanez, V., Geacintov, N.E. and Harvey, R.G. (1990) *Carcinogenesis* **11**, 1667–1672.
25. Geacintov, N.E., Cosman, M., Mao, B., Alfano, A., Ibanez, V. and Harvey, R.G. (1991) *Carcinogenesis* **12**, 2099–2108.
26. Zinger, D., Geacintov, N.E. and Harvey, R.G. (1987) *Biophys. Chem.* **27**, 131–138.
27. Cosman, M. (1991) Ph.D. Dissertation, New York University.
28. DeLeys, R.J. and Jackson, D.A. (1976) *Biochem. Biophys. Res. Commun.* **69**, 446–454.
29. Espejo, R.T. and Lebowitz, J. (1976) *Analyt. Biochem.* **72**, 95–103.
30. Lang, M.C.E., Freund, A.M., de Murcia, G., Fuchs, R.P.P. and Daune, M.P. (1979) *Chem.-Biol. Interactions* **28**, 171–180.
31. Norden, B., Kubista, M. and Kurucsev, T. (1992) *Quart. Rev. Biophys.* **25**, 51–170.
32. Geacintov, N.E., Yoshida, H., Ibanez, V., Jacobs, S.A. and Harvey, R.G. (1984) *Biochem. Biophys. Res. Commun.* **122**, 33–39.
33. Geacintov, N.E., Ibanez, V., Rougee, M. and Bensasson, R.V. (1987) Biochemistry (USA) **26**, 3087–3092.
34. Waring , J. (1970) *J. Mol. Biol.* **54**, 247–279.
35. Swenberg, C.E., Carberry, S.E. and Geacintov, N.E. (1990) *Biopolymers* **29**, 1735–1744.
36. Crawford, L.V. and Waring., M.J. (1967) *J. Mol. Biol.* **25**, 23–30.
37. Bauer, W.R. (1978) *Ann. Rev. Biophys. Bioeng.* **7**, 287–313.
38. Sanger, F., Air, G.M., Barrell, B.G., Brown, N.L., Coulson, A.R., Fiddes, J.C., Hutchinson III, C.A., Slocombe, P.A. and Smith, M. (1977) *Nature* **265**, 687–695.
39. Geacintov, N.E., Gagliano, A.G., Ibanez, V. and Harvey, R.G. (1982) *Carcinogenesis* **3**, 247–253.
40. Jernström, B., Lycksell, P.O., Gräslund, A. and Nordén, B. (1984) *Carcinogenesis* **5**, 1129–1135.
41. Eriksson, M., Nordén, B., Jernström, B. and Gräslund, A. (1988) *Biochemistry (USA)* **27**, 1213–1221.
42. Kolubayev, V., Brenner, H.C. and Geacintov, N.E. (1987) *Biochemistry (USA)* **26**, 2638–2641.
43. Kim, S.-K., Brenner, H.C., Soh, B.J. and Geacintov, N.E. (1989) *Photochem. Photobiol.* **50**, 327–337.
44. MacLeod, M.C. and Tang, M. (1985) *Cancer Res.* **45**, 51–56.
45. Keller, W. (1975) *Proc. Natl. Acad. Sci. (USA)* 72, 4876–4880.
46. Wiesehahn, G. and Hearst, J.E. (1978) *Proc. Natl. Acad. Sci. (USA)* **75**, 2703–2707.
47. Hogan, M.E., Dattagupta, N. and Whitlock, J.P., Jr. (1981) *J. Biol. Chem.* **256**, 4504–4513.
48. Shahbaz, M., Geacintov, N.E. and Harvey, R.G. (1986) *Biochemistry (USA)* **25**, 3290–3296.
49. Carberry, S.E., Shahbaz, M., Geacintov, N.E. and Harvey, R.G. (1987) *Chem.-Biol. Interactions* **66**, 121–145.
50. Carberry, S.E., Geacintov, N.E. and Harvey, R.G. (1989) *Carcinogenesis* **10**, 97–103.
51. LeBreton, P. (1985) in *Polycyclic Hydrocarbons and Carcinogenesis* (R.G. Harvey, Ed.) ACS Symposium Series No. 283, American Chemical Society, Washington, DC, 209–238.
52. Waring, M.J. (1981) *Ann. Rev. Biochem.* **50**, 159–192.
53. Williams, L.D., Egli, M., Gao, Q. and Rich, A. (1992) in *Structure & Function, Volume I: Nucleic Acids* (Sarma, R.H. and Sarma, M.H., Eds.), Adenine Press, Guilderland, NY, pp. 107–125.
54. Scovell, W.M. and Collart, F. (1985) *Nucleic Acids Res.* **13**, 2881–2895.
55. Cohen, G.L., Bauer, W.R., Barton, J.K and Lippard, S.J. (1978) *Science* **203**, 1014–1016.
56. Lee, C.-H., Mizusawa, H. and Kakefuda, T. (1981) *Proc. Natl. Acad. Sci. (USA)* **78**, 2838–2842.
57. Germond, J.E., Rouviere-Yaniv, J., Yaniv, M. and Brutlag, D. (1979) *Proc. Natl. Acad. Sci. (USA)* **76**, 3779–3783.
58. Anderson, P. and Bauer, W. (1978) *Biochemistry (USA)* **17**, 594–601.
59. Boullard, A. and Giacomoni, P.U. (1988) *J. Photochem. Photobiol., B:Biology*, **2**, 491–501.
60. Singh, S.S., Hingerty, B.E., Singh, U.C., Greenberg, J.P., Geacintov, N.E. and Broyde, S. (1991) *Cancer Res.* **51**, 3482–3492.
61. Schwartz, A., Marrot, L. and Leng, M. (1989) *J. Mol. Biol.* **207**, 445–450.

DISTRIBUTION LIST

DEPARTMENT OF DEFENSE

ARMED FORCES INSTITUTE OF PATHOLOGY
ATTN: RADIOLOGIC PATHOLOGY DEPARTMENT

ARMED FORCES RADIOBIOLOGY RESEARCH INSTITUTE
ATTN: PUBLICATIONS DIVISION
ATTN: LIBRARY

ARMY/AIR FORCE JOINT MEDICAL LIBRARY
ATTN: DASG-AAFJML

ASSISTANT TO SECRETARY OF DEFENSE
ATTN: AE
ATTN: HA(IA)

DEFENSE NUCLEAR AGENCY
ATTN: TITL
ATTN: DDIR
ATTN: RARP
ATTN: MID

DEFENSE TECHNICAL INFORMATION CENTER
ATTN: DTIC-DDAC
ATTN: DTIC-FDAC

FIELD COMMAND DEFENSE NUCLEAR AGENCY
ATTN: FCFS

INTERSERVICE NUCLEAR WEAPONS SCHOOL
ATTN: TCHTS/RH

LAWRENCE LIVERMORE NATIONAL LABORATORY
ATTN: LIBRARY

UNDER SECRETARY OF DEFENSE (ACQUISITION)
ATTN: OUSD(A)/R&AT

UNIFORMED SERVICES UNIVERSITY OF THE HEALTH SCIENCES
ATTN: LIBRARY

DEPARTMENT OF THE ARMY

HARRY DIAMOND LABORATORIES
ATTN: SLCHD-NW
ATTN: SLCSM-SE

LETTERMAN ARMY INSTITUTE OF RESEARCH
ATTN: SGRD-ULY-OH

SURGEON GENERAL OF THE ARMY
ATTN: MEDDH-N

U.S. ARMY AEROMEDICAL RESEARCH LABORATORY
ATTN: SCIENTIFIC INFORMATION CENTER

U.S. ARMY ACADEMY OF HEALTH SCIENCES
ATTN: HSMC-FCM

U.S. ARMY CHEMICAL RESEARCH, DEVELOPMENT, AND ENGINEERING CENTER
ATTN: SMCCR-RST

U.S. ARMY INSTITUTE OF SURGICAL RESEARCH
ATTN: DIRECTOR OF RESEARCH

U.S. ARMY MEDICAL RESEARCH INSTITUTE OF CHEMICAL DEFENSE
ATTN: SGRD-UV-R

U.S. ARMY NUCLEAR AND CHEMICAL AGENCY
ATTN: MONA-NU

U.S. ARMY RESEARCH INSTITUTE OF ENVIRONMENTAL MEDICINE
ATTN: SGRD-UE-RPP

U.S. ARMY RESEARCH OFFICE
ATTN: BIOLOGICAL SCIENCES PROGRAM

WALTER REED ARMY INSTITUTE OF RESEARCH
ATTN: DIVISION OF EXPERIMENTAL THERAPEUTICS

DEPARTMENT OF THE NAVY

NAVAL AEROSPACE MEDICAL RESEARCH LABORATORY
ATTN: COMMANDING OFFICER

NAVAL MEDICAL COMMAND
ATTN: MEDCOM-21

NAVAL MEDICAL RESEARCH AND DEVELOPMENT COMMAND
ATTN: CODE 40C

NAVAL MEDICAL RESEARCH INSTITUTE
ATTN: LIBRARY

NAVAL RESEARCH LABORATORY
ATTN: LIBRARY

OFFICE OF NAVAL RESEARCH
ATTN: BIOLOGICAL SCIENCES DIVISION

SURGEON GENERAL OF THE NAVY
ATTN: MEDICAL RESEARCH AND DEVELOPEMENT

DEPARTMENT OF THE AIR FORCE

BOLLING AIR FORCE BASE
ATTN: AFOSR

BROOKS AIR FORCE BASE
ATTN: AL/OEBSC
ATTN: USAFSAM/RZ
ATTN: AL/DEBL

NUCLEAR CRITERIA GROUP, SECRETARIAT
ATTN: OAS/XRS

SURGEON GENERAL OF THE AIR FORCE
ATTN: HQ USAF/SGPT
ATTN: HQ USAF/SGES

U.S. AIR FORCE ACADEMY
ATTN: HQ USAFA/DFBL

OTHER FEDERAL GOVERNMENT

ARGONNE NATIONAL LABORATORY
ATTN: ACQUISITIONS

BROOKHAVEN NATIONAL LABORATORY
ATTN: RESEARCH LIBRARY, REPORTS SECTION

CENTER FOR DEVICES AND RADIOLOGICAL HEALTH
ATTN: HFZ-110

GOVERNMENT PRINTING OFFICE
ATTN: DEPOSITORY RECEIVING SECTION
ATTN: CONSIGNED BRANCH

LIBRARY OF CONGRESS
ATTN: UNIT X

LOS ALAMOS NATIONAL LABORATORY
ATTN: REPORT LIBRARY/P364

NATIONAL AERONAUTICS AND SPACE ADMINISTRATION
ATTN: RADLAB

NATIONAL AERONAUTICS AND SPACE ADMINISTRATION, GODDARD SPACE FLIGHT CENTER
ATTN: LIBRARY

NATIONAL CANCER INSTITUTE
ATTN: RADIATION RESEARCH PROGRAM

NATIONAL DEFENSE UNIVERSITY
ATTN: LIBRARY

NATIONAL LIBRARY OF MEDICINE
ATTN: OPI

U.S. ATOMIC ENERGY COMMISSION
ATTN: BETHESDA TECHNICAL LIBRARY

U.S. DEPARTMENT OF ENERGY
ATTN: LIBRARY

U.S. FOOD AND DRUG ADMINISTRATION
ATTN: WINCHESTER ENGINEERING AND ANALYTICAL CENTER

U.S. NUCLEAR REGULATORY COMMISSION
ATTN: LIBRARY

RESEARCH AND OTHER ORGANIZATIONS

BRITISH LIBRARY (SERIAL ACQUISITIONS)
ATTN: DOCUMENT SUPPLY CENTRE

CENTRE DE RECHERCHES DU SERVICE DE SANTE DES ARMEES
ATTN: DIRECTOR

INHALATION TOXICOLOGY RESEARCH INSTITUTE
ATTN: LIBRARY

INSTITUTE OF RADIOBIOLOGY
ARMED FORCES MEDICAL ACADEMY
ATTN: DIRECTOR

KAMAN SCIENCES CORPORATION
ATTN: DASIAC

NBC DEFENSE RESEARCH AND DEVELOPMENT CENTER OF THE FEDERAL ARMED FORCES
ATTN: WWDBW ABC-SCHUTZ

NCTR-ASSOCIATED UNIVERSITIES
ATTN: EXECUTIVE DIRECTOR

RUTGERS UNIVERSITY
ATTN: LIBRARY OF SCIENCE AND MEDICINE

UNIVERSITY OF CALIFORNIA
ATTN: LABORATORY FOR ENERGY-RELATED HEALTH RESEARCH
ATTN: LAWRENCE BERKELEY LABORATORY

UNIVERSITY OF CINCINNATI
ATTN: UNIVERSITY HOSPITAL, RADIOISOTOPE LABORATORY